



Methods to prepare biosorbents and magnetic sorbents for water treatment: a review

Ahmed I. Osman¹ · Eman M. Abd El-Monaem² · Ahmed M. Elgarahy^{3,4} · Chukwunonso O. Aniagor⁵ · Mohamed Hosny⁶ · Mohamed Farghali^{7,8} · Emanne Rashad⁹ · Marcel I. Ejimofor⁵ · Eduardo A. López-Maldonado¹⁰ · Ikko Ihara⁷ · Pow-Seng Yap¹¹ · David W. Rooney¹ · Abdelazeem S. Eltaweil²

Received: 7 April 2023 / Accepted: 17 April 2023 / Published online: 4 May 2023
© The Author(s) 2023

Abstract

Access to drinkable water is becoming more and more challenging due to worldwide pollution and the cost of water treatments. Water and wastewater treatment by adsorption on solid materials is usually cheap and effective in removing contaminants, yet classical adsorbents are not sustainable because they are derived from fossil fuels, and they can induce secondary pollution. Therefore, biological sorbents made of modern biomass are increasingly studied as promising alternatives. Indeed, such biosorbents utilize biological waste that would otherwise pollute water systems, and they promote the circular economy. Here we review biosorbents, magnetic sorbents, and other cost-effective sorbents with emphasis on preparation methods, adsorbents types, adsorption mechanisms, and regeneration of spent adsorbents. Biosorbents are prepared from a wide range of materials, including wood, bacteria, algae, herbaceous materials, agricultural waste, and animal waste. Commonly removed contaminants comprise dyes, heavy metals, radionuclides, pharmaceuticals, and personal care products. Preparation methods include coprecipitation, thermal decomposition, microwave irradiation, chemical reduction, micro-emulsion, and arc discharge. Adsorbents can be classified into activated carbon, biochar, lignocellulosic waste, clays, zeolites, peat, and humic soils. We detail adsorption isotherms and kinetics. Regeneration methods comprise thermal and chemical regeneration and supercritical fluid desorption. We also discuss exhausted adsorbent management and disposal. We found that agro-waste biosorbents can remove up to 68–100% of dyes, while wooden, herbaceous, bacterial, and marine-based biosorbents can remove up to 55–99% of heavy metals. Animal waste-based biosorbents can remove 1–99% of heavy metals. The average removal efficiency of modified biosorbents is around 90–95%, but some treatments, such as cross-linked beads, may negatively affect their efficiency.

Keywords Adsorption · Biosorbents · Magnetic sorbents · Water treatment · Regeneration · Kinetics

Abbreviation

PPCPs Pharmaceuticals and personal care products

Introduction

Over the past few years, water pollution has become an increasingly urgent global issue due to industries discharging significant amounts of pollutants into water bodies. This situation poses substantial risks to human health and the environment, creating multiple treatment technologies. Among these methods, adsorption holds great promise as

it involves removing contaminants from water by adhering them to an adsorbent material (Abdel Maksoud et al. 2022; Osman et al. 2022a). Due to their unique properties and cost-effectiveness, biosorbents and magnetic sorbents have emerged as cost-effective and environmentally friendly alternatives to conventional adsorbents (Abdel Maksoud et al. 2020). Biosorbents are derived from renewable sources, such as plant-based materials, animal waste, and marine biomass, and can be easily modified to increase their adsorption capacity, making them versatile and efficient for various pollutants (Crini et al. 2019a, b; Osman et al. 2020a). Meanwhile, magnetic sorbents are produced by incorporating magnetic nanoparticles into adsorbent materials, allowing easy separation from water using a magnetic field. This makes them ideal for continuous water treatment, as they can be recovered and reused multiple times.

✉ Ahmed I. Osman
aosmanahmed01@qub.ac.uk

Extended author information available on the last page of the article

This review aims to provide a comprehensive overview of recent advancements in biosorbents and magnetic sorbents for water treatment. The topics covered include preparation methods, adsorption isotherms, mechanisms, applications, and economic evaluation of these materials, as shown in Fig. 1. To the best of the authors' knowledge, this is the first study to critically evaluate adsorbents, with particular emphasis on biosorbents, magnetic sorbents, and other economical sorbents, from their preparation to their ultimate application. Furthermore, it provides a better understanding of adsorption mechanisms and facilitates the effective regeneration of contaminated adsorbents.

Methods to prepare biosorbents

The industrial and technological progress of the past century has resulted in the release of substantial quantities of various organic and inorganic pollutants into the environment (Hosny et al. 2022; Mahmoud et al. 2022a). In order to remove these pollutants, different treatment techniques are continuously researched and implemented. Adsorption is considered one of the most effective techniques for removing pollutants due to its simplicity, low energy demand, and adaptability to various types of pollutants (Abdelfatah et al.

2021; Eltaweil et al. 2022a; Osman et al. 2023). However, the production cost of conventional synthetic adsorbents is prohibitively high, which limits their usage. This has increased the demand for natural adsorbents, also known as biosorbents (Salleh et al. 2011). Various materials can be utilized as biosorbents, including wood biomass, agro-waste such as crop and forest residue, and animal waste materials, e.g., fish scales, crab shells, and chicken feathers. The materials undergo various processes before being used for pollutant removal, as illustrated in Fig. 2. Subsequent sections will provide a detailed discussion of these materials.

Preparation of wooden, herbaceous, bacterial, and marine-based biosorbents

Adopting the circular economy concept in the national development plans of many countries has facilitated the use of waste products for various purposes (Stjepanović et al. 2021). In the case of wood-based production, most waste wood biomass has been used to generate heat and electricity, replacing non-renewable sources with renewable, eco-friendly, and more sustainable alternatives (Uasuf and Becker 2011). However, a significant amount of wood biomass waste remains underutilized or disposed of inadequately, resulting in hazardous environmental issues

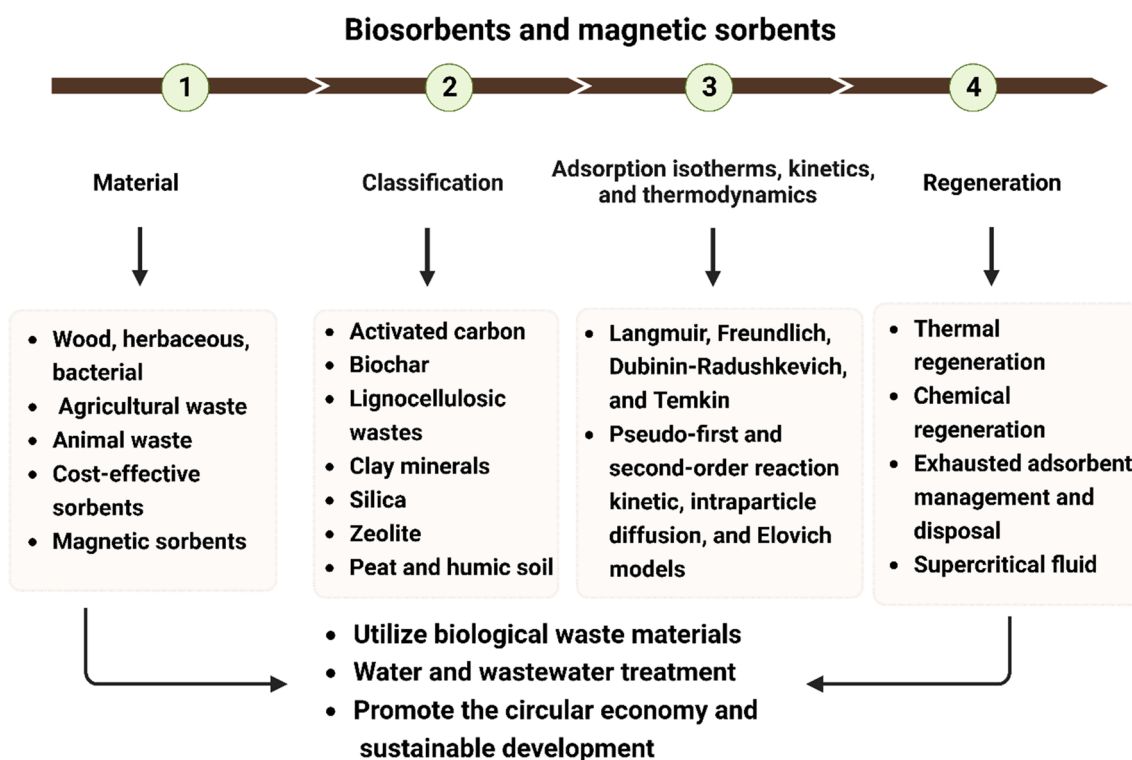


Fig. 1 Main topics presented in this review article. Various materials can be used to prepare these sorbents cost-effectively. By utilizing these sorbents, improved pollutant removal can be achieved, resulting

in a more efficient technology for water treatment. The sorbents can be regenerated and reused to maximize these approaches' cost-effective and sustainable benefits

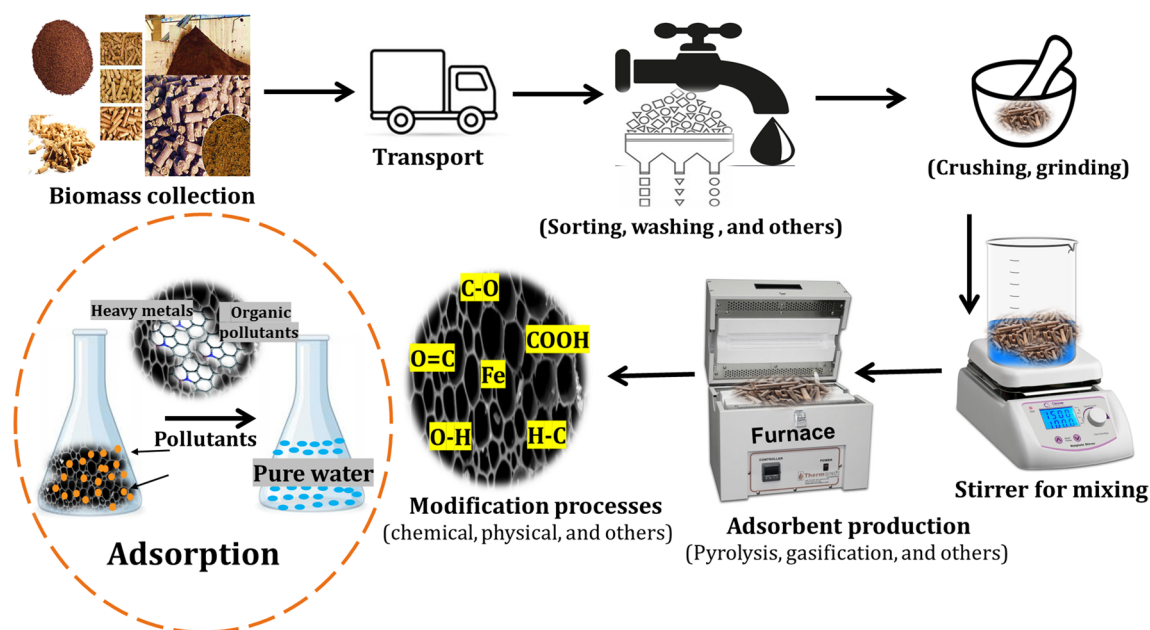


Fig. 2 Biosorbents from synthesis to application. The production and application of biosorbents involve several stages. First, the desired substrates are selected and subjected to washing and drying. Subsequently, physical techniques are employed to increase the surface area

of the feedstock. This is followed by the adsorbent process, which can be carried out using pyrolysis, torrefaction, and gasification methods. The resulting biosorbent can remove contaminants from wastewater, producing purified water suitable for various applications

(Stjepanović et al. 2021). Therefore, recent research articles have focused on utilizing wood biowaste in multiple applications, mainly as adsorbents for various pollutants.

In order to adsorb phosphates from wastewater, aspen wood particles were treated in two stages with carboxymethyl cellulose and ferrous chloride solutions (Eberhardt and Min 2008). The study's novel aspect was using carboxymethyl cellulose, a nontoxic anionic polymer, to create additional binding sites for iron ions, thereby increasing phosphate adsorption capacity. The wood particles were first ground, then treated with a carboxymethyl cellulose solution in deionized water, and left for several hours. They were then filtered via vacuum filtration and dried at 60 °C. The sample was subsequently soaked in an aqueous ferrous chloride solution, filtered, washed, and processed similarly. The positive effect of carboxymethyl cellulose was evident in the adsorption capacity of approximately 4.14 mg g⁻¹, compared to approximately 2.78 mg g⁻¹ for the wood sample treated solely with ferrous chloride.

Similarly, Yang et al. (2022) developed two wooden-based biosorbents for removing congo red and crystal violet using a one-step ball milling approach with Hickory wood feedstock. The biosorbents were synthesized via acidic and alkaline ball milling, while a neutrally-prepared biosorbent served as a control. In the synthesis process, 100 g of 6 mm agate spheres and 1 g of biomass feedstock were added to agate jars. Each jar was filled with 20 ml of sulfuric acid, sodium hydroxide, or deionized water (control). The jars

were subjected to a 12-h ball-milling process at 300 rpm in ambient air, changing the rotation direction every three hours. After ball milling, the remaining biosorbents were rinsed with deionized water, dried for 12 h at 80 °C, ground, and stored in airtight containers. The resulting biosorbents exhibited high removal efficiencies of 87.9% for Congo red using the acidic biosorbent and 76.9% for crystal violet using the alkaline biosorbent, even after five regeneration cycles. The increased oxygen-containing functional groups and pore channels of the biosorbents due to the acidic/alkaline ball milling process resulted in electrostatic interaction, ion exchange, and surface complexation between the biosorbents and the polar dyes. It is worth noting that this low-cost biosorbent production method did not require extensive heat treatment, unlike the biochar preparation method.

Another study targeted the removal of crystal violet from water using a biosorbent prepared by the valorization of jujube shell wood (El Messaoudi et al. 2017). The jujube core was initially crushed to extract the shell, which was then processed using procedures similar to those used for the biosorbent mentioned earlier. To create the modified shell powder, the jujube shell was mixed with sodium hydroxide, stirred at room temperature for one day, filtered and rinsed with water, and finally dried and sieved similarly to the raw powder. The removal efficiency achieved using 0.2 g of raw shell powder was 95.84%, while only 0.1 g of the modified shell powder was required to achieve 98.16% removal efficiency. The modified powder was also found to

have a significantly higher adsorption capacity than the raw powder, with a capacity of 288.18 mg g^{-1} compared to only 59.84 mg g^{-1} for the raw powder. This enhanced adsorption capacity was attributed to irregular cavities and carboxylate groups on the surface of the modified powder, which facilitated the adsorption of crystal violet molecules.

Chemical modifications used in current biosorbent synthesis methods can lead to secondary pollution, making it essential to search for eco-friendly and green alternatives (Zhang et al. 2012). In this concern, a recent study by Zhang et al. (2022b) investigated using an ultrasound-assisted and hydroalcoholic-freezing combination modification method for preparing a biosorbent made of waste peach wood branches to remove methylene blue. Initially, the peach wood branches were ground into powder (control sample), mixed with ethanol, stirred for a few minutes, sonicated in a water bath at $70 \text{ }^\circ\text{C}$, centrifuged, and subjected to freeze-drying at $-60 \text{ }^\circ\text{C}$. The resulting biosorbent had a porous structure with fewer impurities than the control sample, providing more adsorption sites and improving the overall removal efficiency to 94.91%. After removing impurities with an ultrasound-assisted hydroalcoholic cleaning process, the remaining cellulose, lignin, and hemicellulose were responsible for methylene blue adsorption via electrostatic, ion–dipole interactions, and π electrons transfer from the biosorbent to methylene blue. Additionally, the stability of this biosorbent was confirmed by observing a removal efficiency of 81.79% after five recycling times.

A green and cost-effective method for producing a highly efficient and easily recyclable biosorbent for removing nickel ions from wastewater was achieved through the esterification of paulownia wood using eco-friendly chemicals, phosphoric acid, and urea, commonly used in food and fertilizer production (Huo et al. 2022). The Paulownia wood was first made into chips, mixed with sodium hydroxide, and heated for one hour at $100 \text{ }^\circ\text{C}$, followed by rinsing with hot deionized water to produce the control wood biosorbent. The chemically modified (phosphorylated) biosorbent was prepared by suspending the control biosorbent in water and mixing it with phosphoric acid and urea. The mixture was then dried at $80 \text{ }^\circ\text{C}$ for 12 h, rinsed with hot water, and left to dry in the open air. The positive effect of phosphorylation was evident in the significant increase in the adsorption capacity, from 18.5 mg g^{-1} for the unmodified biosorbent to 130.2 mg g^{-1} for the phosphorylated biosorbent. This increase was attributed to the complexation and electrostatic attraction between the negatively charged phosphate groups on the phosphorylated biosorbent surface and the positively charged nickel ions. The high adsorption capacity was also attributed to the protection and stabilization of the phosphorylated biosorbent achieved by urea.

In contrast to biosorbents prepared by Richards et al. (2019) from wood biomass, natural softwood chippings

exhibited very low efficiency in removing copper and zinc ions from aqueous solutions, with only about 3% efficiency for both metals. This was due to the low cation release from the wood biomass in both metal solutions, resulting in a very low cation exchange rate. However, when using *Fucus vesiculosus* algal biomass as a biosorbent, the removal efficiencies were much higher, with 67% and 55% for copper and zinc ions, respectively. To prepare the unmodified biosorbent, the algae were collected, rinsed with water, air-dried, crushed, rewashed, and air-dried. A chemically treated algal biosorbent was produced to enhance the removal efficiency by shaking the dried algal powder with a calcium nitrate solution for one day, followed by rinsing with water and air drying.

Furthermore, modified algal biosorbents were also prepared for the same purpose. A chemically modified biosorbent was produced by treating the dried algal powder with a calcium nitrate solution for one day, then rinse it with water and air drying. A thermally modified biosorbent was also prepared by drying the crushed algae at $100 \text{ }^\circ\text{C}$ for two days after rinsing it with water. Surprisingly, both modified biosorbents showed lower efficiencies than the untreated biosorbent without any explanation provided by the authors. The chemically modified biosorbent exhibited 62% and 52% efficiency against copper and zinc ions, respectively, while the thermally modified biosorbent exhibited 59% and 42% efficiency against copper and zinc ions, respectively. The high efficiency of the untreated biosorbent was attributed to the presence of functional groups such as alcohols, carboxylic acids, esters, and amides that have a high affinity for both metals.

Various herbaceous materials have been investigated as efficient biosorbents in multiple research articles. One such material is *Phytolacca americana* L., which Wang et al. (2018a) used to remove lead ions (Pb^{2+}) from aqueous solutions. To prepare the biosorbent, the plant material was processed similarly to the biosorbents discussed previously. A modified biosorbent was created by soaking the plant material in a diluted nitric acid solution and shaking it for six hours at room temperature. This was followed by washing to neutralize the pH and drying the modified biosorbent similarly to the raw biosorbent. The modification with nitric acid played a crucial role in improving the adsorption efficiency from 81.97 to 93.29% by increasing the surface porosity and creating cracks that served as additional adsorption sites for lead ions. The adsorption mechanism was electrostatic interaction and ion exchange through the hydroxyl, carboxyl, and amine functional groups.

Phragmites australis, also known as the common reed, is a cosmopolitan aquatic plant species that pose various environmental issues, including depletion of dissolved oxygen and reduction of biological diversity (El-Borady et al. 2021; Hosny et al. 2021). Nevertheless, due to its

high cellulose and lignin content, it was utilized by Southichak et al. (2006) as a biosorbent to remove heavy metals, such as nickel ions. The biosorbent was prepared in the same way as previously mentioned. The raw biosorbent was then modified by treating it with sodium hydroxide, washing it with water to neutralize the pH, and oven-drying it at 90 °C. The adsorption efficiency of the raw biosorbent was only 14% against a nickel concentration of 1.1 ppm, but it significantly increased to 81% for the treated biosorbent. This improvement was primarily attributed to the enhanced surface area of the treated sorbent ($20 \text{ m}^2 \text{ g}^{-1}$), compared to only $3.49 \text{ m}^2 \text{ g}^{-1}$ for the raw sorbent. Surprisingly, the removal efficiency of the treated biosorbent against a nickel concentration of 0.9 ppm increased from 92% in the first cycle to almost 99% in the second and third cycles. This behavior was attributed to the slight increase of the biosorbent's negative zeta potential after being recycled using hydrochloric acid, resulting in improved adsorption of positively charged nickel ions.

Shahnaz et al. (2020) conducted a study to remove hexavalent chromium using a chemically modified biosorbent made from *Acacia auriculiformis*. The plant material was processed like the previously mentioned biosorbents, then treated with sulfuric acid and pyrolyzed at 400 °C. The resulting powder was neutralized with a sodium bicarbonate and water mixture, dried, and mixed with ethylenediaminetetraacetic acid for two days at room temperature before being washed and dried. The modified biosorbent achieved a higher removal efficiency of 57.51% compared to 40.65% for the pristine biosorbent. This increase was attributed to the complexation of the pristine biosorbent with chelating agents, which increased the number of active functional groups, such as carboxyl and hydroxyl groups, that interacted with chromium ions.

Due to their high surface area and other positive properties, nanomaterials have found numerous applications. In a recent study, Herrera-Barros et al. (2020) investigated using alumina nanoparticles to modify an oil palm-based (bagasse) biosorbent to remove cadmium and nickel from wastewater. The preparation process involved shredding, rinsing, drying, and grinding the oil palm into fine pieces, followed by mixing the pristine powder with dimethyl sulfoxide, tetra ethyl-o-silicate, and alumina nanoparticles while stirring for 12 h. The biosorbent was then rinsed and dried at room temperature. However, the chemical modification of the bagasse biosorbent did not significantly improve its adsorption efficacy. While the removal efficiency increased slightly for cadmium and nickel, the improvement was insignificant enough to justify the modification process's additional cost and environmental impact. Therefore, it may be more cost-effective and environmentally friendly to rely on unmodified biosorbents.

To enhance the adsorption efficiency of biosorbents, surfactants can be utilized to reduce surface tension and increase the rate of ionic exchange. Bhatti et al. (2007) conducted a study using *Moringa oleifera* as a biosorbent to remove zinc ions from aqueous solutions. The plant was processed by being rinsed, dried, and ground into a fine powder before being mixed with three different surfactants: Triton, sodium dodecyl sulfate, and acetyl trimethyl ammonium bromide. After each surfactant was added and washed to reach a pH of approximately 7, the biosorbent was air-dried. The results showed that acetyl trimethyl ammonium bromide had the highest removal efficiency at 85.6%, followed by Triton (84.12%), sodium dodecyl sulfate (80.82%), and the unmodified biosorbent (74%). This was attributed to the high number of carbon atoms in acetyl trimethyl ammonium bromide, which created more positive sites for improved ionic exchange with zinc ions than other surfactants.

Yeast, including commercial dry baker's yeast (*Saccharomyces cerevisiae*), has been used by researchers as a category of biological material for preparing biosorbents. do Nascimento et al. (2019) utilized this yeast and successfully removed 76% of copper ions. Similarly, De Rossi et al. (2020) used the same yeast to remove hexavalent chromium ions from real wastewater. Encapsulating the yeast with alginate beads led to an efficacy of approximately 95%. To prepare the biosorbent, the yeast was first rinsed with water and mixed with a sodium alginate solution in phosphate buffer for 10 min. The mixture was then added to a calcium chloride solution and left for two hours for the capsules to form. These capsules were then rinsed and oven-dried at 50 °C for 24 h. The significant removal efficiency was attributed to the surface pores formed by the dried alginate beads.

Using the same biosorbents, baker's yeast was treated with ethylenediamine tetra-acetic acid di-anhydride by Yu et al. (2008) to remove lead and copper ions. The preparation procedures involved two main steps; firstly, the baker's yeast was mixed with a glutaraldehyde solution for 24 h at room temperature, rinsed, and subjected to freeze drying. Secondly, ethylenediamine tetra-acetic acid di-anhydride was mixed with a solution of *N,N*-dimethylacetamide containing yeast crosslinked biomass that was prepared in the first step. Subsequently, the mixture was washed to remove the unreacted reagent after being stirred for 4 h at 60 °C and freeze-dried. This treatment improved the active adsorption sites, leading to a removal efficiency of more than 90% for both metals through complexing these ions with ethylenediamine tetra-acetic acid of the modified biosorbent.

In another study, Chwastowski and Staroń (2022) investigated how modifying a biosorbent made from coconut fibers with *Saccharomyces cerevisiae* impacted the removal of lead ions. Initially, the fibers were rinsed and dried at 50 °C for 72 h. The researchers then mixed the fibers with sterilized yeast cells and left the mixture

to incubate at 28 °C for 24 h. The study found no significant difference in the removal efficiency before and after the modification, with both the unmodified and modified biosorbents achieving a removal efficiency of 99.32% against a lead concentration of 1000 ppm. However, the modified version demonstrated a slightly improved efficiency of 99.87%, attributed to the accumulation of lead ions in the yeast cells. As the lead concentration increased, the efficiency of the modified biosorbent decreased and became lower than the unmodified version. This was due to the toxic effect of lead ions on the yeast cells, resulting in their death and the subsequent blocking of active adsorption sites.

Jalali et al. (2002) utilized *Sargassum hystrix*, a type of brown algae, as a source of biosorbents for removing lead ions. Marine biomass has become a popular and environmentally friendly option due to its simplicity and cost-effectiveness. The algal biomass was prepared conventionally by rinsing it with water, drying it under the sun, oven-drying it, and finally grinding it into powder. The study found that the obtained removal efficiency was 98%, and it is worth noting that the efficiency remained constant even after ten regeneration cycles. This high efficacy was attributed to the algal polysaccharides, particularly alginates, which contain carboxyl and sulfate functional groups that act as adsorption sites (Volesky 1994).

Several research studies have confirmed the effectiveness of modifying biosorbents, including marine-based ones, with surface functional groups like amine, carboxyl, and phosphate to enhance their removal efficacy (Jayakumar et al. 2021). For example, *Oscillatoria princeps* was modified using three different amine ligands; tetraethylene tetramine, *para*-amino benzamidine, and polydopamine to enhance the removal efficiency of reactive red 120 dye (Bayramoglu et al. 2022). The study found that the removal efficiency of the unmodified biosorbent was approximately 33.1% but significantly increased to 99.7%, 81.4%, and 59.8% after being modified with tetraethylene tetramine, *para*-amino benzamidine, and polydopamine, respectively. This increase in efficiency was attributed to the increased number of adsorption sites after modification and the electrostatic attraction between the amine groups on the aliphatic chains of the ligands and the dye's sulfonyl groups. The higher efficiency of the tetraethylene tetramine-treated biosorbent compared to the other modified biosorbents was due to its numerous primary and secondary amine groups. Overall, various biosorbents have been found to be effective in removing dyes, heavy metals, and other pollutants, as listed in Table 1, with algal biomass exhibiting the highest efficiency even after ten regeneration cycles.

Preparation of agricultural waste-based biosorbents

Due to their wide availability, eco-friendliness, and facile conversion to biosorbents by straightforward processes such as washing, drying, and grinding, agricultural waste materials are an efficient candidate for removing various organic and inorganic pollutants (Bhatnagar et al. 2015). The utilization of such a type of waste materials offers numerous positive aspects, such as minimizing the number of released waste materials, producing materials that could be of a high value as well as treating wastewater by removing organic and inorganic contaminants (Escudero et al. 2019; Peng et al. 2023). In this regard, peels of overripe *Cucumis sativus*, commonly known as cucumber, were used by Lee et al. (2016) to remove acid blue 113 dye. The biosorbent was conventionally prepared by washing the whole plant with water, followed by removing the plant's outer layer, cutting it into small pieces, oven drying, and finally, the peels were ground into fine powder. The obtained removal efficiency was 97.6%, as indicated in Table 2, at an acidic pH level of 2 due to the electrostatic attraction between the positively charged adsorption sites and the negatively charged sulfonate groups of the dye molecules.

Similarly, Ali (2018) used banana peels to support silicon dioxide nanoparticles to produce a nanocomposite of cellulose/silicon dioxide and employed this composite in the biosorption of methylene blue. Silicon dioxide nanoparticles were first synthesized through the alkaline hydrolysis of tetraethylorthosilicate in ethanol. Then the peel powder was similarly prepared to the abovementioned article. Subsequently, the powder was mixed with the nanoparticles solution and stirred for 16 h, dried at 80 °C, and eventually calcined at 550 °C for one hour. Upon characterizing both biosorbents, the surface area of the raw biosorbent was found to be 1.9 m² g⁻¹, whereas, for the modified biosorbent, the surface area significantly increased to 8.9 m² g⁻¹. Consequently, the adsorption capacity increased from 21 to 78.75 mg g⁻¹ by the modified biosorbent. Also, the removal efficiency increased from 86.5 to 99.6% by increasing the pH from 4 to 10. Such a result indicated the quintessential role of the electrostatic attraction between the negatively charged biosorbent and the cationic dye molecules and the chemical adsorption.

Similarly, sugarcane bagasse was treated with phosphoric acid to produce a biosorbent for methyl red dye adsorption (Saad et al. 2010). The bagasse powder was added to a phosphoric acid solution and heated at 150 °C for one day, followed by water rinsing and overnight mixing with sodium carbonate to remove acid residues. Lastly, the mixture was neutralized by washing with deionized water, 24 h-drying at 150 °C, and ground into fine powder. This treatment increased the adsorption efficacy from 64.2 to 83.2%, which was attributed to the enhanced anion-exchange reaction

Table 1 Methods to prepare wooden, herbaceous, bacterial, and marine-based biosorbents

Preparation method	Feedstock material	Target pollutant	Removal% or q_m (mg g ⁻¹)	References
Two-stage treatment of aspen wood particles with carboxymethyl cellulose and ferrous chloride solutions	Refined aspen wood fiber	Phosphates	4.14 mg g ⁻¹	Eberhardt and Min (2008)
Acidic and alkaline one-step ball milling	Hickory wood	Crystal violet	76.9%	Yang et al. (2022)
		Congo red	87.9%	
Valorization of wood	Jujube shell	Crystal violet	98.16%	El Messaoudi et al. (2017)
Ultrasound-assisted and hydroalcoholic-freezing combination modification	Waste peach wood branches	Methylene blue	94.91%	Zhang et al. (2022b)
Esterification of wood by phosphoric acid and urea	Paulownia wood	Nickel	130.2 mg g ⁻¹	Huo et al. (2022)
Conventional method	Unmodified wood chippings	Copper	3%	Richards et al. (2019)
		Zinc	3%	
	<i>Unmodified macro algae (Fucus vesiculosus)</i>	Copper	67%	
		Zinc	55%	
Treatment with a nitric acid solution	<i>Phytolacca americana</i> L	Lead	93.29%	Wang et al. (2018a)
Treatment with sodium hydroxide solution	<i>Phragmites australis</i>	Nickel	92%	Southichak et al. (2006)
Sulfuric acid treatment combined with ethylenediaminetetraacetic acid complexation	<i>Acacia auriculiformis</i> shells	Hexavalent chromium	57.51%	Shahnaz et al. (2020)
Modification of oil palm with alumina nanoparticles	Oil palm (<i>Elaeis guineensis</i>)	Cadmium	87%	Herrera-Barros et al. (2020)
		Nickel	81%	
Modification of <i>Moringa oleifera</i> with surfactants	<i>Moringa oleifera</i> treated with Triton	Zinc	84.12%	Bhatti et al. (2007)
	<i>Moringa oleifera</i> treated with sodium dodecyl sulfate		80.82%	
	<i>Moringa oleifera</i> treated with cetyl trimethyl ammonium bromide		85.6%	
Conventional biosorption assays	Commercial dry baker's yeast (<i>Saccharomyces cerevisiae</i>)	Copper	76%	do Nascimento et al. (2019)
Encapsulation with alginate beads	Commercial dry baker's yeast (<i>Saccharomyces cerevisiae</i>)	Hexavalent chromium	95%	De Rossi et al. (2020)
Modification of baker's yeast with ethylenediaminetetraacetic acid dianhydride	Commercial dry baker's yeast (<i>Saccharomyces cerevisiae</i>)	Lead and copper	More than 90%	Yu et al. (2008)
Modification of coconut fibers by <i>Saccharomyces cerevisiae</i>	Coconut fibers	Lead	99.87%	Chwastowski and Staroń (2022)
Conventional preparation of algal biosorbents	Brown algae (<i>Sargassum hystrix</i>)	Lead	98%	Jalali et al. (2002)
Chemical modification of algal biomass with amine ligands (tetraethylene tetramine, <i>para</i> -amino benzamidine, and polydopamine)	Blue-green algae (<i>Oscillatoria princeps</i>)	Reactive red 120	99.7%	Bayramoglu et al. (2022)
			81.4%	
			59.8%	

Various techniques are used to modify these biosorbents to improve their efficiency. In addition, different feedstock materials used, types of target organic and inorganic pollutants, and the reported removal efficiencies of these biosorbents were reported. q_m is the maximum adsorption amount of Langmuir isotherm

Table 2 Common methods to prepare biosorbents from agricultural waste materials

Preparation method	Feedstock material	Target pollutant	Removal%	References
Conventional preparation of agro-waste biosorbents	Peels of overripe <i>Cucumis sativus</i>	Acid blue 113	97.6	Lee et al. (2016)
Synthesis of cellulose/silicon dioxide nanocomposite	Banana peels	Methylene blue	99.6	Ali (2018)
Treatment of agro-waste biosorbent with phosphoric acid	Sugarcane bagasse	Methyl red	83.2	Saad et al. (2010)
The two-stage process of chemical activation accompanied by carbonization followed by surfactant modification	Orange peels	Congo red	98	Karaman et al. (2022)
Combined acidic and alkaline treatment of an agricultural waste material	Tangerine peels	Cadmium	97.9	Abdić et al. (2018)
		Cobalt	94.7	
		Hexavalent chromium	88.9	
		Copper	97	
		Manganese	92.4	
		Nickel	93.5	
		Lead	93	
Thermochemical treatment of agricultural waste-based biosorbent	Corn husk (<i>Zea mays</i>)	Lead	100	Rwiza et al. (2018)
Formation of crosslinked composites beads containing copper-tolerant <i>Aspergillus australensis</i> biomass	<i>Aspergillus australensis</i>	Copper	79	Contreras-Cortés et al. (2019)
Ultrasound treatment of seaweed-based biosorbent	Seaweed (<i>Kappaphycus alvarezii</i>)	Methylene blue	100	Kumar et al. (2022)
Conventional preparation of forest waste-based biosorbents	<i>Inga marginata</i> <i>Tipuana tipu</i>	Gentian violet	77.65	Franco et al. (2021)
			68.71	
Treatment of forest waste biosorbent with phosphoric acid	Kenaf fiber	Copper	88.2	Razak et al. (2020)

The possible modifications applied to these preparation methods to enhance their pollutants' removal efficiencies and the employed feedstock materials in preparing the biosorbents were listed. The detected removal efficiencies, q_m is the maximum adsorption amount of Langmuir isotherm

between the dye and functional groups on the biosorbent surface.

Treating biosorbents with surfactants to enhance their removal performance of various organic and inorganic pollutants was indicated in previous research works, such as the one conducted by Karaman et al. (2022) on Congo red dye. The raw biosorbent was made of orange peel waste, similar to the abovementioned studies. The modified biosorbent was prepared in two steps; chemical activation accompanied by carbonization and modification with the surfactant cetyl trimethyl ammonium bromide. Firstly, the powder was magnetically stirred with zinc chloride solution and then dried at 110 °C, followed by a carbonization process in a muffle furnace at 500 °C for one hour. Secondly, the carbonized powder was rinsed with hydrochloric acid followed by water, oven-dried at 110 °C, mixed with the surfactant, shaken for one day, rinsed, and dried. The removal efficiency was boosted from 61% by the pristine biosorbent to almost 98% using the treated biosorbent. Such a significant difference

was related to the enhancement of surface area from 102 to 1169 m² g⁻¹ and the improved pores' formation after the modification process. Also, van der Waals forces between the dye and the surfactant molecules were considered one of the main factors for increasing the adsorption efficacy.

One more study targeted the removal of eight different heavy metals by a chemically-modified biosorbent made of tangerine peels (Abdić et al. 2018). The peel powder was prepared using the same steps mentioned above and then mixed with nitric acid at the average room temperature for one day, followed by thorough washing to neutralize the pH and air-dried. Secondly, the powder underwent a further alkaline treatment by mixing the neutralized powder with sodium hydroxide for three to four hours and then processed in the same manner as the first step. The observed removal efficiencies using the modified biosorbent were 97.9%, 94.7%, 88.9%, 97.0%, 92.4%, 93.5%, 93.0%, and 96.8% for cadmium, cobalt, hexavalent chromium, copper, manganese, nickel, lead, and zinc, respectively. These removal

efficiencies were about 40% higher than the unmodified biosorbent for all eight metals. Such an improved performance was accredited to the increased adsorption sites and the enhanced ionic exchange between the negatively charged functional groups in the cell wall of tangerine peels and the positively charged metal ions upon chemical modification.

Another sort of common agricultural waste material that could be harnessed in producing biosorbents for wastewater treatment is corn husk. In this line, a recent study (Rwiza et al. 2018) targeted the adsorption of lead ions using a thermochemically treated corn (*Zea mays*) husk biosorbent. Conventional experimental procedures, from rinsing and drying to grounding, were employed to prepare the raw corn husk biosorbent. Subsequently, biochar material was produced by pyrolyzing at 500 °C for 1 h. Afterwards, the biochar powder was chemically treated using two different reagents; firstly, mixed in an equal ratio with zinc chloride in water, followed by stirring, heating, filtration, and drying. The resulting powder was re-carbonized using the same conditions, removed excess zinc chloride by nitric acid, and finally washed to have a pH range of 5–6. Secondly, another chemically modified biosorbent was prepared similarly using potassium hydroxide. The observed removal efficiency for the raw biosorbent was about 82% but reached almost 100% using the two thermochemically biosorbents. Such a result was accredited to the improved chemical cation exchange because of the increased oxygen-containing functional groups, including carboxyl and hydroxyl groups (Gaskin et al. 2008), along with the enhanced adsorption sites after chemical treatment.

Fungi-based materials constitute another important type of biosorbent that showed high efficacy and well applicability in many research works, such as the one carried out by Contreras-Cortés et al. (2019) to adsorb copper ions on the surface of crosslinked composites beads containing copper-tolerant *Aspergillus australensis* biomass with an efficiency of 79%. The dead fungi powder was prepared in a broth containing potassium hydrogen phosphate, sodium nitrate, sucrose, yeast extract, and others. Subsequently, the broth was inoculated, and the produced biomass was filtered, rinsed, sterilized in an autoclave, dried, and eventually ground into fine powder. To prepare the chitosan beads, chitosan solution was mixed with the prepared fungal powder, then sodium alginate solution was added to synthesize the polymerization gel. Furthermore, the gel was mixed with a tripolyphosphate solution to formulate the crosslinked composite beads. A comparison between the unmodified composite beads and the crosslinked composite beads revealed higher removal efficiency for the unmodified beads since the crosslinking step blocked some active adsorption sites. However, the mechanical stability of the crosslinked beads was higher, particularly in the acidic medium, which is better for avoiding chitosan beads

dissolution that could result in forming other secondary pollutants (Sánchez-Duarte et al. 2017).

Applying the ultrasound energy in modifying biosorbents is another option to produce highly efficient biosorbents, such as the ultrasound seaweed-based (*Kappaphycus alvarezii*) biosorbent synthesized by Kumar et al. (2022) to remove methylene blue. The seaweed powder was prepared similarly to the aforementioned raw biosorbents. Subsequently, the powder was mixed with ethanol and subjected to a probe-based ultrasound treatment at 30 °C with a variation in ultrasound power, solid–liquid ratio, and contact time. Such treatment created more cavities on the biosorbent surface and increased the surface area from 0.77 m² g⁻¹ to almost 1 m² g⁻¹, leading to complete removal efficiency (100%).

Forest waste materials are another category of eco-friendly biosorbents that attracted the researchers' interest due to their wide availability, low cost, simple preparation techniques, facile modification, and high efficacy (Gemici et al. 2021). In this regard, Franco et al. (2021) investigated the removal of gentian violet dye using the pods of two forest species; *Inga marginata* and *Tipuana tipu*. The pods were rinsed separately and then dried at 60 °C inside a greenhouse for two days. Subsequently, the dried materials were ground, washed with ethanol followed by water, and ultimately dried one more time inside the greenhouse. Some negatively charged functional groups, including carbonyl and hydroxyl groups on the biosorbents' surface led to the adsorption of the cationic dye molecules by 77.65% and 68.71% using the biosorbents of *Inga marginata* and *Tipuana tipu*, respectively.

Within the same biosorbents category, Razak et al. (2020) examined the adsorption of copper ions by a phosphoric acid-treated biosorbent based on Kenaf fiber. The pristine biosorbent was produced similarly to the abovementioned biosorbent. However, the pristine powder was mixed with dimethyl formamide solution for one day at room temperature to prepare the modified one. Subsequently, the solution was filtered, followed by adding urea in a fresh dimethyl formamide solution and phosphoric acid addition. Furthermore, the mixture was refluxed, filtered, and washed with ethyl alcohol, followed by water. Finally, the filtered powder was mixed with sodium hydroxide, rinsed with water, and dried. The observed adsorption capacity of the treated biosorbent was 25.2 mg g⁻¹ with an efficiency of 88.2% compared to just about 15 mg g⁻¹ using the untreated biosorbent when the target sample was real wastewater released from the electroplating industry. A substantial difference was attributed to the increased surface area from 78.38 to 150.82 m² g⁻¹, accompanied by an increased number of pores that serve as adsorption sites and the presence of oxygen-containing functional groups bind the target pollutant.

In conclusion, acid treatment is the most common modification technique for improving the efficacy of various biosorbents. Additionally, ultrasound and thermochemical treatments positively influence the performance of biosorbents. However, some treatment types might have a negative effect on the biosorbents' efficiency, such as using cross-linked beads. Such a conclusion could be supported or refuted by undertaking further research work.

Preparation of animal waste-based biosorbents

The industrial revolution, advanced medical care, overpopulation, economic growth, and welfare are all interrelated reasons behind the substantial food and animal consumption rates worldwide. Subsequently, it releases loads of animal waste into the environment, such as fish scales, crab shells, and chicken feathers. Therefore, it is essential to make the utmost use of these wastes by turning them into biosorbents and employing them in wastewater treatment.

In this regard, Ighalo and Eletta (2020) conducted experiments using biosorbents derived from fish scales to eliminate zinc and lead ions from aqueous solutions. Scaling scales involved a few simple steps, beginning with a thorough rinsing with water and then a detergent. Subsequently, the scales were mixed with nitric acid to remove metal oxides and other waste materials on the scales' surface and then washed with water. Lastly, the scales were oven-dried and ground into fine powder. The detected removal efficiencies for zinc and lead ions were 96.4% and 98.7%, respectively, as indicated in Table 3. Such a result was accredited to many adsorptive constituents, including esters and carboxylic acids.

Regarding applying the same sort of biosorbents in the remediation of sediments, Pal and Maiti (2020) investigated the adsorption of cadmium and lead using chemically, hydrothermally, and chemically hydrothermally biosorbents made from fish scales. The raw powder was prepared as mentioned above and then chemically modified using two different reagents, hydrochloric acid and sodium hydroxide, by simply mixing and stirring each one, followed by washing and drying. The powder was dissolved in deionized water for the hydrothermal treatment and heated for 3 h at 150 °C in a stainless-steel autoclave, followed by rinsing and oven drying. Furthermore, the raw powder was dissolved in hydrochloric acid instead of water and processed similarly to the hydrothermally treated biosorbent to produce the hydrothermally-acidic biosorbent. The observed efficiencies were 43.3%, 60.9%, 76.5, 77.4%, and 95.9% for cadmium ions using raw biosorbent, alkaline-treated, acid-treated, hydrothermally-treated, and hydrothermally-acidic treated biosorbents, respectively. While for lead ions, the obtained efficiencies were 51.2%, 65.3%, 78.8%, 83.3%, and 97.2% using the same order of biosorbents.

Continuing with the abovementioned study, the enhanced efficacies of all treated biosorbents indicated the positive effect of treatments in removing the inorganic and the organic materials blocking the active adsorption sites on the biosorbent surface. The chemical treatments were specifically responsible for blocking lipids and proteins, creating more pores, and increasing the surface area. Additionally, the hydrothermal treatment resulted in slightly better adsorption efficiencies attributed to the enhanced adsorption sites as a consequence of removing inorganic minerals from the biosorbent surface. As a result, it was expected that the combination of the acid and hydrothermal treatments would yield greater removal efficiencies for both metals.

Extracting several materials from biological waste materials and using them as biosorbents is another viable option by which a product with the added value could be produced from such waste. In this respect, Aziz et al. (2022) extracted hydroxyapatite from two different bio-waste materials, fish scales, and camel bones, and employed it to remove bisphenol A. Both scales and bones were firstly and separately processed using the abovementioned experimental procedures and then dissolved in hydrochloric acid, followed by adding sodium hydroxide solution while keeping the mixture heated and stirred for 12 h. Subsequently, white precipitates started settling out of the solution and were collected, washed, oven-dried, and ground. This heat treatment helped improve the porosity of both biosorbents allowing the bisphenol A molecules to get adsorbed on their surfaces. Therefore, efficient adsorption performance was detected with removal efficacies of 83.51% and 79.38% using scales-based and bone-based biosorbents, respectively.

Another class of animal waste materials that are released from the seafood industry, restaurants, and homes daily is crab shell waste. Crab shells contain various organic and inorganic constituents that help produce biosorbents with high adsorption efficacy. Therefore, many research studies were focused on investigating these waste materials, such as the one that targeted the adsorption of copper and lead using a crab shell-based biosorbent (*Cancer pagurus*) (Richards et al. 2019). The shells were rinsed with a surfactant, followed by water, and ground into fine powder. The observed removal efficacy of copper was 31%, while 18% was against zinc ions. The formation of coordination bonds between the metals and the amino acids and carboxyl functional groups on the biosorbent surface governed the removal of these ions. Moreover, the increased concentration of calcium ions released from the biosorbent surface into the solution indicated the ionic exchange mechanism. Also, it was concluded that chitin molecules, a major constituent of crab shells, acted as binding sites for the metal ions.

Concomitantly with the same biosorbents category, the removal of lead and zinc ions was targeted by the crab shells of *Clistoeloma sinensis* (Zhou et al. 2016). Four different

Table 3 Methods to prepare animal waste-based biosorbents

Preparation method	Feedstock material	Target pollutant	Removal%	References
Conventional preparation of biosorbents	Fish scales of <i>Micropogonias undulatus</i>	Zinc	96.4	Ighalo and Eletta (2020)
Alkaline treatment of animal waste-based biosorbent	Fish scales	Lead	98.7	Pal and Maiti (2020)
		Cadmium	60.9	
Acidic treatment of animal waste-based biosorbent		Lead	65.3	
		Cadmium	76.5	
Hydrothermal treatment of animal waste-based biosorbent		Lead	78.8	
		Cadmium	77.4	
Combined hydrothermal and acid treatments of animal waste-based biosorbent		Lead	83.3	
		Cadmium	95.9	
Thermal extraction of hydroxyapatite from animal waste materials	Fish scales	Bisphenol A	83.51	Aziz et al. (2022)
	Camel bones		79.38	
Conventional preparation of animal waste-based biosorbent	Untreated crab shells (<i>Cancer pagurus</i>)	Copper	31	Richards et al. (2019)
		Zinc	18	
Chemical modification of crab shells-based biosorbents	Fresh crab shells (<i>Clisto-coeloma sinensis</i>)	Lead	99.95	(2016)
		Zinc	99.72	
	Boiled crab shells (<i>Clisto-coeloma sinensis</i>)	Lead	99.90	
		Zinc	99.70	
	Deproteinized crab shells (<i>Clisto-coeloma sinensis</i>)	Lead	99.99	
		Zinc	99.89	
Demineralized crab shells (<i>Clisto-coeloma sinensis</i>)	Lead	10.17		
	Zinc	1.50		
Extraction of biopolymers from shrimp shell wastes	Shrimp shells	Copper	98.97	Mohanasrinivasan et al. (2014)
		Zinc	86.15	
		Ferrous iron	65.2	
		Hexavalent chromium	37.51	
Modification of chicken feathers-based biosorbent with graphene oxide nanoparticles	Chicken feathers	Nickel	99	Zubair et al. (2022)
		Cobalt	92	
		Lead	91	
		Cadmium	90	
		Zinc	90	
		Chromate	90	
		Selenium	99	
Arsenic	96			
Calcination of eggshell waste-based biosorbent	Eggshells	Yellow 28	93.2	Slimani et al. (2014)
Mechanical ball milling of eggshell waste-based biosorbent	Unmodified eggshells	Copper	91.36	Mohammad et al. (2022)
	Nano-sized eggshells		97.21	

Animal waste-based biosorbents can remove multiple pollutants, including zinc, lead, cadmium, bisphenol A, and others

biosorbents were prepared from the same material, including a fresh biosorbing sample that was prepared via rinsing with water and air drying. Additionally, a portion of this sample was then ground to prepare the boiled biosorbent. At the same time, to produce the deproteinized biosorbent, the powder was mixed and stirred with sodium hydroxide for six hours. Lastly, the demineralized biosorbent was prepared by mixing the boiled one with hydrochloric acid at average room temperature for 48 h. The obtained removal

efficiencies of lead ions were 99.95%, 99.90%, 99.99%, and 10.17% using the fresh, boiled, deproteinized, and demineralized biosorbents, respectively. At the same time, the efficiencies of these biosorbents in the same order against zinc ions were 99.72%, 99.70%, 99.89%, and 1.50%.

The abovementioned percentages indicated that the presence of minerals with a biosorbent structure is a quintessential factor in boosting the removal efficacy against both metals. The lowest effective biosorbent was the demineralized

one. The primary mechanism for lead adsorption was the precipitation of lead ions on the surface of the biosorbent as lead carbonate with the aid of the dissolved calcium carbonate from the shells. At the same time, the chelation of zinc ions with carbonyl and hydroxyl functional groups, along with the coordination between zinc and carbonate components of the crab shell, was considered the main removal mechanism.

Extracting biopolymers from shrimp shells is another sustainable route for preparing biosorbents such as chitosan, extracted from shrimp shell waste material and used as a biosorbent to remove heavy metal ions (Mohanasrinivasan et al. 2014). Firstly, the shrimp shells were demineralized using hydrochloric acid, followed by acid removal using water. The second step was producing chitin via deproteinization, which was conducted by mixing the demineralized shells with 5% sodium hydroxide for one day at 90 °C and then drying. Subsequently, the chitin was subjected to deacetylation to produce chitosan by mixing with a higher concentrated sodium hydroxide (70%) under stirring for three days. Lastly, the pH of the residual solid was neutralized by washing with water and then filtering, drying, and crushing. The detected removal efficiencies were 98.97%, 86.15%, 65.2%, and 37.51% for copper, zinc, ferrous iron, and hexavalent chromium ions, respectively. This result was accredited to the main role of polysaccharides existing in chitosan as active adsorption sites for these metal ionic species.

In line with the abovementioned technique, chicken feathers constitute another renewable, widely available, and sustainable source of biopolymers and proteins, such as keratin (Tsfaye et al. 2017). Accordingly, a recent study used keratin to produce an efficient nano-biosorbent by modifying it using graphene oxide nanoparticles to remove several cationic and anionic heavy metals with efficacies of more than 90% (Zubair et al. 2022). The feathers were pretreated in a similar procedure to other types of biosorbents. Then they were stirred with ethylenediamine tetra-acetic acid, urea, tris-base, and sodium sulfite at 90 °C for two days. Subsequently, they were sonicated for half an hour to extract keratin. Secondly, keratin was precipitated with hydrochloric acid and mixed with graphene oxide, and then the precipitate was centrifuged, rinsed, dried, and ground into a fine powder biosorbent. Keratin has high stability due to its crosslinking structure, so many functional groups in its internal structure and side chains are unavailable for adsorbing pollutants. Consequently, they became more exposed and exfoliated upon modification by graphene oxide, which was in line with the substantial increase in the surface area of the modified biosorbent ($19.50 \text{ m}^2 \text{ g}^{-1}$) compared to the unmodified one ($1.06 \text{ m}^2 \text{ g}^{-1}$). Thus, the observed removal efficacies against both anionic and cationic metals were higher than 90%, as indicated in Table 3, whereas the efficacies of the unmodified one ranged from 20 to 70%.

Eggshell wastes are commonly produced in most of the world's countries regardless of their economic well-being. They represent another green, facile, and cost-effective biosorbent material, whether prepared in a pristine or modified form. Therefore, such a kind of waste material always attracts researchers' interest, such as Slimani et al. (2014), who examined the adsorption efficacy of physically treated egg shells by calcination in removing basic yellow 28 dye with an efficiency of 93.2%. The raw biosorbent was prepared by the same conventional experimental procedures used for most biosorbents, including washing, drying, and grinding. In contrast, the calcined biosorbent was prepared by heating the ground powder for two hours at 900 °C. The adsorption mechanism was found to be governed by van der Waals along with dipole forces by observing that the adsorption capacity decreased from 9 mg g^{-1} at 15 °C to 5 mg g^{-1} at 45 °C.

Mechanical ball milling is a commonly used technique for preparing various nanomaterials and nano-biosorbents. Mohammad et al. (2022) in preparing an eggshell-based biosorbent to remove toxic copper ions from water. The raw biosorbent material was prepared similarly to the previously mentioned biosorbents. In contrast, for the nano-biosorbent, the raw biosorbent powder was crushed into nano-sized powder using a ball milling machine. Although the obtained removal efficiencies were primarily comparable, as they were 91.36% and 97.21% for the raw and the mechanically treated biosorbents, respectively, the removal rate of the latter was about 17 times faster than the former. The main reason behind that difference was the high surface area of the modified biosorbent ($21.2 \text{ m}^2 \text{ g}^{-1}$) which was 1.6 times higher than the unmodified powder. The major driving force of biosorption was the electrostatic attraction between positive copper ions and negative biosorbent particles at an almost neutral pH (6).

This section summarizes the preparation methods of different biosorbents using various source materials, including wooden, bacterial, algal, and herbaceous materials. Additionally, agricultural wastes, fungi, and forest waste materials, as well as animal wastes (e.g., fish scales, camel bones, crab and shrimp shells, eggshells, and chicken feathers), as shown in Fig. 3, could be employed in the adsorption of several organic and inorganic pollutants. Such a fact is based on their availability worldwide, eco-friendliness, low cost, facile modification, and high adsorption efficacy. As shown in Fig. 4, numerous modification techniques could be applied to enhance the performance of biosorbents, and they are mainly categorized into chemical, physical, and mechanical techniques. Therefore, the main target of biosorbent preparation is two-fold: first, to use the unwanted biological waste materials that always end up being released into the environment and polluting water systems. The

Fig. 3 Categorization of common biosorbent materials. Biosorbent materials can be broadly categorized into woody and herbaceous-based biosorbents, crop residue and biomass-based biosorbents, and animal waste-based biosorbents. Examples of animal waste-based biosorbents include fish scales, eggshells, and chicken feathers. Among bacteria-based biosorbents, commercial dry baker's yeast (*Saccharomyces cerevisiae*) and blue-green algae-based biosorbents are commonly used. Biosorbents from agricultural waste, such as fruit peels, sugarcane bagasse, and corn husk, are also widely used

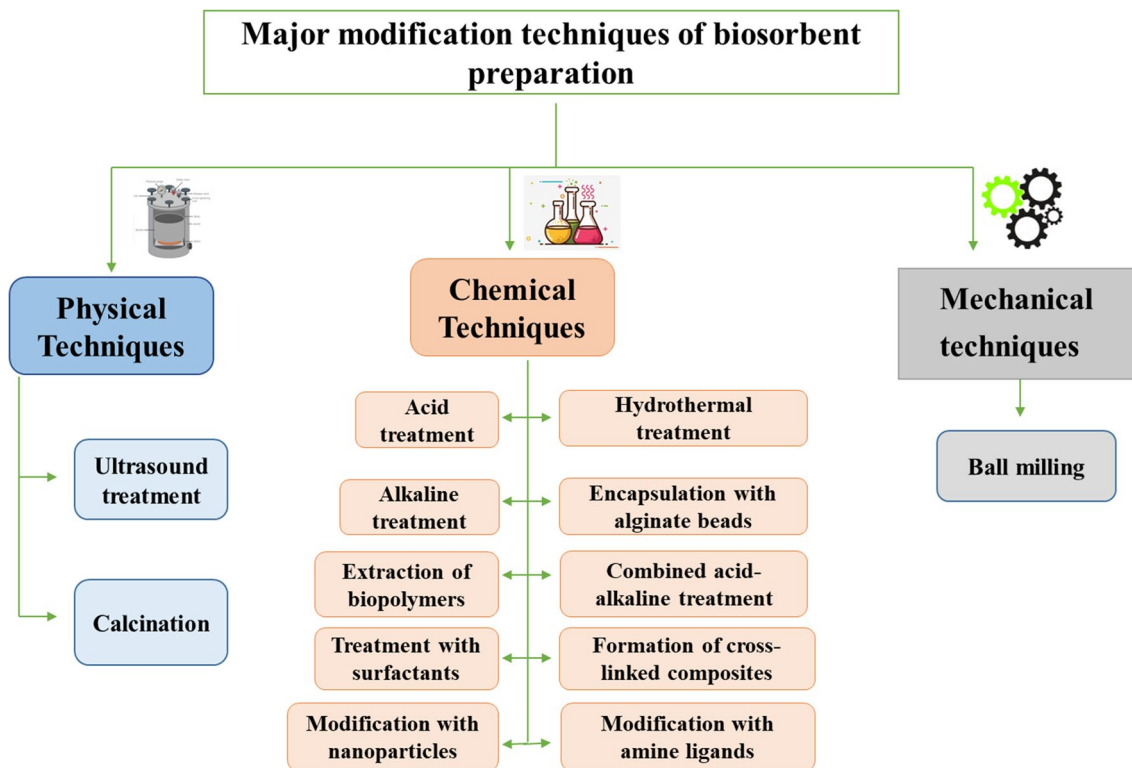
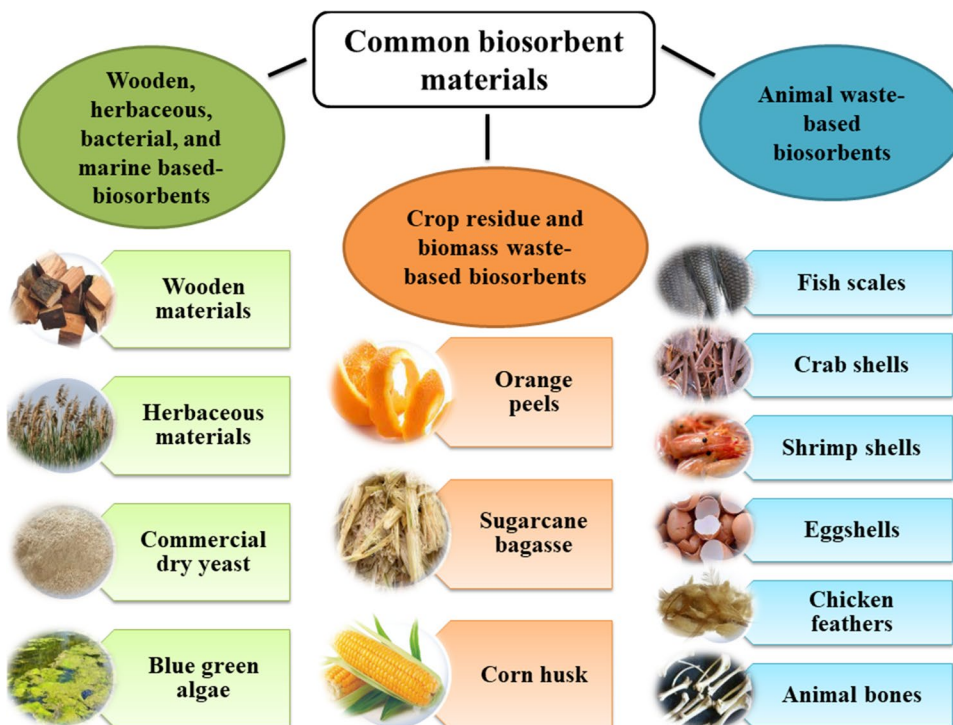


Fig. 4 Classification of major modification techniques of biosorbents' preparation. Mechanical techniques such as ball milling are used—physical techniques involving ultrasound treatment and calcination.

Chemical techniques include acid treatment, alkaline treatment, treatment with surfactants, and others. A combination of multiple treatment types is also applied in biosorbents' preparation

second target is to advocate circular economy principles and sustainable development by using pollutants (i.e., biosorbents) to remove other pollutants.

Methods to prepare magnetic sorbents

Due to magnetic sorbents' outstanding properties, sustained studies have been executed to foster their preparation approaches. Notably, the preparation method mainly controls the magnetic sorbents' shape, morphology, magnetic property, and particle size. Generally, the most applied approaches to synthesizing magnetic sorbents are coprecipitation, hydrothermal, thermal decomposition, polyol, microwave, sol–gel, and micro-emulsion, as revealed in Table 4 and Fig. 5.

Coprecipitation approach

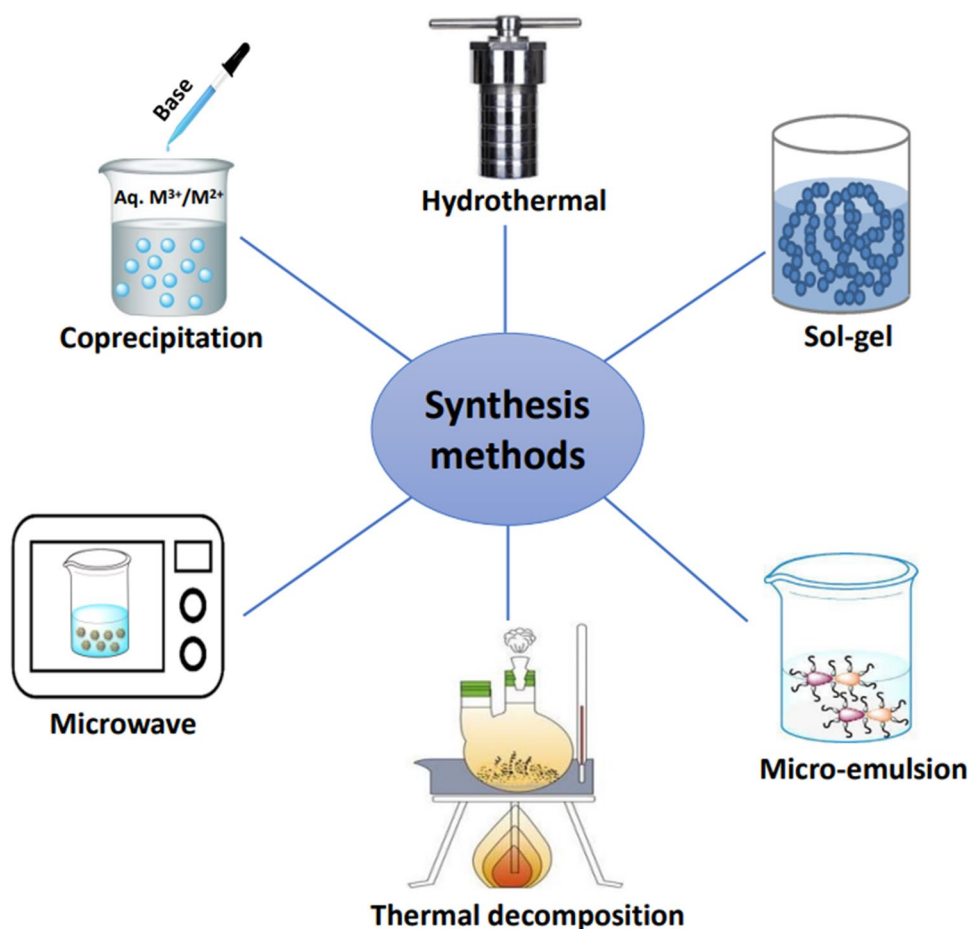
Coprecipitation is one of the most straightforward conventional approaches that is widely utilized for fabricating magnetic sorbents. Typically, the approach is proceeded by mixing a divalent metal ions (M^{2+}) precursor with a trivalent metal ions precursor (M^{3+}) in fundamental conditions. Furthermore, the fabricated magnetic sorbents by the coprecipitation approach could be easily functionalized by adding functional substances to the reaction mixture. Notably, the magnetic nature, structure, particle size, and morphology of the synthesized magnetic sorbents by coprecipitation are controlled by some key parameters, including the type of metal salts, M^{2+}/M^{3+} ratio, and the process temperature and pH (Wu et al. 2008). Also, the precipitating agent type impacts the magnetic sorbent specifications since the crystallinity and magnetic saturation of the fabricated particles by ammonium hydroxide are higher than those prepared by

Table 4 Preparation approaches of magnetic sorbents

Preparation method	Controlling parameters	Advantage	Disadvantage
Coprecipitation	Type of metal salts M^{2+}/M^{3+} ratio Temperature pH Precipitating agent	Simplicity Easy-functionalization Eco-friendly solvent High yield Short reaction time	Lack of particles uniformity Low reproducibility
Hydrothermal	Reaction temperature Reaction pressure Precursor concentration Reaction time	Synthesis in water Excellent magnetic property High surface area Narrow size distribution High product purity	Slow kinetic rate High temperature and pressure
Micro-emulsion	Oil/water ratio	High magnetic property Small particles' size	Large amounts of emulsifier Low yield High cost
Thermal decomposition	The precursor: surfactant: solvent ratio Annealing temperature Reaction time	Narrow size distribution Size and shape control Good magnetic property High crystallinity	High temperature and pressure Safety issues of the reactants Solubility in organic solvents
Polyol	Precursor concentration Reaction temperature	Excellent magnetic property Application in hyperthermia Special morphology High crystallinity	Production of elemental metals Poly-dispersed particle size
Microwave-assisted pyrolysis	Microwave power Radiation time	Superb adsorption property High surface area High total pores volume Rapid crystallization	Needs specific apparatus
Chemical reduction	Reducing agent type Precursor concentration	Simple Safe Easy to be performed in the laboratory Proceeding at room temperature	Oxidation probability of magnetic metal sorbents
Arc discharge	Temperature Power supply Pressure Electrode geometry	Efficient Cheap Eco-friendly Nontoxic	Low efficiency Difficulty in size controlling Limited in industry

The controlling parameters of the preparation approaches of magnetic sorbents are listed. The advantages and disadvantages of different preparation methods are clarified. M^{2+}/M^{3+} is divalent metal ions precursor/trivalent metal ions precursor ratios

Fig. 5 Preparation approaches of magnetic sorbents. Magnetic sorbents could be prepared via coprecipitation using a precipitating agent. Further, the sol–gel method is a popular method for preparing magnetic sorbents. Heating in a reactor (hydrothermal process), microwave-assisted process, or direct thermal decomposition could be used to prepare magnetic sorbents. Other methods, such as micro-emulsion, could also prepare magnetic sorbents. M^{3+} and M^{2+} refer to the metal valences



sodium hydroxide (Faraji et al. 2010). Coprecipitation possesses remarkable merits, such as producing a high yield, having a short reaction time, and utilizing water as an eco-friendly solvent.

On the other hand, a high base condition is one of the demerits of the coprecipitation method since such conditions decrease the uniformity of the produced magnetic particles. In addition, the low reproducibility is another disadvantage of the coprecipitation method (Husnain et al. 2017). The coprecipitation method is a simple, efficient, economical procedure for producing magnetic sorbents but lacks uniformity and reproducibility.

Hydrothermal approach

Hydrothermal is an approach for fabricating magnetic sorbents by chemical reactions in an autoclave. Hydrothermal needs specific conditions such as elevated temperature ranging from 150 to 200 °C and high pressure reaching 2000 psi (Lv et al. 2009). Noteworthy, the saturation magnetization of magnetic sorbents could be enhanced by adjusting the reaction temperature (Attallah et al. 2016). In addition, elevated temperature leads to fast nucleation

and growth, resulting in the fabrication of small particles, which increase the surface area and the adsorption efficacy of the magnetic sorbents. Whereas the generated high pressure in the reactor could reduce the volatilization of the reactants as well as improve the purity of the produced particles (Sari et al. 2018).

Furthermore, the metal salt precursors significantly influence the size and morphology of the fabricated magnetic substances. Interestingly, the synthesized magnetic materials via the hydrothermal method have higher crystallinity and narrower size distribution than those manufactured by the other preparation approaches. The long hydrothermal time increases the size of the magnetic particles, while the short time produces uniform particles ranging from 10 to 50 nm (Xu and Teja 2008). Nevertheless, the hydrothermal approach has shortcomings, such as a slow reaction rate and high temperature and pressure requirements (Eltaweil et al. 2022b). In brief, the hydrothermal method needs high temperature and pressure, and it overcomes the metal salt effect on the produced size and morphology. Still, the reaction time should be well-adjusted to control the particle size.

Thermal decomposition approach

Thermal decomposition is one of the popular approaches for preparing monodispersed magnetic sorbents via the decomposition of organometallic precursors in boiling organic liquids (Duan et al. 2015). The size and morphology of produced magnetic particles by the thermal decomposition method depend on the ratio between metal precursor, surfactant, and solvent, in addition to the domination of the other factors, such as annealing temperature and reaction time on the structural and magnetically nature of the fabricated magnetic substances by thermal decomposition method (Patsula et al. 2016). However, thermal decomposition suffers the safety issue since it requires harsh conditions like boiling organic liquids at elevated temperatures and using vapor phases without air. Nevertheless, how metal oxides can be synthesized without oxygen is still questionable. Pioneering studies pointed out that the protons of water could oxidize the formed metal hydroxide to metal oxide (Gul et al. 2019). It could be concluded that thermal decomposition suffers extreme operating conditions; moreover, the produced magnetic particles' size and morphology depend on metal precursor ratios, surfactant, and solvent.

Microwave-assisted pyrolysis approach

Microwave-assisted pyrolysis involves using heat to shorten the preparation time, yield a high product, and enhance the adsorption property (Abdel Maksoud et al. 2021). Such an approach could heat the prepared substances without transferring the heat throughout the furnace, saving time and energy (López-Quintela et al. 2004). Notably, the characteristics of the fabricated magnetic adsorbents via microwave-assisted pyrolysis are controlled by the power of the microwave and the radiation time. The surface area of magnetic adsorbents can be ameliorated by raising the power of the microwave owing to the increase in the quantity of volatile matter (Vidal-Vidal et al. 2006). Furthermore, the increment in the radiation time and microwave power increase the pores' volume, enlarging the micro-pores, decreasing the micro-pores number, and increasing the total pores' volume (Chin and Yaacob 2007). More importantly, the microwave-assisted pyrolysis method has an advantage over the other preparation approaches, which is rapid crystallization since the microwave provides central heating to the reaction solution.

Chemical reduction approach

Chemical reduction is the simplest solution-phase approach to fabricating magnetic adsorbents, especially metal nanoparticles (Eltaweil et al. 2020). The process proceeds as follows; simple reduction to the metal precursor by reducing

agent at room temperature. Chemical reduction distinguishes by its safety, simplicity, and ease of being performed in the laboratory (El-Monaem et al. 2021, 2022). Nevertheless, the metals could be oxidized during the fabrication via chemical reduction, which is the major disadvantage of this approach. To overcome this limitation, adjusting the ratio between metal precursor and reducing agent, utilizing freshly prepared reducing agent, performing the process quickly, and washing the fabricated metal particles well with an ethanolic solution is essential.

Polyol approach

Polyol is a liquid phase approach that proceeds by the divalent metal ions precursor (M^{2+})/trivalent metal ions precursor (M^{3+}) oxidative alkaline hydrolysis in a polyol solvent. Although the particle size of the produced magnetic substances by the polyol method is poly-dispersed, the magnetism of the particles is pretty high. In addition, their unique morphology, "flower-like structure", renders them suitable for performed applications at high temperatures (Hugouenq et al. 2012). Interestingly, the increment in the precursors' concentration increases the particle size. Furthermore, the crystallinity of the particles is controlled by raising the reaction temperature (Yang et al. 2014). Advanced heating sources like ultrasonic and microwaves have revealed great results in the polyol process. However, the preparation of metal oxides by the polyol method is limited due to the production of elemental metals (Wee et al. 2017). Overall, the polyol method is a liquid-phase approach that can produce magnetic substances with high magnetism and a unique flower-like structure suitable for high-temperature applications. However, the method's limitations in producing metal oxides due to the production of elemental metals must be considered.

Micro-emulsion approach

Micro-emulsion method involves the fabrication of magnetic sorbents via the precipitation in an oil/water medium. Notably, the oil/water ratio could adjust the micro-emulsion medium since oil acts as a surfactant and water is a co-solvent. Micro-emulsion produces magnetic substances with unique advantages such as relatively small particles' size, uniformity, and superior magnetic property. Nonetheless, there is a restriction to applying the micro-emulsion approach in the laboratory owing to its low yield, high cost, and the need for large quantities of emulsifiers (Liu et al. 2020b). In conclusion, the micro-emulsion method is promising for producing magnetic sorbents with small particle sizes, uniformity, and superior magnetic properties. Still, its limited yield, high cost, and high emulsifier requirements restrict its applicability in the laboratory.

Arc discharge approach

The arc discharge is a common approach for preparing magnetic sorbent encapsulated into a carbon layer. The arc discharge is executed by placing the metal precursor into the cavities of the graphite electrode, and then arc discharge is applied to evaporate the solvents of the precursor (Ansari et al. 2022). The quality and quantity of the yielded magnetic sorbent by arc discharge are controlled by the process temperature, power supply, applied pressure, and electrode geometry (Arora and Sharma 2014). The arc discharge method possesses economic and environmental merits; efficient, cheap, eco-friendly, and nontoxic (Aljohani et al. 2021). However, this approach cannot be applied in the industry since controlling the magnetic particle size is impossible. Excessive studies have focused on overcoming this bottleneck to exploit the unique advantage of arc discharge.

Other preparation methods to prepare cost-effective sorbents

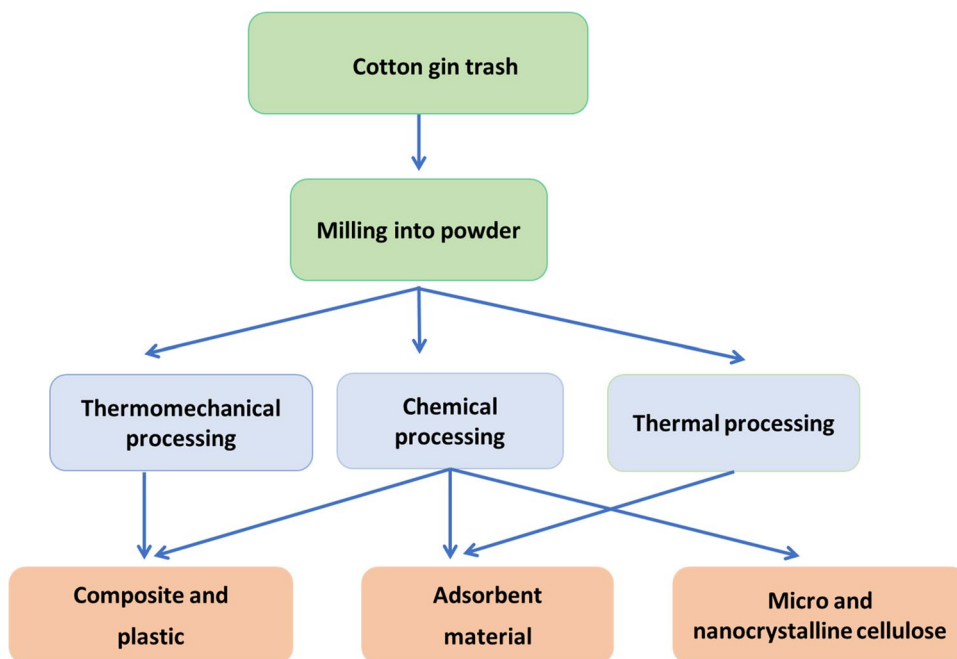
Nowadays, cost-effective sorbents prepared from industrial wastes have drawn particular attention due to their abundant resources, low cost, and excellent adsorption efficiency. Many industrial wastes that cost nothing have exhibited an auspicious adsorption behavior toward various contaminants. Interestingly, most of these industrial wastes could be used as sorbents after a simple treatment via cleaning with water and acid like dolochar, bagasse fly ash, and others.

While there are wastes that need some processing before use as sorbents, as follows.

Cost-effective sorbents-derived cotton gin trash

Figure 6 represents the pretreatment approaches of cotton gin trash for material fabrication. Raw cotton gin trash consists of many fractions like sticks, leaf parts, and motes, so the first step involves milling these fractions to a powder (Haque et al. 2020). The milled cotton gin trash could also easily interact with chemicals such as solvents, polymers, and others, facilitating its surface modification. Then, the size of the milled cotton gin trash could be reduced by "mechanical processing", in which the speed of the shaft and impellers is relatively high in the presence of water as a solvent to form a slurry (Chranioti et al. 2016). Interestingly, the drying step impacts the morphology of the fabricated cotton gin trash since the produced cotton gin trash powders by spray drying are more spherical than those dried in an oven (Haque et al. 2021). Next, after the mechanical processing, "chemical processing" is sometimes conducted to facilitate the cotton gin trash properties. For example, the hydrophilicity of cotton gin trash could be improved by succinylation, while acetylation is performed to enhance cotton gin trash hydrophobicity. In addition, the mechanical strength of cotton gin trash is reinforced by polyvinyl alcohol. Also, "thermal processing" could be carried out to diminish the moisture content in cotton gin trash powder and increase the interaction with polymers. Notably, the thermal processing could be performed at low temperatures (50 °C) or high temperatures (150 °C), taking into consideration

Fig. 6 Cotton gin trash consists of fractions like sticks, leaf parts, and motes. These parts should be milled into powder. Thermal processing is used to eliminate moisture content in cotton gin trash powder. Milled cotton gin trash is treated with chemicals through a chemical modification process. Polyvinyl alcohol could be used to enforce cotton gin trash mechanical strength



reduces the treatment time at high temperatures and vice versa (Holt et al. 2012; Sutivisedsak et al. 2012). In summary, various pretreatment methods, including milling, chemical and mechanical processing, drying, and thermal processing, can convert raw cotton gin trash into material suitable for fabrication.

Cost-effective sorbents-derived red mud

Red mud is a rich resource for fabricating efficient adsorbents, but it needs excessive neutralization to reduce its dangerous environmental effects. Several neutralization or activation routes have been adopted to fabricate a cost-effective sorbents-based red mud, as clarified in Fig. 7.

Seawater neutralization is a simple and popular route for red mud neutralization. This approach exploits the soluble ions into seawater (mainly calcium and magnesium) to neutralize the red mud via the precipitations of the hydrotalcite compounds and carbonate and hydroxide minerals (Kannan et al. 2021). The increase in the washing of red mud by seawater increases its surface area, reaching $31 \text{ m}^2 \text{ g}^{-1}$, and decreases pH to ~ 8.5 (Rai et al. 2013). In brief, seawater neutralization is an effective and straightforward method for neutralizing red mud using soluble ions present in seawater.

Combined treatment involves the enhancement of the adsorbability of red mud via a series of treatment routes. For instance, in the first stage, red mud is treated by seawater (Bauxsol™), and the second stage involves the combined acid-thermal treatment of Bauxsol™. Finally, sulfate salts of ferric and aluminum are used for further treatment of Bauxsol™ (Taneez and Hurel 2019). It was found that the combined treatment route significantly enhances the surface area of red mud, reaching about $130 \text{ m}^2 \text{ g}^{-1}$ (Sahu et al. 2013). It could be concluded that the combined treatment

route can significantly increase the surface area of red mud through a series of treatment routes involving seawater, acid-thermal treatment, and sulfate salts of ferric and aluminum.

Thermal activation means the treatment of red mud at an elevated temperature ranging from 200 to 1000 °C for a pyrolysis time in the range of 1–3 h. The X-ray diffraction analysis revealed hematite, bayerite, gibbsite, sodalite, quartz, calcite, and titanium dioxide crystalline phases. In addition, the crystallinity of hematite enhanced with the raising in pyrolysis temperature above 600 °C. Moreover, the surface area of the red mud improved at 500 °C, which is most likely due to the water exclusion. Nonetheless, the adsorption performance declined when the pyrolysis temperature exceeded 700 °C (Smiljanić et al. 2011; Taneez and Hurel 2019). To summarize, the thermal activation of red mud at elevated temperatures can lead to the formation of various crystalline phases and an increase in the surface area of red mud. Still, the adsorption performance is negatively impacted at temperatures above 700 °C.

Acid treatment includes neutralizing red mud with acids such as sulphuric, nitric, and hydrochloric acid to remove the alkali salts and inorganic and organic impurities. The acid neutralization of red mud can be executed via two approaches; the first is simple treatment by acid (0.1–1.0 M), followed by washing with distilled water and drying at 100 °C. At the same time, the second approach involves the reflux of red mud in an acidic solution for 1–2 h and then precipitating the red mud in an ammonia solution. Finally, the precipitated red mud was washed with distilled water and dried at 100 °C (Joseph et al. 2019; Qi 2021). Generally, acid treatment is an effective method to remove impurities from red mud. There are two approaches to achieving acid neutralization, the simple treatment and reflux method, followed by washing and drying.

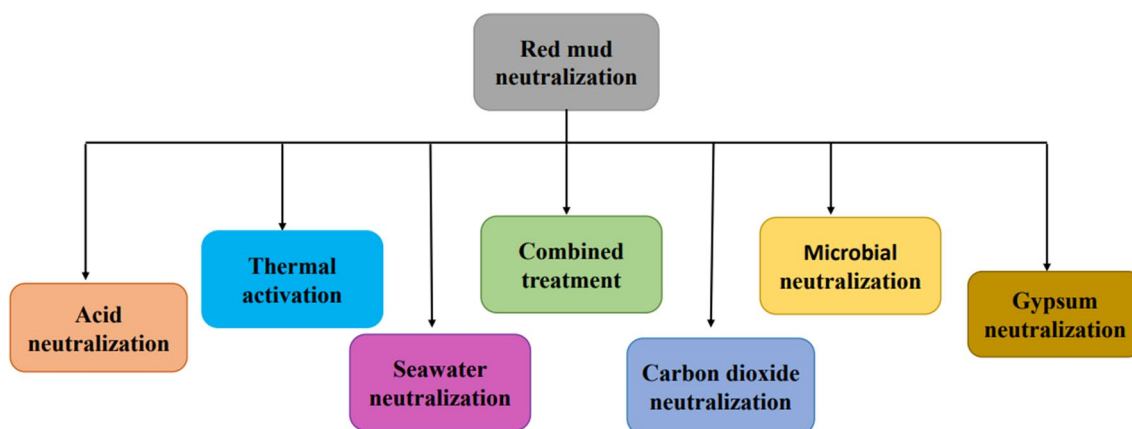


Fig. 7 Treatment approaches to fabricate cost-effective sorbents-derived red mud. Red mud is a good resource for the efficient adsorbent. Red mud needs excessive treatment to make it safe for use. Acid, microbial, gypsum, carbon dioxide, and seawater neutraliza-

tions could be employed for red mud before use. Thermal activation below 700 °C can lead to a higher crystallinity and an increase in the surface area of red mud

Adsorbent classifications and their wastewater treatment applications

The sorption application and uptake efficiency are often a function of a given adsorbent's class and physicochemical features. Accordingly, these adsorbents vary in selectivity, adsorption capacity, shelf life, and synthesis cost (Syeda and Yap 2022). Also, there are obvious distinctions in their respective active surface, pore diameters, quality of pore distribution, and surface functional groups. The following subsection discusses applying an array of adsorbents in the adsorption of varying pollutants. The different adsorbents used in wastewater treatment were broadly classified as activated carbon, biochars, lignocellulosic biomass, clay minerals, silica, zeolite, and peat and humic soil (Chen et al. 2019b; Osman et al. 2020b, 2022b).

Similarly, the common pollutants encountered in wastewater treatment were also classified. Figure 8 presents the different classes of adsorbents and pollutants considered in this review. The applicational benefits and drawbacks of the different adsorbent classes considered in this review are outlined in Table 5.

Activated carbon adsorbents

Activated carbons are porous carbon materials produced by carbonizing chemically dehydrated carbonaceous materials

or by oxidizing chars (Heidarinejad et al. 2020). Both fossil and renewable carbonaceous materials serve as activated carbon precursors. Other non-conventional activated carbon precursors, such as ionic liquids (Zhang et al. 2014a), organic salts (Xu et al. 2012), and deep eutectic solvents (Iwanow et al. 2017, 2020) still exist. To obtain high-quality and low-cost activated carbon adsorbents, non-fossil and renewable materials with high carbon and volatile components and low ash content are recommended. However, coal-based activated carbons exhibit superior mechanical properties to those from lignocellulosic materials.

Dyes are one of the most typical aquatic pollutants successfully adsorbed using activated carbon and are often classified following their chemical structure and industrial application (Liu et al. 2022b). The adsorption of different classes of dye, including cationic (Ahmed 2016; Corda and Kini 2018), dispersed (Mittal et al. 2022; Shukla and Dhiman 2017), reactive (Giannakoudakis et al. 2016; Silva et al. 2016), direct (Ho 2020; Imran et al. 2012), vat (Ho 2020; Nagy 2018), and acid (Biglari 2017; Naraghi et al. 2017) dyes onto activated carbon have been extensively studied. However, it was noted that irrespective of the dye class, efficient adsorption is always a function of high surface area. The larger the surface area, the more available active sites for binding dye molecules. The weak adsorptive interaction between the π -electrons of the activated carbon basal planes and the loose electrons of the aromatic rings of the dye molecule also accounts for the efficient dye adsorption

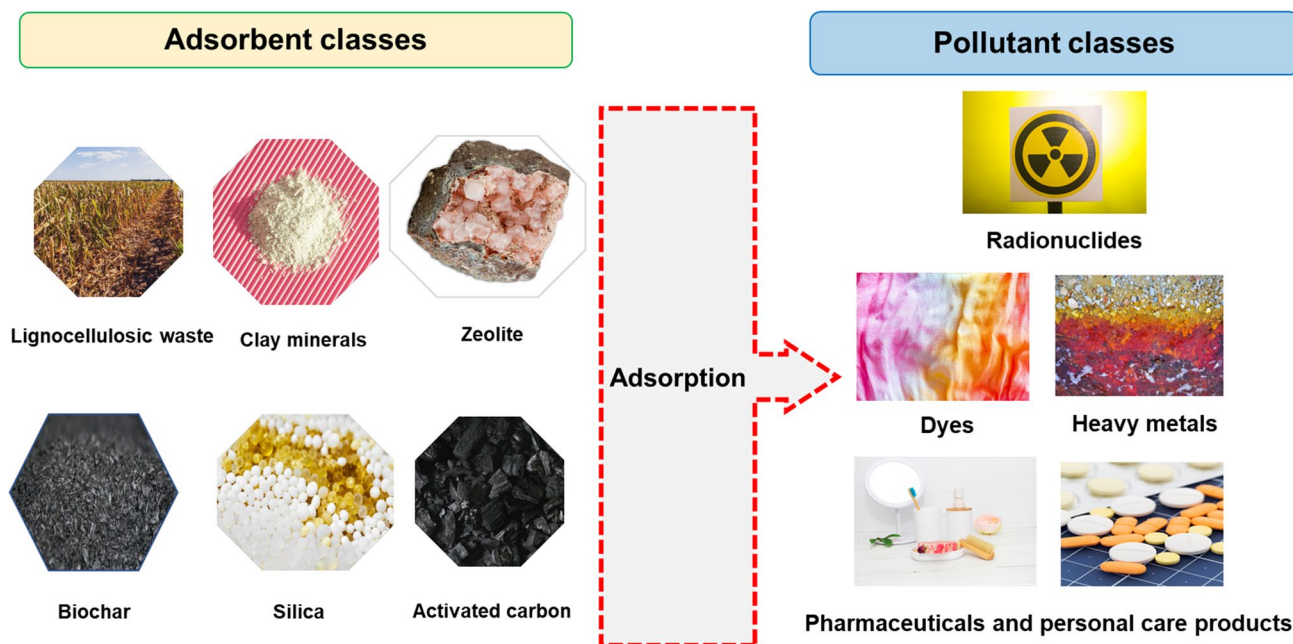


Fig. 8 Broad classification of adsorbents and pollutants. The adsorption capacity and ultimate success of the adsorption process depend on the degree of adsorbent-adsorbate compatibility. The respective

physicochemical properties and the structural/ionic composition of the adsorbent are significant for establishing the desired adsorbent-adsorbate affinity

Table 5 Benefits and drawbacks of adsorbent classes in wastewater treatment processes

Adsorbent class	Application in water treatment		References
	Benefits	Drawbacks	
Activated carbon	<p>Activated carbon is readily sourced from local precursors</p> <p>Due to their high porosity and surface area, activated carbons are highly effective</p> <p>Activated carbon is very suitable for batch conditions</p> <p>They are efficient in adsorbing a wide variety of contaminants</p> <p>They are readily recyclable</p> <p>In most cases, the spent activated carbon is not hazardous</p> <p>They are eco-friendly adsorbents</p> <p>The feedstock is highly available, and the cost of production is low</p> <p>Spent biochar is readily and cheaply recyclable</p> <p>The specific surface area which aids efficient pollutant adsorption is high</p> <p>They are efficient for the adsorption of organic and inorganic species from wastewater</p> <p>They have abundant functional groups for efficient adsorption</p>	<p>Not suitable for adsorbing low molecular weight pollutants, water streams with high solids, oil, and grease</p> <p>Activated carbon as a standalone operation cannot produce treated water of high purity</p> <p>Spent adsorbent disposal is challenging</p>	<p>Ling et al. (2019) and Thompson et al. (2016)</p>
Biochar	<p>They are eco-friendly adsorbents</p> <p>The feedstock is highly available, and the cost of production is low</p> <p>Spent biochar is readily and cheaply recyclable</p> <p>The specific surface area which aids efficient pollutant adsorption is high</p> <p>They are efficient for the adsorption of organic and inorganic species from wastewater</p> <p>They have abundant functional groups for efficient adsorption</p>	<p>Biochar, as an adsorbent, is highly pH sensitive</p> <p>The cost of system maintenance can be relatively high</p> <p>The process efficiency continuously decreases with usage; hence continuous regeneration or desorption may be needed for prolonged use</p> <p>Their small particle size and low density make separating from treated water difficult</p>	<p>Marciniczyk et al. (2022), Srivatsav et al. (2020) and Tan et al. (2016)</p>
Lignocellulosic wastes	<p>Being generated from agro-wastes, they are natural, efficient, and of low production cost</p> <p>Their adsorptive application promotes waste-to-wealth initiatives</p> <p>They have good regenerative potential</p> <p>Easy to prepare and have a good surface structure for effective adsorption</p> <p>Excellent for heavy metals</p>	<p>Mostly need modification to improve the adsorption capacity</p>	<p>Çelebi (2020), Maia et al. (2021) and Nindjio et al. (2022)</p>
Clay and clay minerals	<p>They are inexpensive, as they mainly occur naturally</p> <p>They are eco-friendly and non-toxic</p> <p>They have a high surface area and large ionic exchange propensity</p>	<p>They are usually of low adsorption capacity, therefore, need modification for effective adsorption</p> <p>The regeneration of spent clay minerals is complex</p> <p>It is always tricky separating the adsorbent-adsorbate mixture after adsorption</p>	<p>Jadhav and Jadhav (2021) and Uddin (2017)</p>
Silica	<p>Exhibit high adsorption capacity at low temperatures</p> <p>It has high porosity suitable for the efficient adsorption of macromolecular species</p> <p>It is non-toxic and adequate as packings in column adsorption</p> <p>They are not pH sensitive</p>	<p>Relatively expensive</p> <p>Not readily recyclable</p> <p>Exhibit low adsorption capacity compared with other conventional adsorbents</p>	<p>Hamad and Idrus (2022)</p>

Table 5 (continued)

Adsorbent class	Application in water treatment		References
	Benefits	Drawbacks	
Zeolite	<p>Zeolite has very high selectivity for specific pollutants</p> <p>They are suitable for the adsorption of some trace pollutants due to their cage-like surface structure</p> <p>They have high uptake capacity, with hydrothermal stability</p>	<p>Due to the high selectivity index, the adsorption capacity of zeolite is often limited</p> <p>There is always a high blockage risk during column operations due to the microporous structure of zeolites</p>	Alver and Metin (2012) and Zhou et al. (2023)
Peats and humic soil	<p>Spent zeolites are easy to replace</p> <p>Peats have high adsorption capacity and improved surface area and porosity</p> <p>They are considered non-toxic and eco-friendly</p> <p>They have high selectivity index and strong cation exchange capacity</p>	Peats have low mechanical strength	Crini et al. (2019a), Hamad and Idrus (2022) and Younas et al. (2021)

The specific characteristics of the various adsorbents in relation to their ability to selectively adsorb certain substances, their capacity for adsorption, longevity, and affordability are determined by factors such as the type of precursor material, the physicochemical properties of the adsorbent, the treatment method used, and the properties of the adsorbate

(Chatterjee et al. 2005; Giannakoudakis et al. 2016). Thus, efficient adsorption of dye molecules onto activated carbon is significantly influenced by the surface area present for physisorption and active sites for chemisorption.

Lead (Largitte et al. 2016; Shi et al. 2018), chromium (Ugwu and Agunwamba 2020; Yang et al. 2015), copper (Natrayan et al. 2022; Ugwu and Agunwamba 2020), zinc (Tuomikoski et al. 2019; Ugwu and Agunwamba 2020), cobalt (Kakavandi et al. 2018; Peres et al. 2018), manganese (Tran et al. 2018), iron (Goher et al. 2015), and arsenic (Yin et al. 2019) have been reportedly adsorbed using activated carbon. However, for improved adsorption efficiency, the adsorbate solution pH, the activated carbon surface charge, textural characteristics, and surface chemistry should be considered (Li et al. 2010; Liu et al. 2022c). It was noted that when the activated carbon surface is composed mainly of alkaline/basic groups, the point of zero charges (pH_{pzc}) value is expected to be higher than pH 7.0. In such a situation, electrostatic interaction and exchange of ions between the negative activated carbon surface groups, π -electrons of the activated carbon, and the heavy metal cations are realized at the acidic pH ranges (Aniagor et al. 2022). Similarly, in the presence of abundant acidic surface groups, the pH_{pzc} is less than pH 7.0, and efficient cation adsorption via an electrostatic interaction mechanism is achieved when the solution pH tends to the alkaline pH ranges (Hashem et al. 2021b). Also, the issue of ionic speciation and precipitation strongly affects the effective adsorption of heavy metals, and to circumvent such a limitation, the appropriate solution pH must be adopted. In conclusion, the heavy metals' adsorption onto activated carbon is a function of the adsorbents' surface area, pore volume, and the number of surface groups.

The effectiveness of activated carbon for adsorbing different pharmaceuticals and personal care products (PPCPs) (Bursztyn Fuentes et al. 2022; El Naga et al. 2019; García-Rosero et al. 2022; Kim et al. 2022) and other emerging pollutants (Ahn et al. 2022; Moreno-Marenco et al. 2020) have been documented. The adsorption generally occurs via pore-filling/size exclusion, hydrogen bonding, π - π electro-donor acceptor, electrostatic interactions, and hydrophobic interaction mechanism (Ahn et al. 2022; Liu et al. 2022a; Pamphile et al. 2019). Accordingly, the pore-filling mechanism is a function of the adsorbate's molecular size and the adsorbent pore properties (Moreno-Marenco et al. 2020). Aside from the pore-filling, all the mechanisms mentioned above are controlled by the activated carbon's surface charge, acid dissociation constant (pKa) of the organic pollutants, and pH variation within the bulk adsorbate phase (Kim et al. 2022). During the comparative adsorption of caffeine, ibuprofen, and triclosan, due to the size exclusion mechanism, a higher adsorption capacity was recorded when there is a high correlation between the molecular size of the adsorbate and pore diameter of the activated carbon (Kaur et al. 2018).

Furthermore, El Naga et al. (2019) noted that the phenolic and carboxylic acid groups on the activated carbon, respectively, donated hydrogen bonds to the oxygen atoms in diclofenac molecules up to $\text{pH} \sim 10$ and $\text{pH} \sim 4.9$, hence the improved uptake via hydrogen bonding. Also, strong electron acceptor groups like the chlorine atoms in most PPCPs and other emerging organic pollutants lower the π -electron density on their respective phenyl ring, thus improving π - π interactions with the activated carbon surface (El Naga et al. 2019). Therefore, the sorption efficiency of the PPCPs and other emerging organic pollutants on activated carbons depends on the solution pH, the adsorbate's molecular features, and the nature of the mutual adsorbate-adsorbent interaction, as well as the surface and pore properties of the activated carbon.

Activated carbon adsorbent has been applied for the adsorption of different radionuclides such as cobalt-60 (Hamed et al. 2016), europium (Hamed et al. 2016; Moloukhia et al. 2016), cesium (Khandaker et al. 2021; Moloukhia et al. 2016), radon (Karunakara et al. 2015), thoron (Karunakara et al. 2015), uranium (El-Magied et al. 2021; Nezhad et al. 2021), radioactive iodine (Chien et al. 2011; Li et al. 2014), selenium (Elgazzar et al. 2020), molybdenum (Elgazzar et al. 2020), strontium (Elgazzar et al. 2020; Moloukhia et al. 2016), lanthanum (Elgazzar et al. 2020), and technetium-99 (Li et al. 2014). All the studies highlight the importance of oxygen-based functional groups and activated carbon π -electrons. Consequently, the radionuclides could either form complexes/cation exchange with the oxygen-based groups (Khandaker et al. 2021), interact with aromatic π -electrons of the activated carbon basal planes (Cho et al. 2020), or physically bind onto the activated carbon pores (Khandaker et al. 2018). During the adsorption of uranium ions, Nezhad et al. (2021) and Rout et al. (2016) noted that improved adsorption is achieved at decreasing solution acidity since the electron lone pair from the negatively charged oxygen-based groups form complexes with empty uranium ions orbitals. Therefore, it is concluded that highly porous activated carbon with either positive or negative oxygen-containing surface groups can efficiently adsorb arrays of radionuclides from wastewater.

In conclusion, adsorption onto activated carbon is a function of the adsorbents' surface area, pore volume, and the number of surface groups, irrespective of the pollutant class. Furthermore, the weak adsorptive interaction between the π -electrons of the activated carbon basal planes and the loose electrons of the aromatic rings also accounts for the efficient adsorption of organic pollutants.

Biochar

The term “char” refers to the residue obtained from the pyrolysis of carbonaceous materials (Armah et al. 2022),

while biochar strictly implies the solid products from the pyrolysis of agro and animal waste materials (Chen et al. 2019c). Biochar is distinguished from activated carbon because of its low pyrolysis temperature requirement, which is always below $700\text{ }^{\circ}\text{C}$, and the absence of any activation step (Ighalo et al. 2022a). The high porosity of biochar is comparable to that of activated carbon, but biochars also have a high ion exchange capacity compared to activated carbons. Such high biochar ion exchange capacity is linked to residual carboxylic, phenolic, hydroxyl, and carbonyl groups on the graphitic backbone (Zhao et al. 2021). Meanwhile, the percentage composition of each functional group on the biochar varies as the precursor material and thermochemical conversion technique are adopted (Amin et al. 2016). Thus, the creation of efficient and affordable adsorbents for wastewater decontamination is greatly aided by the physicochemical and porous features of biochar.

The application of biochar for azo (Gurav et al. 2021; Guy et al. 2022), reactive (Acemioğlu 2022; Muralikrishnan and Jodhi 2020), vat (Gupta et al. 2022; Vigneshwaran et al. 2021a), basic (Praveen et al. 2021; Silva et al. 2021), disperse (Das et al. 2021), and acid (Gao et al. 2021; Jose et al. 2022) dye adsorption has been reported in the literature. Notably, dye adsorption onto biochar generally proceeds via physical interaction (Guy et al. 2022), ion exchange (Goswami et al. 2016), and electrostatic interaction (Nguyen et al. 2021) mechanisms. The physical interaction mechanisms include pore filling, hydrophobic effect, π - π interactions, and n - π interactions. The pore-filling mechanism is always facilitated and favored by biochar's enhanced surface area and pore volume (Goswami et al. 2016). Similarly, the abundant carbonyl, hydroxyl, carboxyl, phenyl, and amine functional groups on the biochar are advantageous for π - π interactions with the aromatic rings of the different dye molecules (dos Reis et al. 2021). Siddiqui et al. (2019) reported efficient adsorption via a hydrogen bond donor-acceptor interaction between the hydroxyl group of modified biochar and the hydrogen bond receptor present in the methylene blue molecules. Also, non-covalent π - π and n - π interactions were reported between the aromatic rings of biochar and the Evans blue dye (Guy et al. 2022). Electrostatic attraction and ions exchange mechanism was noted as important sorption mechanisms during the adsorption of methylene blue dye (Pirbazari et al. 2014; Yang et al. 2019a). Consequently, electrostatic interaction predominates when the dye molecules and biochar surface contain opposite charges, while ion exchange mechanism involves ionic exchange between the surface groups of the biochar and the charges on the dye molecules. In conclusion, dye adsorption onto biochar occurs significantly through the hydrophobic effect, electrostatic attraction, hydrogen bonding, and π - π interaction. However, for biochar with highly developed porosity and

specific surface area, efficient dye adsorption is mostly via a pore-filling mechanism.

Heavy metal adsorption onto modified and unmodified biochar has been successfully demonstrated (Amabilis-Sosa et al. 2022; Li et al. 2022b; Sun et al. 2022). Several properties, such as elemental distribution, surface area, and surface charge, have been identified as key factors influencing adsorption (Bai et al. 2023; Liu et al. 2023). Ion exchange, surface complexation, electrostatic interactions, precipitation, and π - π interaction mechanisms are some main processes during cation adsorption. According to Chu and Nguyen (2023), the adsorption of hexavalent chromium onto magnetic biochar involves ion exchange, surface complexation, and redox reactions. Consequently, the sorption mechanism mentioned above is possible following the involvement of the biochar's carboxyl, hydroxy, and carbonyl groups. Qi et al. (2023) also affirmed that the surface complexation involving the oxygen-based functional groups of the biochar was critical to the successful adsorption of lead, cadmium, and copper ions. Conversely, the influence of pore-filling and electrostatic attraction between ionic copper species and the surface of magnetic biochar have been reported (Sun et al. 2023b). Therefore, biochar with improved porosity, specific surface area, and large oxygen group amounts exhibit high adsorption capacity for heavy metal species.

PPCPs and other emerging organic pollutants are adsorbed onto modified and non-modified biochar via chemical and physical adsorption (Nayyar et al. 2022; Zhang et al. 2022a). Chemisorption interaction occurs via electrostatic interactions and ion exchange, while physisorption occurs via pore-filling, π - π interaction, and other weak interaction mechanisms (Keerthanan et al. 2020; Liu et al. 2022a). Choudhary and Philip (2022) ruled out the role of electrostatic interaction during the sorption of methylparaben, carbamazepine, ibuprofen, and triclosan onto biochar. Instead, the predominance of non-electrostatic interaction (such as hydrogen bonding, electron donor-acceptor, and hydrophobic interactions) that is driven by the hydrophobic and hydrophilic moieties on the respective PPCPs, was proposed. Mayakaduwa et al. (2017) reported the role of chemisorption and physisorption interaction during the adsorption of carbofuran onto biochar. The study further noted that during chemisorption, the carbonyl groups interact with the nitrogen atoms of the carbofuran molecule via a nucleophilic addition reaction.

Similarly, the hydroxyl and carbonyl groups of the biochar can also interact with the heterocyclic ring of the carbofuran via π - π and hydrogen bonding-driven physisorption. The occurrence of an n - π interaction between the nucleophile-like oxygen groups on the biochar and π electron cloud of caffeine molecules was reported by Keerthanan et al. (2020). Thus, it is concluded that high π -electron density on

the biochar and abundant electrophilic groups in the PPCPs makes for efficient PPCPs uptake.

The adsorption of different radionuclides such as europium (Frišták et al. 2017), uranium (Ahmed et al. 2021a, b; Guilhen et al. 2019), and thorium (Chen et al. 2019d) onto raw and modified biochar has been reported. The studies generally highlighted the involvement of chemisorption, electrostatic interaction, and surface complexation reaction mechanisms. Also, oxygen-containing functional groups' significance in facilitating the abovementioned mechanisms was identified. For improved adsorption of radionuclides, different authors (Li et al. 2019b; Liu et al. 2021b) incorporated iron and sulfur into their biochar samples. It is believed that the iron and sulfur species promoted the reduction of most radionuclides, especially uranium, and enhanced their removal from wastewater. Ahmed et al. (2021a) and Li et al. (2019b) applied magnetic biochar for uranium adsorption. They suggested the possibility of surface complexation between the oxygen-based groups, such as the hydroxyl, carbonyl, iron oxide, and uranium molecules. Based on spectroscopic evidence, Ahmed et al. (2021b) also verified the binding of uranyl ions on surface groups of oxidized biochar.

In conclusion, the creation of efficient and affordable biochar for wastewater decontamination is greatly aided by the physicochemical and porous features of the adsorbent. The high porosity of biochar is comparable to that of activated carbon, but biochars also have a high ion exchange capacity compared to activated carbons. Such high ion exchange capacity of biochar is linked to residual carboxylic, phenolic, hydroxyl, and carbonyl groups on the graphitic backbone.

Lignocellulosic wastes

This class of adsorbent is generally sourced from plant materials and by-products of agro-material processing in various industries (Syeda et al. 2022). Many authors have previously developed efficient lignocellulosic adsorbents from tree bark, fruit peels, seeds, husk, and leaves. According to Aniagor et al. (2022), these lignocellulosic wastes are generated in large quantities, and their disposal is often challenging. Consequently, successfully utilizing these lignocellulosic wastes as adsorbents in wastewater treatment offers the advantage of cost-effectiveness and mitigates the environmental problems associated with their indiscriminate disposal. The high presence of relevant organic functional groups at the surface of these agricultural wastes makes them efficient in adsorbing varying classes of pollutants (Wakkel et al. 2019).

The adsorption potentials of the raw lignocellulosic wastes have been previously investigated (Hashem et al. 2022b; Ighalo et al. 2022b). However, it has been reported that this adsorbent class's functional group and sorption site could be greatly enhanced through surface chemical functionalization and other pre-treatment methods (Hashem et al.

2021a). Cavalcante et al. (2022) utilized grape winery waste functionalized with 3-aminopropyl tri ethoxy silane as an adsorbent for methyl orange dye uptake. The study noted the positive impact of chemical grafting on the adsorption performance of the modified material, as significant electrostatic interactions occurred between the ammonium group of the grafted adsorbent and the sulfur trioxide group on methyl orange dye species. Besides from electrostatic interaction, van der Waals, π – π interactions, and hydrogen bonds between the remaining functional groups of the dye molecules and the modified adsorbent were also reported. Other biomasses such as *Dodonaea viscosa* (Hopbush) plant, apricot (*Prunus armeniaca* L.) seed shell wastes, lupine seed powder, *Lepidium sativum* seed powder and olive waste have been respectively utilized in the adsorption of methyl red (Gul et al. 2022), acid blue 193 (Hashem et al. 2022a, c), acid orange 142 (Hashem et al. 2022b) and methylene blue (Ferkous et al. 2022) dyes. Incidentally, all the studies mentioned above affirmed the predominance of the electrostatic interaction mechanism.

Studies have shown that heavy metal adsorption onto lignocellulosic waste biosorbents occurs mostly via chelation, ion exchange, electrostatic interaction, and complexation with relevant surface groups (Aniagor et al. 2021; Mohamed et al. 2021). Also, the role of sodium, potassium, calcium, and magnesium in the adsorbent towards improved ion exchange process has been highlighted (Akar et al. 2012). Furthermore, certain functional groups, like the acetamide, carboxyl, phenolic, amino, alcohols, and ester groups, can substitute hydrogen ions with cations or donate electron pairs to form complexes with the metal ions in solutions (Kwikima et al. 2021). The predominance of electrostatic interaction and ion exchange mechanism was also reported during the adsorption of lead ions onto sugarcane waste (Hashem et al. 2021b) and respective adsorption of four different heavy metals onto husk cedar cones, pine nut oil cake, baffle walnut, pectin (Salishcheva et al. 2021). Therefore, the organic functional groups on lignocellulosic wastes play a crucial role during heavy metal adsorption from wastewater.

Lignocellulosic waste has also proven effective for PPCPs adsorption. Among the PPCPs investigated are bisphenol A, tetracycline, oxytetracycline, chlortetracycline, diclofenac, trimethoprim, and aflatoxin B1 species (Abdullah et al. 2021; Li et al. 2019c; Vázquez-Durán et al. 2021). It was, however, observed that the efficient sorption occurs majorly via the electrostatic and non-electrostatic mechanisms. Vázquez-Durán et al. (2021) used unmodified lignocellulosic adsorbents prepared from kale and lettuce wastes to adsorb carcinogen aflatoxin B1. The study concluded that adsorption occurred mainly via electrostatic, hydrophobic, and dipole–dipole interactions and hydrogen bonding.

Furthermore, complexation between the aflatoxin B1 and the chlorophyll content of the agro-waste also drove

the sorption process. Similarly, an ion exchange mechanism could occur involving the carbon and oxygen-based functional groups on the acid-treated banana bunches, coconut bunches, and bisphenol A (Abdullah et al. 2021). Conde-Cid et al. (2019) also reported the influence of electrostatic attractions between different antibiotics and variable charge components in the mussel shell and pine bark. Also, cationic bridges between antibiotics and non-crystalline minerals of the respective adsorbents were reported. In conclusion, the adsorption of PPCPs and other emerging organic contaminants reportedly occurred mainly through various electrostatic and non-electrostatic interactions between the individual drug molecules and the adsorbent's surface functional groups. Notably, no recent studies were found on the adsorption of radionuclide onto lignocellulosic waste adsorbent, and the reason for this observation is unknown. Therefore, it is suggested that the researcher further explore the potential of lignocellulosic waste for radionuclide adsorption. Also, effective surface functionalization and pretreatment could be necessary to improve the sorption capacity of lignocellulosic wastes for radionuclides adsorption.

Overall, lignocellulosic adsorbents have been successfully synthesized from tree bark, fruit peels, seeds, husk, and leaves. The successful utilization of these lignocellulosic wastes as adsorbents in wastewater treatment offers the advantage of cost-effectiveness and mitigates the environmental problems associated with their indiscriminate disposal. However, the functional group and sorption site of this type of adsorbent could be greatly enhanced through surface chemical functionalization and other pre-treatment methods.

Clay minerals

The classification of clay minerals is based on the respective layer type, interlayer order, and layer net charge (Bergaya and Lagaly 2013). However, the extensive application of clay minerals is hinged on their low cost, ready availability, ecofriendliness, high specific surface area, and ion exchange capacities (Uddin 2017). Thus, clay minerals constitute the active adsorptive groups on natural clay. However, despite their abundance, naturally occurring clay minerals have limited and variable adsorptive capacities due to their inherent impurities and mineralogical composition variations (Jaber et al. 2013; Zhang et al. 2010). Controlled fabrication of synthetic clay minerals is being explored to obtain a pure and homogenous clay mineral phase. These synthetic clay minerals are applied as advanced functional materials in specialized systems and the synthesis of specialized consumer goods. Therefore, regarding the layer structure, natural and synthetic clay minerals are widely used in many process industries and as an adsorbent in water treatment.

Several researchers have recorded massive success in the adsorption of dyes using modified and unmodified clay minerals. Dyes such as methylene blue (Amrhar et al. 2021; Çiftçi 2022), crystal violet (Cao et al. 2020; Sarma et al. 2019), brilliant green (Sarma et al. 2019), malachite green (Sevim et al. 2021), basic blue 9 (El Kassimi et al. 2021; Lawchoochaisakul et al. 2021), basic yellow 28 (El Kassimi et al. 2021; Lawchoochaisakul et al. 2021), acid green 25 (Yap and Priya 2019), methyl orange (Akbour et al. 2020; Lawchoochaisakul et al. 2021), rhodamine B (Ouachtak et al. 2020; Yu et al. 2019), and congo red (Yu et al. 2019) have been successfully investigated and reported in the literature. Notably, dyes have charged and neutral parts, but Haounati et al. (2021) noted that clay adsorbent provides suitable sites for both species. The cationic dye molecules interact with the negative charge sites of the clay minerals through electrostatic attraction. At the same time, the neutral species are adsorbed onto the external surface of the clay mineral via hydrogen bonding with the hydroxyl groups (de Queiroga et al. 2019). Aside from hydrogen bonding, this surface attachment can also occur via intermolecular π - π stacking attraction (Dobe et al. 2022; Thirumoorthy and Krishna 2020). Thus, dye adsorption onto clay minerals majorly proceeds via electrostatic attraction, hydrogen bonding and intermolecular attraction. Similarly, the sorption efficiency is a function of the solution pH, initial dye concentration and adsorbent dose.

The adsorption of different heavy metal cations, including trivalent chromium, hexavalent chromium (Essebaai et al. 2022; Mdalose et al. 2021), lead (Jabłońska 2021; Jiang et al. 2021a; Sun et al. 2023a), zinc (Jabłońska 2021; Jiang et al. 2021a), nickel (Jabłońska 2021), cadmium (Szewczuk-Karpisz et al. 2022; Tonk et al. 2022; Zeng et al. 2023), and barium (Atun and Bascetin 2003; Mundim et al. 2022) have been reported. The efficiency of clay and clay minerals in heavy metal adsorption has been linked to the clay's high cation exchange capacity, high specific surface area, and high swelling properties (Essebaai et al. 2022). According to Szewczuk-Karpisz et al. (2022), heavy metals usually adsorb onto the inner-sphere complexes of the clay minerals via ionic exchange and on the silicon monoxide and aluminium oxide surface groups. Furthermore, at low pH (acidic sorption environment), negatively charged sites of the clay mineral adsorbent establish electrostatic interaction with the target heavy metal, forming outer-sphere complexes (Mundim et al. 2022). In summary, heavy metal adsorption onto clay and clay minerals mainly occurs via ion exchange and electrostatic attraction mechanisms. The solution pH also influences sorption efficiency since the charges on the surface groups of the clay minerals vary considerably with pH variation.

Clay minerals adsorbents also have proven effective for the adsorption of PPCPs. Among the PPCPs investigated

are propranolol, ibuprofen, amoxicillin, diclofenac-sodium, imipramine, paracetamol, p-chlorophenol, and tetracycline species (Chauhan et al. 2020a, b; del Mar Orta et al. 2019; Ji et al. 2019; Martín et al. 2019; Obradović et al. 2022; Sun et al. 2017; Zhang et al. 2021). It was, however, observed that efficient sorption occurs majorly via an ionic exchange mechanism (de Farias et al. 2022; del Mar Orta et al. 2019; Martín et al. 2019; Obradović et al. 2022). Furthermore, a complex mechanism involving hydrophobic interactions between the nonpolar groups of the PPCPs and clay minerals and an electrostatic interaction mechanism was reported while adsorbing Ibuprofen and diclofenac-sodium (Obradović et al. 2022). Zhang et al. (2021) reported improved adsorption of tetracycline species onto montmorillonite via partial cation exchange, surface complexation, and hydrogen bond/Vander Waal interaction. Therefore, it is concluded that the ionic exchange mechanism accounts for most PPCPs adsorption onto clay minerals.

The adsorption of different radionuclides, including cesium, strontium, uranium, europium, plutonium, iodine, cobalt, zirconium, and selenium, onto modified and unmodified clay minerals, have been successfully investigated (Akemoto et al. 2021; Pavón González and Alba 2022; Soliman et al. 2019; Zabulonov et al. 2021). Generally, one or a combination of electrostatic interaction, surface complexation, and ionic exchange mechanisms play a significant role in the adsorption of radionuclides onto clay minerals (Akemoto et al. 2021; Alamudy and Cho 2018). In addition, clay minerals' expandability and basal spacing enhance their cation exchange capacity and affinity for radionuclides (Philipp et al. 2022; Soliman et al. 2019). The influence of environmental factors such as temperature, pH, organic matter content, contact time, initial adsorbate concentration, and ionic strength also impacts the adsorption of radionuclides (Fan et al. 2019). Zabulonov et al. (2021) reported a low distribution coefficient for cesium radionuclide at low solution pH and enhanced strontium uptake due to the high probability of strontium ionic fixation in diffuse clay ionic layers. Philipp et al. (2022) reported improved uranium adsorption with increasing ionic strength and solution alkalinity. According to the study, at pH < 8.0, the main sorption driving force was cation exchange, which depends on ionic strength. Beyond this pH, there was a sequential surface de-protonation, thus enhancing surface complexation. The positive impact of solution temperature on the clay expandability and the mobility and effective collision of the radionuclide molecules was also highlighted (Soliman et al. 2019). Thus, it is concluded that the sorption capacity of clay minerals for radionuclides is a function of the expandability of the clay particles, as well as the pH and the ionic strength of the adsorbate solution.

To sum up, clay minerals are widely used in adsorption due to their affordability, availability, eco-friendliness, high

specific surface area, and ion exchange abilities. However, despite their abundance, their adsorptive capacities are limited and inconsistent due to inherent impurities and variations in mineralogical composition. Therefore, chemical modification is necessary to enhance their adsorption capabilities.

Silica

Silica is an inorganic solid material often applied as an efficient adsorbent in water treatment, either in its raw or chemically modified state. They exhibit a considerably high surface area, chemical inertness, improved pore properties, and many surface functional groups, which can provide grafting sites (Lahiri and Liu 2021). Many recent publications have demonstrated the versatility of silica-based adsorbents in wastewater treatment.

Different types of dye have been successfully adsorbed onto varieties of silica-based adsorbents (Arasi et al. 2021; Benvenuti et al. 2020; Koyuncu and Okur 2021); however, it was noted that the functionalization of these silica adsorbents greatly enhanced their dye adsorptive capacity. Consequently, different surface-modified silica-based adsorbents (Bensedira et al. 2022; Cao et al. 2020; Gomaa et al. 2022; Li et al. 2020d; Zein et al. 2020) have been used to adsorb different dyes. Specifically, Kalkan and Nadaroglu (2021) adsorbed acid fuchsin dye onto laccase-modified silica fume. The optimum uptake was established at pH 5.0, with a hydrogen bond forming between the adsorbent's sulfate and amine groups and the positively charged acid fuchsin dye molecules. Also, during the adsorption of reactive wool dyes, Gemeay et al. (2020) reported the role of the sulfonate and oxygenated groups for enhanced hydrogen bonds and electrostatic interaction. Pham et al. (2021) synthesized a silica-based adsorbent with a high positive surface charge via functionalization with poly-diallyl-dimethylammonium chloride. Based on the study, efficient dye uptake was achieved following a complex formation between the oxygen atoms on the sulfonic group of the azo dye and the adsorbents' amine groups. Al-Shehri et al. (2021) investigated the impact of incorporating neodymium into the three-dimensional structure of mesoporous silica. The results show an improved adsorption capacity via electrostatic interaction, as the surface modification introduced a large number of negative binding sites that are necessary for adsorbing the positively charged nitrogen atoms of the dye species. Also, the possible formation of a coordination bond between the nitrogen lone pairs of the neutral amino groups and the neodymium atoms was further postulated. Therefore, irrespective of the nature of the silica-based adsorbent, the solution pH, which directly influences the degree of electrostatic interaction, plays a crucial role during dye uptake.

Different forms of raw and functionalized silica-based adsorbents have been successfully investigated for the adsorption of heavy metal ions. The surface functionalization techniques mainly involve introducing relevant surface groups to enhance interaction with heavy metal cations. Although many studies have demonstrated the usefulness of surface functional groups in pollutant binding, it should be noted that some functional groups exhibit superior cation binding capacities than others. Through successful silylating reactions, Shao et al. (2020) incorporated the sulfoacid, thiol, amino, carboxyl, and ethylenediamine tetra-acetic acid groups onto silicon dioxide nanoparticles. Further, they tested the lead ion adsorption potentials of the respective adsorbents. It was reported that the ethylenediamine tetra-acetic acid-decorated silicon oxide, with improved geometrical adaptability, depicted the highest adsorption capacity. Other studies by Vareda et al. (2020), Wang et al. (2020c), and Albayati et al. (2019) also highlighted the role of nitrogen-containing functional groups, having similar electrostatic interaction mechanisms in heavy metal adsorption. Radi et al. (2019) explored the potential of porphyrin-modified silica for adsorbing lead, zinc, cadmium, and copper ions. The study concluded that efficient uptake occurred through the direct complexation of porphyrins with the cations via a so-called 'sitting-atop' interaction. Conclusively, it was noted that efficient cation uptake is hinged upon successfully introducing sufficient negatively charged groups on the silica adsorbents that could interact with the different cations.

Studies exist on the adsorption of PPCPs and other emerging organic pollutants onto modified silica adsorbents (Ighalo et al. 2022c; Igwegbe et al. 2021). Modified nano-silica (Pham et al. 2020b) and polycation-modified nano-silica (Pham et al. 2020a) were used for the adsorption of ciprofloxacin and beta-lactam cefixime. Both studies reported that the main adsorption driving force was the electrostatic interaction between the anionic surface charge of the respective drugs and the protonated adsorbent surface. Besides, Jodeh et al. (2022) recorded high adsorptive capacity while adsorbing trimethoprim onto a chelating matrix synthesized via a reaction between 1.5-dimethyl-1H-pyrazole-3-carbaldehyde, 3-aminopropyltrimethoxysilane and silica gel. According to the study, efficient drug binding occurred via complexation between the nitrogen atoms of the adsorbent and π -electrons originating from the benzene and pyrimidine rings in the drug. Also, low adsorption enthalpy values were recorded throughout the entire sorption process due to the hydrogen bond formation and the formation of a water bridge between the nitrogen/oxygen-containing groups of the trimethoprim and the amine groups of the adsorbent (Jodeh et al. 2022). Dipyrindyl-based organo-silica nanosheets were successfully synthesized and utilized for adsorbing clofibric acid,

ketoprofen, and naproxen sodium from wastewater (Guo et al. 2020). It was noted that the adsorption of naproxen sodium occurred via π - π interaction, while partition and π - π stacking predominated during the ketoprofen adsorption. Conversely, clofibrac acid uptake was controlled by multiple interaction mechanisms, including hydroxyl- π interaction, partition, π - π interaction, and π - π stacking. In conclusion, the adsorption of PPCPs and other emerging organic contaminants reportedly occurred mainly through various physical interactions between the respective drug molecules and the adsorbent's surface functional groups.

The adsorption of different radionuclides such as cesium (Bu et al. 2019; El-Shazly et al. 2021b; Zhuravlev et al. 2022), uranium (Tripathi et al. 2018), europium (Garcia et al. 2019; Wang et al. 2020b), cobalt (El-Shazly et al. 2021a), and strontium (Zhuravlev et al. 2022) onto raw and modified silica-based adsorbent has been reported. Bu et al. (2019) investigated the adsorption of cesium ions onto the tobermorite 9 Å, tobermorite 14 Å, and jennite. Accordingly, cesium adsorption onto tobermorite 14 Å and tobermorite 9 Å, respectively, occurred via the ionic adsorption at the octahedral hexaqua calcium (II) complex surface and cation exchange at the tetrahedral silicate surface. Similarly, electrostatic interaction via complexation with surface hydroxyl groups controlled the cesium adsorption onto jennite (Bu et al. 2019). The influence of the cation exchange mechanism was also highlighted during cesium adsorption onto insoluble ferrocyanide composites (El-Shazly et al. 2021b). Tripathi et al. (2018) evaluated the feasibility of uranium adsorption onto hollow amorphous silicon oxide nanotubes. A robust electrostatic attraction was established between the deprotonated silicon oxide nanotube surface and the uranyl hydroxyl cation during uptake. Using sodium lauryl sulfonate-modified silicon dioxide adsorbent, Wang et al. (2020b) reported that the oxygen-containing functional groups from sulfur trioxide were responsible for the europium ions adsorption. According to Jose et al. (2020), the europium ions often interact with sulfur trioxide anion in preference to the sodium lauryl sulfonate chain. It is thus concluded that the adsorbent's surface charge, solution pH and structural orientation significantly impact the type of the dominant sorption mechanism during radionuclide sorption.

Overall, surface complexation, hydrogen bonding, and electrostatic interaction are the primary mechanism responsible for pollutant binding onto silica adsorbents. Furthermore, efficient binding of organic pollutants occurred via complexation between the silicate groups of the adsorbent and π -electrons originating from the benzene and pyrimidine rings in the respective organic pollutants.

Zeolite

Zeolites are porous materials with improved ion exchange capacity, mainly composed of hydrated aluminosilicate minerals (El-Nahas et al. 2020). This class of adsorbent exhibit a negatively charged framework, which stems from substituting tetra atomic silicate cation for aluminium cation within the structural backbone. Unmodified zeolite adsorbents have proven efficient for adsorbing different classes of dyes, except the anionic dyes, due to the anionic nature of the zeolite surface. However, different functional groups and complexes have been successfully incorporated into the zeolite structural framework for improved dye adsorption capacity.

Gollakota et al. (2020) investigated the potential adsorption of rhodamine 6G onto a novel zeolite material. During the study, two main sorption mechanisms were identified: electrostatic interaction between the deprotonated silanol groups and the cationic dye species and hydrogen bonding due to the interactions between the silanol and amine functional groups of zeolite and the cationic dye species. Similarly, while adsorbing basic fuchsin dye onto tetra propyl ammonium bromide-modified magnetic zeolite, Mohammed et al. (2020) observed the deprotonated silanol, silicon oxide groups of the adsorbent interacted with the cationic dye species, to entrench efficient uptake at increasing pH up to pH 5.0. Meanwhile, between pH 5.0–9.0, efficient dye uptake was achieved following the complexation between the neutral silanol groups of the adsorbent and electrons lone-pair from primary amine groups. Also, a robust electrostatic attraction was reported as the predominant mechanism during the sorption of acid red 66 dye onto Linde-type A zeolite (Al-dahri et al. 2022), methylene blue dye onto synthetic zeolite mixture (Youssef et al. 2021), methyl orange dye onto pillar(5)arene modified zeolite (Yang et al. 2019b) and methylene blue dye onto zeolite/cerium oxide nanocomposite (Nyankson et al. 2020). Furthermore, Phouthavong et al. (2020) reported the efficient binding of methylene blue species onto the 3-dimensional pore system of silica-rich magnetic zeolite via a pore-filling mechanism. Thus, the solution pH regulates the extent of dissociations and charge distributions of the zeolite functional groups.

Different studies have successfully investigated and established raw and modified zeolite's heavy metal adsorption capacity. Meanwhile, the strong influence of the electrostatic attraction mechanism during the cation binding was reported by most authors. Gollakota et al. (2023) evaluated the potential adsorption of cadmium and zinc ions onto ionic liquid functionalized zeolite X. They affirmed the dominance of electrostatic attraction to complexation between the silanol groups of the adsorbent and the cationic species. According to Guo et al. (2023), a coordination interaction with the nitrogen/oxygen-containing groups of the functionalized zeolitic imidazole frameworks-functionalized resulted in

efficient sequestration of lead and copper ions. Similarly, the exchange of ions within the zeolitic structure by the heavy metal cations was also reported during the adsorption of copper (Dasgupta et al. 2021) and chromium ions (Huang et al. 2022) onto zeolite. However, the mechanism of heavy metal adsorption onto zeolite is mainly via cation exchange within the zeolitic structure and silanol groups-assisted electrostatic interactions.

The adsorption of PPCPs and other emerging organic contaminants onto zeolite-based adsorbents has been reported mainly through hydrophobic and electrostatic interaction mechanisms (Belviso et al. 2021; Goyal et al. 2018). However, a zeolite-based adsorbent capable of efficient adsorption of different organic pollutants was generally synthesized via chemical functionalization. Smiljanić et al. (2020, 2021) comparatively investigated the adsorption of ibuprofen, naproxen, diclofenac sodium, and ketoprofen onto natural zeolites that are respectively loaded with monolayer and bilayer of cationic surfactant. During sorption onto the loaded zeolite, the anionic drug species interact electrostatically with the cationic surfactant head. The alkyl chains of surfactants complex with the hydrophobic heads of the drugs via hydrophobic interaction. Besides from the interactions mentioned above, there was an ionic exchange between the counter chloride anion on the surfactant molecule and the anionic drug species in the case of zeolite with a bilayer of surfactant (Smiljanić et al. 2020). Using a two-step computational analysis, Lin et al. (2020b) investigated the possible adsorption of four linear siloxanes and derivatives onto a myriad of hypothetical pure-silica zeolites. It was observed that the most robust adsorption energy and electrostatic interaction were recorded for the compound with the smallest particle sizes and significant electronegativity differences between the bonded atoms. The dominance of hydrophobic interactions was also reported during the adsorption of ketoprofen, hydrochlorothiazide, and atenolol in their neutral state with high-silica commercial zeolites (Sarti et al. 2020). Thus, the affinity of zeolite-based adsorbents for organic and nonpolar molecules could be improved through surface modification with the right reagent, noting that the adsorption of organic and non-polar molecules is a function of the adsorbent's physicochemical properties.

The effectiveness of zeolite in the adsorption of different radionuclides has been established in the literature, and electrostatic interaction was noted as the major sorption mechanism involved (Li et al. 2022a). Salam et al. (2020) and Ai et al. (2022) investigated the sorption of uranium ions from wastewater. They observed that the complexation of thiol and hydroxyl with uranyl ions between pH 5.0–6.0 facilitated sorption. Adsorption of strontium radionuclide onto microporous Linde Type A zeolites of varying crystal sizes also proceeded with predominant electrostatic interaction (Kwon et al. 2020). The study also observed that adsorbents

with a crystal size of 2 μm showed better adsorption capacity and selectivity for strontium ions than those with smaller crystal sizes of 100 nm and 500 nm. Li et al. (2020c) blended the aspartic acid molecules with the bilayer cetyltrimethylammonium bromide cations onto zeolite Y. The modified zeolite Y adsorbent was utilized for adsorbing cesium, strontium, and uranium ions. It was, however, reported that the monovalent cesium ions were adsorbed better and faster than the bivalent strontium and uranium ions. Notably, higher consumption of aspartic acid ligands occurred during the formation of a coordination compound with bivalent ions than with monovalent ions, hence the decreased adsorption capacity. However, the crystal size significantly affects the affinity between the zeolite adsorbent and radionuclides.

In conclusion, zeolites exhibit a negatively charged framework due to substituting tetra atomic silicate cation for aluminium cation within the structural backbone. The silanol and amine functional groups of zeolites facilitate the occurrence of hydrogen bonding and electrostatic interaction, which are the two main identified sorption mechanisms.

Peat and humic soil

Peats and humus are soil materials mainly comprising decaying organic matter, detrital minerals, and plant debris such as lignin, cellulose, and hemicellulose. Its different constituents' polar organic functional groups confer high pollutant adsorption and ion exchange capacity on peat soil. It has been shown that the predominant physical and chemical properties of any given peat soil are a function of the origin and nature of the decayed plant materials and the moisture relations during and after the peat formation (Kolay and Taib 2018).

The presence of cellulose, hemicellulose, and lignin compounds, originating from decaying plant biomass makes for the efficient uptake of dye molecules by peat soil. Rahmayanti et al. (2021) studied the adsorption of naphthol blue black and indigo sol blue dyes onto peat soil humin. The dominance of electrostatic interaction via protonation of the carboxyl and hydroxyl groups of the peat humin was recorded between pH 2.0 and 5.0. At the same time, the hydrogen bonding mechanism predominated between pH 7.0 to pH 8.0. Dzieniszewska et al. (2019) adsorbed five different dyes: reactive blue 19, reactive blue 81, reactive black 5, acid black 1, and acid blue 9, onto low-moor peat in the presence of sodium chloride, sodium carbonate, and ethanoic acid auxiliaries within the adsorbate solution. In the presence of ethanoic acid, the peat surface charges protonated, thus enhancing the anionic dye adsorption via an electrostatic interaction mechanism (Dzieniszewska et al. 2019).

Similarly, the reactive dye species' increased intermolecular force and dimerization were observed in the presence of salts. The dominance of the electrostatic interaction and

ion exchange mechanisms was also highlighted during the adsorption of malachite green dye onto coco peat (Kumari and Dey 2019) and modified sphagnum peat moss samples (Abu-Saqer and Lubbad 2019). Therefore, it is concluded that the different functional groups inherent in the peat soil's cellulose, lignin, and hemicellulose content are responsible for both electrostatic and non-electrostatic interactions involved during the uptake of different classes of dyes.

Different studies have successfully investigated and established the heavy metal adsorption capacity of raw and modified peat soil. Kasiuliene et al. (2019a) studied the adsorption of hexavalent chromium, trivalent chromium, copper, arsenic, and zinc onto raw and iron-modified peat. It was reported that peat magnetization negatively impacted the adsorption of chromium, copper, and zinc due to the screening/shielding effect of the iron coating on some surface organic groups and active sites. Conversely, due to their high affinity for iron hydroxide and improved surface area, arsenic was better adsorbed onto the iron-modified peat. Furthermore, the solution pH for optimal adsorption of hexavalent chromium, trivalent chromium, copper, and zinc was established at pH 1.5–3.0, 4.0–5.5, 5.0, and 7.0–9.0, respectively. Bartzak et al. (2018) recorded the optimum adsorption of nickel and lead ions onto peat at pH 5.0. The electrostatic attraction between the negative surface charge on the peat and the metal cations, as well as the progressive exchange of adsorbent cations by the nickel and lead ions, was also highlighted in the study. Besides from magnetization, Pchelomov et al. (2021) also observed that the oxidation of peat soil humin with potassium persulfate improved its capacity for adsorbing zinc, lead, copper, and nickel. According to the study, the oxidative treatment increased the amount of carboxylic, ketone, and quinoid groups on the adsorbent structure. In addition to the already stated studies, other literature on the successful adsorption of iron (Ashraf et al. 2019), chromium (Ashraf et al. 2019), nickel (Ashraf et al. 2019), copper (Lodygin 2019; Naymushina and Gaskova 2019), zinc (Lodygin 2019), lead (Lodygin et al. 2020; Pelinsom Marques et al. 2020), and cadmium (Lodygin et al. 2020; Pelinsom Marques et al. 2020) onto peat-based adsorbent still exist. In summary, heavy metal adsorption potentials of raw and modified peat mostly occur via ion exchange and/or electrostatic interaction mechanisms. However, a proper pH adjustment on the respective heavy metal wastewater can greatly enhance uptake.

The adsorption of PPCPs and other emerging organic contaminants onto peat and humic-based adsorbents is primarily a function of the available functional groups and organic carbon content of the peat soil, as well as the adsorbate speciation and solution pH (Chen et al. 2017). Guo et al. (2017b) reported the successful adsorption of sulfamethazine antibiotics onto peat soil humin. During the study, the interactions between the sulfonamide group

of the sulfamethazine antibiotics, which act as π -electron-acceptors, and the benzene rings on the adsorbent ensured efficient sorption. Chen et al. (2017) investigated the adsorption of sulfamethoxazole and sulfapyridine antibiotics onto peat. For the neutral sulfamethoxazole species, the dominant mechanism was the hydrophobic partitioning between the sulfonamide group of the adsorbate and the organic matter of the peat soil. At the same time, cation bridging and slight contribution of van der Waals forces controlled the sorption of deprotonated sulfamethoxazole species (Chen et al. 2017).

Furthermore, the dispersive and electrostatic interactions between the sulfapyridine's pyridine group and the peat's aromatic carbon ring were responsible for efficient adsorption. Only a few earlier studies were found on the adsorption of PPCPs and other emerging organic contaminants on peat and humic-based adsorbent. This observation could be related to the fact that this class of adsorbent is open to and compatible with a wide range of surface functionalization required for the efficient sorption of structurally complex pollutants such as PPCPs and other emerging organic contaminants.

Due to the abundant presence of carboxyl and phenolic hydroxyl groups on peat and humic soil, the adsorption of varying radionuclides mainly occurs via cation exchange and electrostatic interaction mechanisms (Belousov et al. 2021). Komissarov and Ogura (2019) and Belousov et al. (2021) observed a variation in the adsorption of cesium and strontium radionuclides onto different peat soils at varying solution pH. The studies reported enhanced uptake via electrostatic attraction between the sorbent's deprotonated carboxyl and phenolic functional group and the radionuclide cations at acidic pH ranges. Meanwhile, when the solution pH was increased beyond pH 6.0, Belousov et al. (2021) recorded a decreased adsorption for both radionuclides due to decreasing adsorbate-adsorbent bond strength. Similarly, the possible formation of stable complexes between the oxygen-based groups of the peat soil and the respective radionuclide cations was postulated (Belousov et al. 2021). Bordelet et al. (2018) also highlighted the key role of carboxylic and phenolic functional groups of peat soil during the adsorption of uranium and radium radionuclides. The study further reported that the optimum uptake of uranium and radium onto peat soil occurred between pH 3.0 to 6.0. This observation aligns with the result obtained by Belousov et al. (2021). Thus, the interaction of the deprotonated groups on the peat soil and the cationic species of the radionuclide remains the dominant sorption mechanism.

In summary, the polar organic functional groups of the peat adsorbent's cellulose, hemicellulose, and lignin constituents are responsible for high pollutant adsorption and ion exchange capacity. Also, the main adsorption mechanisms are the electrostatic interaction, hydrogen bond formation, and possible formation of stable complexes

between the oxygen-based groups of the peat soil and the respective pollutants.

Adsorption isotherms

Isotherm modeling is an applicable technique for expecting adsorption behaviors and studying the correlation between adsorbents and contaminants at an equilibrium medium. A comprehensive understanding of the isotherm models would significantly enhance the behavior of the adsorption method and pollutant-adsorbent design (Dada et al. 2021). Moreover, isotherm modeling could provide insight into the removal method of pollutants, such as maximum adsorption capacity, strength, and adsorption state (Majd et al. 2021). Adsorption isotherms are produced when an adsorbent and an adsorbate come across for a sufficiently extended period for the interface concentration to be in equilibrium with the absorption of the contaminant at a constant temperature (Al-Ghouti and Da'ana 2020). Adsorption isotherm is critical for fundamental studies for designing, optimizing, and troubleshooting manufacturing adsorption experiments. Various factors could be influenced during the adsorption process, such as pH, temperature, initial concentration, and adsorbent characteristics (Ahmad et al. 2022; Huang et al. 2021b). These impacting parameters affect the adsorption modeling. For instance, temperature, pollutant dosage, and adsorbent properties could completely influence the level of selecting the proper isotherm model (Duan et al. 2020).

Various isotherm models with differing factors have been established and utilized in a broad series of manufacturing removal methods via adsorption involving oil and gas factories, food manufacturing, and water remediation activities. The proper isotherm model affords the necessary details for evaluating the adsorbent acts, incorporating the adsorption mechanism, adsorption capacity, and fundamental characteristics of the removal method. Numerous adsorption isotherm models have been applied throughout the previous years to review the thermodynamic equilibrium correlation among pollutants and adsorbents at steady temperatures.

Following the sum of factors, adsorption models are categorized as one-factor, two-factor, and three-factor models. The isotherm model is regularly employed to study adsorption processes, capability, and adsorbent characteristics in different pollutants studies. Nevertheless, because of some model constraints, not all isotherm models could be suitable for expressing the data and explaining the pollutant's adsorption method.

Langmuir adsorption isotherm

The Langmuir isotherm model, one of the fundamental empirical models, presumes the pollutant and adsorbent material in a standard method utilized for homogenous surfaces (Al-Ghouti and Da'ana 2020). A further supposition of this model is the reversibility of the adsorption–desorption process (Langmuir 1916, 1918). The Langmuir isotherm could be gained from this equation, inferring that:

$$q_e = \frac{q_m}{1 + K \cdot C_e} \times K \cdot C_e$$

where q_m , L is the maximum adsorption amount of Langmuir isotherm (mg g^{-1}), and k is Langmuir isotherm constant ($\text{dm}^3 \text{mg}^{-1}$).

Due to its simplicity and homogenous monolayer adsorption, Langmuir is the most frequently used optimal isotherm in the adsorption of heavy metals. Most of the heavy metal adsorption research described in the literature used monolayer chemisorption techniques. Chitosan aerogel was synthesized by Fan et al. (2021) to remove copper from contaminated water, and the equilibrium data were compared using Langmuir and Freundlich models. The outcome showed that the Langmuir model is the most appropriate one to describe the adsorption process. Using Pinewood sawdust biochar, naphthalene, phenanthrene, and anthracene compounds were effectively removed from the contaminated aqueous solution. The isotherm models revealed the complete success of the Langmuir equation in elucidating the contaminants' uptake (Rashad et al. 2022).

Freundlich adsorption isotherm

The Freundlich isotherm model is a broadly applied practical principle that relies on tentative findings since it explicitly explains the removal of organic/inorganic toxins on numerous adsorbent materials. Herbert Freundlich initially suggested the model in 1906 (Freundlich 1907) as an expansion of Henry's standard. The primary assumption in enhancing the Freundlich adsorption isotherm model in 1906 is that the adsorbent material has a heterogeneous surface comprising numerous active adsorption sites. Following this perspective, the quantity removed is the amount of adsorption on all active sites until the adsorption capacity reduces exponentially at the end of the adsorption process. The Freundlich model could also be employed for multilayer adsorption. When chemisorption is the major adsorption mechanism, the Freundlich model describes monolayer adsorption, whereas it explains multilayer adsorption when physisorption is the major mechanism. The Freundlich isotherm model has both linear and nonlinear models, which are defined as follows:

$$q_e = K \cdot C_e^{\frac{1}{N}}$$

$$\log q_e = \log K_f + \frac{1}{N} \log C_e$$

where K_f (mg L^{-1}) and N are the Freundlich isotherm model's coefficients for the adsorption removal and strength coefficients, respectively, the infinite surface coverage that is anticipated mathematically indicates multilayer adsorption on the surface since the Freundlich model does not expect the overload of the adsorbent. The value $1/N$ is temperature-dependent and depends on the adsorption conditions like surface heterogeneity or adsorption capacity (Febrianto et al. 2009).

To examine experimental data of chromium, arsenic, cadmium, and lead adsorption with graphene oxide, Abbasi et al. (2021) employed linear and nonlinear regression of Freundlich models. The data analysis revealed that the nonlinear Freundlich adsorption isotherm model outperformed the linear form in estimating the quantity of heavy metals removed by graphene oxide.

Dubinin–Radushkevich isotherm

The Dubinin–Radushkevich isotherm model presupposes a multilayer structure with van Der Waal's forces relevant to physical adsorption (Al-Ghouti and Da'ana 2020). The Dubinin–Radushkevich adsorption model, an empirical isotherm, depicts the adsorption of vapors and gases via a pore-filling mechanism on micropore adsorbent surfaces, such as biochar, activated carbon, and metal–organic framework. To explain the pore size, adsorption capacity, and removal of microporous non-polar contaminants, Dubinin and Radushkevich designed the Dubinin–Radushkevich formula in 1946 (Dubinin 1947). The Dubinin and Radushkevich model is beneficial for different water pollutants removal applications, including measuring adsorption capability, evaluating the mechanism of the adsorption method, and figuring out the average adsorption energy (Chen et al. 2022b). The Dubinin and Radushkevich isotherm model depends on temperature variations. The following formula can be used to apply the Dubinin and Radushkevich adsorption model:

$$\varepsilon = RT \ln \left(1 + \frac{1}{C_e} \right)$$

ε (kJ mol^{-1}) is Polanyi potential, R is the gas constant $8.314 \text{ J mol}^{-1} \text{ K}^{-1}$, and $T(K)$ is the absolute temperature.

Elgarahy et al. (2020) inspected the subsequent remediation of Congo red anionic dye and copper metal ions on the multifunctional alginate beads. Calculating the mean sorption energy permitted researchers to differentiate between

mercury's physical and chemical adsorption utilizing the Dubinin–Radushkevich model.

Temkin isotherm

The Temkin model presumes a multi-layer chemisorption process containing a parameter that reflects relations between the adsorbent and the pollutant (Temkin 1940). Temkin isotherm model disregards great and little concentration amounts while accounting for adsorbent–contaminant contact. The Temkin isotherm is merely appropriate to specific ion concentrations. This model assumes that the binding energy is uniformly distributed and that the adsorption heat of all molecules in the layer drops linearly rather than logarithmically when the surface coverage upsurges as a function of temperature (Elgarahy et al. 2022). The Temkin model equation is stated as follows.

$$q_e = \frac{RT}{b} \ln (A \times C_e)$$

where A (L g^{-1}) is the constant of equilibrium binding; b (J mol^{-1}) is the adsorption heat constant. The above-mentioned equation can be solved by plotting q_e versus $\ln C_e$, which yields a straight line, and A and b can be calculated from the slope and intercept.

Cadmium, Nickel, Copper, lead, and Zinc metal ions were discarded from the contaminated solution utilizing crab shell-derived chitin, and the experimental findings were modeled using the Langmuir, Freundlich, Temkin, and D-R isotherms to describe the adsorption mechanisms. It was revealed that the Temkin model successfully fitted the adsorption method. The heat of adsorption value from the Temkin isotherm shows that the chitin and heavy metal interaction is likely physisorption rather than ionic interaction (Boulaiche et al. 2019).

Brunauer, Emmett, and Teller isotherm

In 1938, Brunauer, Emmet, and Teller suggested a theoretical isotherm model that relied on multimolecular adsorption. This model was first applied in gas–solid equilibrium techniques (Brunauer et al. 1938). The Brunauer, Emmett, and Teller isotherm model is a Langmuir version with several additional assumptions, such as (1) the adsorption method is multilayer homogeneous; (2) the first layer's adsorption force is persistent (i.e., The adsorption energy of each additional layer is equivalent to the heat of condensation. The interactions between the adsorbent and the adsorbate have no impact on the fusion heat that is used to generate this energy.), and (3) adsorption and desorption rates are equal (Wang and Guo 2020). There are numerous variations of the Brunauer, Emmett, and Teller isotherm model, but the

following describes its extinction model at the liquid–solid interface:

$$q_e = \frac{q_{\text{mBET}} C_{\text{BET}} C_e}{(C_s - C_e) \left[1 + (C_{\text{BET}} - 1) \left(\frac{C_e}{C_s} \right) \right]}$$

where q_{mBET} (mg g^{-1}) is the maximum adsorption capacity of Brunauer, Emmett, and Teller isotherm; C_s (mg L^{-1}) is the adsorbate solubility; C_{BET} (mg L^{-1}) is the Brunauer, Emmett, and Teller isotherm adsorption constant, a parameter related to the binding intensity for all layers.

Saccharomyces cerevisiae that had been chemically and thermally modified was used by De Rossi et al. (2018) to examine chromium removal from contaminated solution. The Brunauer, Emmett, and Teller isotherm was effectively applied to model the chemically treated bio-sorption isotherms. The BET isotherm posits that the adsorbent material was soaked with chromium following the Langmuir isotherm; therefore, the monolayer had become saturated, and more biosorption took place on the numerous layers of the material, resulting in a more remarkable ability to absorb chromium. Nevertheless, relatively than a feasible adsorption isotherm, Brunauer, Emmett, and Teller isotherm model is currently considered a technique for characterizing various biosorbents (Majd et al. 2021). Additionally, it has been utilized to investigate the specific surface area, total pore volume, and pore size of various carbonaceous materials (Najafloo et al. 2021; Zeng et al. 2020).

Adsorption kinetics

Kinetic models help to define the functional performance, comprehend the adsorbent–pollutant correlations, and afford perceptions into the multifaceted adsorption method. Despite several compound equations that have been established, e.g., Elovich, Avrami, Bangham, or layer diffusion models, the utmost applied models are the pseudo-first-order and pseudo-second-order equations. The kinetic explanation is a critical dynamic process by removing different pollutants from contaminated solutions since it could describe the equilibrium period, reaction order, and reaction side and consequently define the behavior and the rate-governing phase of the contaminant catching from the wastewater onto the adsorbent material. Kinetic models stipulate vision with result data essential for operating a successful biosorption model.

Generally, the biosorption method that relies basically on time could be categorized into different kinetic models such as pseudo-first-order (Lagergren 1898), pseudo-second-order (Ho and McKay 1999), Weber and Morris model (Weber Jr and Morris 1963), Boyd model (Okewale et al. 2013), Bingham's model (Malana et al. 2011), and Elovich model (Zeldowitsch 1934). Nevertheless, some challenges occur in the use of

these kinetic models. The first is that the pseudo-first-order and Pseudo second order models that are most commonly applied are empirical models with no apparent physical implication. With these empirical kinetic models, examining the molecule removal routes is difficult. It is essential to create the physical importance of observed kinetic patterns. The following is that while the physical implications of the differential kinetic models, such as the phenomenological external/internal and adsorption in active sites models, are well defined, the methods for explaining them are challenging. The mass transfer systems consuming these models have not been carefully examined. The complex explaining methods impede the applications of these models. The third one is that in some published papers, the kinetic models are employed in inappropriate manner due to some statistical interference.

Three phases make up the adsorption molecules transfer kinetics. External diffusion comes first. In this stage, the pollutant invades the aqueous medium around the adsorbent material—the concentration variations between the surface of the adsorbent and the overall contaminated solution fuel the external diffusion. Internal diffusion is the second phase. Internal diffusion defines the diffusion of the pollutant in the apertures of the used material. The third step is the adsorption of water pollutants in the active pore volumes of the adsorbent material (Elgarahy et al. 2021).

Pseudo-first-order reaction kinetic

This model is the utmost applied for the liquid–solid adsorption method and relies on the pseudo-first-order equation (Lagergren 1898). The pseudo-first-order model identifies the adsorption kinetics of molecules in an adsorbent surface by the following ordinary first-order differential equation Eq. (35) (Rodrigues and Silva 2016):

$$\ln(Q_e - Q_t) = \ln(Q_e) - K_1 t$$

where Q_e : the amount of adsorbate in the adsorbent at equilibrium (mg g^{-1}); Q_t : the amount of adsorbate in the adsorbent at time t (mg g^{-1}); K_1 : constant rate of Lagergren's first order; and t : time of contact (min).

Pseudo-second-order reaction kinetic

Adsorption takes place on two surface sites in pseudo-second order kinetics (some authors call it “Blanchard's model”), and therefore, can be expressed by the following second-order differential equation Eq. (37) (Naderi et al. 2018).

$$\frac{t}{Q_t} = \frac{1}{K_2 \times Q_e^2} + \frac{1}{Q_e} t$$

where Q_e is the amount of adsorbate in the adsorbent at equilibrium (mg g^{-1}); Q_t is the amount of adsorbate in the

adsorbent at time t (mg g^{-1}); K_2 is a constant rate of the pseudo-second-order; and t : time of contact (min).

Intraparticle diffusion model

In general, the adsorption process by porous carbonaceous materials involves four stages; (1) the border layer surrounding the particle receives the solute from the aqueous solution, (2) transfer of the solute to the adsorbent surface from the boundary layer, (3) the solute is transported to the adsorbent sites by diffusion in the micro- and macropores, and (4) interactions between the particles of the solute and the active sites of the adsorbent: Adsorption, complexation, and precipitation. The following equation could interpret this model:

$$Q_t = K_{ID} \sqrt{t} + I$$

Q_t is the amount of adsorbate in the adsorbent at time t (mg g^{-1}); K_{ID} is the constant rate of intraparticle diffusion; t : time of contact (min); and I is the intercept of intraparticle diffusion kinetic model. To test this isotherm, it is suitable to graph Q_t as a function of the square root of the contact time and to note the coefficient of determination R^2 .

Elovich model

In recent years, the adsorption of contaminants from aqueous solutions and the kinetics of gas adsorption on solids has been extensively described using the Elovich equation (Ho 2006). This model matches the following equation (Chien and Clayton 1980).

$$Q_t = \beta \ln(\alpha\beta) - \ln(t)$$

where Q_t : the amount of adsorbate in the adsorbent at time t (mg g^{-1}); b : the number of sites available for adsorption; a : the initial adsorption rate ($\text{mg g}^{-1} \text{min}$); and t : time of contact (min).

Adsorption thermodynamics

Thermodynamics provides insight into the intrinsic energetic variations connected to the adsorption method, which is essential to explain the method's adsorption behavior, irreversibility, and naturalness. The thermodynamic parameters, ΔG° , ΔH° , and ΔS° , are typically assessed after implementing equilibrium tests at changed heats, which include a vast quantity of tentative studies, restraining the obtainable information for thermodynamic factor approximation. The description of these thermodynamic functions is the following: Gibbs free energy is essential for identifying the spontaneity of the system. When ΔG° is negative, the adsorption is

considered spontaneous, while $\Delta G^\circ > 0$ suggests non-spontaneity, demonstrating that the method involves energy from the environments to be expatriate to the equilibrium (Guo et al. 2017a).

Generally, the contaminant-biosorbent systems are spontaneous because an absorption slope mostly rules the adsorption process. Henceforth, its Gibbs-free energy is further beneficial in defining whether adsorption is preferred at advanced or lesser temperatures. Consequently, the enthalpy change indicates the outcome energy or the consumed energy. Adsorption is endothermic if the shift in Enthalpy is more significant than zero, while it is exothermic when it becomes less than zero (Vilela et al. 2019).

Most of the reactions are exothermic; nonetheless, one practicable identification of the endothermic mechanism is that when particles are nearby to be attached to the adsorbent material, they miss a portion of their hydration cover. This dehydration method uses energy that surpasses the exothermic behavior of connecting particles to the surface (Anastopoulos and Kyzas 2016). Ultimately, entropy change designates if the haphazardness rises or declines, subsequently, the adsorption method (Dirbaz and Roosta 2018). Gibbs free energy and Van't Hoff models are the furthestmost applied equations to evaluate thermodynamic factors (Akram et al. 2017; Lombardo and Thielemans 2019; Maity et al. 2018; Marques et al. 2019). The Clausius-Clapeyron model is not commonly applied because the change in enthalpy value could be deviated upon its use. Nevertheless, it is used favored in the solid–gas adsorption methods (Li et al. 2019a; Wang et al. 2018d).

Accurately calculating the thermodynamic values is essential for determining more details about the nature of the contaminant adsorption method (endothermic/exothermic/spontaneous/viability). Gibb's free energy variation, enthalpy, and entropy could be calculated at various temperatures by the following equations;

$$K_c = \frac{C_s}{C_e}$$

C_s and C_e represent the equilibrium value of the contaminant onto the adsorbent surface and in aqueous media, correspondingly. In contrast, an equilibrium constant, K_c , states the proportion of pollutant concentration on the adsorbent to the dissolved in an aqueous medium.

Mechanistic understanding of biosorption

Biosorption as a multidimensionally successful method has become emerging recently. It is elaborated as an advanced substitute to other traditional approaches for wastewater treatment (Demey et al. 2019). In the physicochemical

phenomenon, the sorbate particles (pollutants) gather on another particle (sorber) surface, as shown in Fig. 9. High-quality effluents are generated in this manner. The term "biosorption" is also defined simply, even though the "bio" prefix indicates a biological entity's involvement.

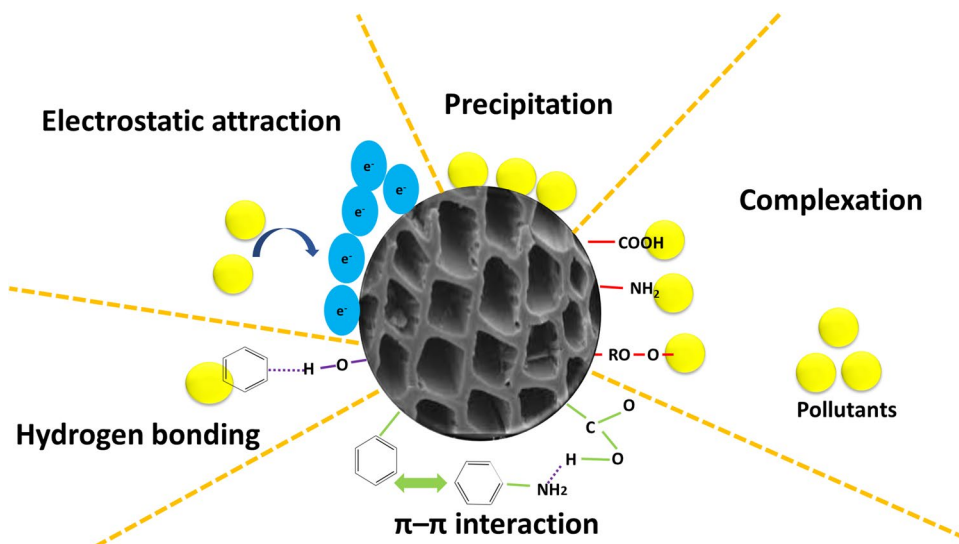
Regarding the sorption mechanism, both bioabsorption and biosorption dimensions are implicated. A material in such a state combined with another substance in a different state over absorption. It also covers the uptake of gases or liquids by solids or water. However, adsorption remains in a physical connection wherein a sorber and sorbate interact to form a contact (Maksoud et al. 2020). Biosorption requires all aspects of the interaction between some pollutants and the biological environment and is a submissive, metabolically independent process (biosorbent). It is essential to numerous processes that naturally take place throughout several scientific fields (Elgarahy et al. 2021; Tee et al. 2022).

Selection of biosorbents

The most crucial factor influencing the choice of biosorbent is well known to be its compatibility. An essential factor to consider when choosing a biosorbent is the cost and source of the biomass. Dead biomass is preferred over living biomass when making various biosorbents (Adewuyi 2020). Utilizing dead biomass has several advantages. It can be summed up as follows; (1) no need for growth requirements to remain included in the aqueous solution (e.g., media, nutrients); (2) no toxicity restrictions; (3) potential for reuse of exhausted adsorbent and pollutants, respectively, and (4) simpler statistical modeling of contaminants removal (Chan et al. 2022; Thirunavukkarasu et al. 2021). The selected biosorbent would also meet several other requirements, including eco-friendliness, ease of application, feasibility, and sustainability. This guarantees its prospective capacity

to eradicate various toxins from wastewater (Priya et al. 2022). There is a critical demand for more diverse excellent qualities that are described by biosorbents. This involves its excellent stability, high removal efficacy toward the targeted contaminants, and ease of regeneration (SafaÇelik et al. 2022). Regeneration and biosorbent adaptation to several models (such as batch and fixed bed reactors) would be heavily considered. Accessible waste should receive the utmost attention based on the concept of waste as wealth. Due to their environmental friendliness, their use offers several advantages. It is economically advantageous because it solves disposal issues and brings in money for several sectors. The abundant biological materials have structural differences that are notable (Sayin et al. 2021). Various ligands, including alcohol, aldehydes, carboxylic, hydroxyl, phosphate, thiol, ketones, phenolic, and ether compounds, make up their structure. Due to their variable levels of presence, they can interact with target pollutants in a variety of ways. A potential replacement for traditional methods is biosorption (Yaashikaa et al. 2021). It depends on how bio-wastes are used to remove various types of water pollutants. Its theory is designed to get two uses out of such bio-pollutants. This is accomplished by reusing them to actively contribute to trash minimization and maximize their usefulness (Gupta et al. 2019). As a result, it permits achieving the reduction concentrations supported by global or domestic rules and the World Health Organization (Hespanhol and Prost 1994). It distinguishes itself by exceptional qualities, including low production and running costs, adaptability, simplicity, and great efficiency. Several biosorbents based on activated carbon (Boulika et al. 2022), agriculture wastes (Bushra et al. 2021), bio-calcium carbonate (Arslanoğlu 2021), biochar (Xiang et al. 2022), bio-nanocomposites (Motaghi et al. 2021), bio-hydrogels (Wan et al. 2022), chitosan (Chen et al. 2022a), macroalgae (Elgarahy et al. 2019), and microalgae

Fig. 9 Adsorption mechanisms of biosorbents. This figure depicts the accumulation of pollutant molecules on the surface of an adsorbent. The bond strength between the adsorbent and adsorbate, which occurs through specific mechanisms, will influence the number of cycles required in the adsorption and desorption processes



(Shalaby et al. 2021) were used to purify different water pollutants.

For the treatment of wastewater, marine algae are regarded as an effective and alternative base sorbent. It considers the availability of renewable resources worldwide. Based on its hue and colloid content, it can be grouped. Oceans typically contain three basic kinds of organisms algal phyla, Chlorophyta, Phaeophyta, and Rhodophyta (Mokhtar et al. 2017). Recent research has shown that using microalgae is a sustainable substitute. Afshariani and Roosta (2019), for instance, researchers identified the batch and continuous removal of methylene blue in a contaminated solution. The ultimate sorption stayed attained at pH 9 and 30 °C, reaching 87.69 3.22 mg g⁻¹. To find a more effective leather dye adsorbent, defatted microalgae biomass (also known as microalgae biofuel waste) was inspected (da Fontoura et al. 2017). Acid Blue 161 solutions were applied in biosorption analyses. At room temperature and 40 °C, respectively, the highest concentration of a dye adsorbed was 75.78 mg g⁻¹ and 83.2 mg g⁻¹. The findings showed that biomass remarkably eliminated the dye amounts in real tannery waste effluents by 76.65%. Alginate, carrageenan, and polycolloid comprise the algal cell wall, primarily made up of polysaccharides. These ingredients are capable of removing several types of water contaminants (Daneshvar et al. 2017).

Macro and microalgae were used as strong contenders for eradicating heavy metals and synthetic dyes from aquatic systems (Chen et al. 2019a; da Rosa et al. 2018). *Enteromorpha flexuosa*, a green macroalga, was tested for its capacity to absorb crystal violet and methylene blue cationic dyes from aqueous media (Elgarahy et al. 2019). The findings demonstrated that the removal efficacy of 90.3% and 93.4% under ideal variable circumstances, respectively, were attained. The primary component of green algae is cellulose, coupled with many proteins and polysaccharides to form glycoproteins (Jayakumar et al. 2014). These compounds have several functional groups (e.g., amino, hydroxyl, carbonyl, and carboxyl). They are interestingly crucial to sorption (Rangabhashiyam et al. 2016). Brown algae are distinguished by having a wide variety of metabolites, including halogenated substances, polyphenols, terpenoids, laminarins, fucoidans, mannitol, and alginates (Saravana et al. 2018; Farghali et al. 2023). Salts of calcium, phosphate, and sodium make up alginates. The primary naturally occurring components of the cell wall of brown seaweed are sodium salts. Its weight is almost between 30 and 40%. These polysaccharides are linear anionic and water-soluble (Fernando et al. 2019). For extracting alginate from brown seaweed, various pre-extraction treatment techniques were employed (Saravana et al. 2018). Numerous researchers have tested the usage of biochar synthesized from microalgae as another type of sorbent for removing heavy metals from

contaminated solutions (Amin and Chetpattananondh 2019). Many trials on the efficacy of cobalt eradication employing biochar have been implemented in a batch scheme. The equilibrium numbers matched the Freundlich, Temkin, and D-R isotherm models. The Langmuir biosorption amount became 1.117 mg g⁻¹ (Bordoloi et al. 2017). It has been identified that biochar synthesized from water hyacinths (*Eichhornia crassipes*) was a successful sorbent to remove several heavy metals from contaminated water and prevent the harmful effects of the existing invasive species. The further value of harvesting aqueous hyacinth medium as biomass for biochar is that it has fewer invading species effect on delicate aquatic environments. The cadmium removal from a contaminated medium by applying biochar-alginate capsules was studied, with maximal sorption amounts varying from 24.2 to 45.8 mg g⁻¹ (Liu et al. 2020a).

Recently, batch biosorption of the rare-earth element ytterbium from the aqueous media using alginate and sericin particles chemically crosslinked with poly(vinyl alcohol) was explored. The equilibrium point revealed that at 55 °C, ytterbium had a maximum biosorption capacity of 0.642 mmol g⁻¹. Calcium carbonate was used as the pore-forming agent to create sodium alginate-based beads with varying amounts of the pore-forming agent to increase alginate gel beads' sorption capabilities. According to the experimental findings, copper (II) adsorption's capability rose by at least twofold (from 13.69 to 33.88 mg g⁻¹). Alginate-PEI beads were functionalized by phosphorylation and used for the sorption of neodymium (III) and molybdenum in another recent method of alginate modification (VI). While the phosphorylation of molybdenum (VI) significantly limits the enhancement, it considerably increases the sorption of neodymium (III). Because molybdate species have a strong affinity for amine groups, the phosphorylation of alginate-polyethyleneimine (PEI) beads enhanced neodymium(III) maximal sorption capacity from 0.61 to 1.46 mmol g⁻¹. However, the neodymium (VI) uptake increase is much less pronounced (from 1.46 to 2.09 mmol g⁻¹).

Chitin is a precursor of chitosan. It is primarily extracted from waste shellfish, such as crab or shrimp shells (Elwakeel et al. 2018). Chitosan sorbent can be cross-linked by different crosslinking agents either (e.g., citric acid, sodium tripolyphosphate, and polyaspartic acid sodium salt) or covalent (e.g., epichlorohydrin, trimethylol propane, and triglycidyl ether) to improve its stability (Jóźwiak and Filipkowska 2020). The Reactive Black 5 dye removal efficacy was significantly impacted by ionic crosslinking using the chitosan hydrogel. After 24 h of the sorption procedure, chitosan cross-linked with sodium citrate and sulfosuccinate had a greater sorption capacity of 46.7% and 37.2%, respectively, than chitosan, which had not been cross-linked. Moreover, after 24 h of sorption, it was noticed that the removal efficiency of the chitosan cross-associated with glutaraldehyde

and trimethylolpropane triglycidyl ether reduced to 35.3% and 26.6% lesser than that of unmodified chitosan. The unmodified chitosan displayed the maximum sorption removal (2307.0 mg g^{-1}) once the sorption equilibrium had been reached.

In comparison, the sorption potential of the crosslinked hydrogels (ionically/covalently) ranged from 2005 to 2164 mg g^{-1} and from 2083.0 to 2183.0 mg g^{-1} , respectively (Józwiak and Filipkowska 2020). Chitosan-based magnetic sorbent decorated with polypyrrole was synthesized to remove anionic methyl orange and cationic crystal violet dye from wastewater. The removal performance was measured at 88.11% and 92.89% under optimized operational conditions for crystal violet and methyl orange dyes. Though the pseudo-first-order kinetic model more closely matched methyl orange, the pseudo-second-order better reflected crystal violet adsorption. The results from the reaction equilibrium for the two dyes closely fitted the Langmuir isotherm model, which owned a maximum sorption capacity of 62.89 and 89.29 mg g^{-1} for crystal violet and methyl orange dyes, respectively. Chitosan can also be altered by becoming immobilized on another polymer. For instance, ethoxy-functionalized 4-methyl-2-(naphthalen-2-yl)-N-propylpentanamide efficaciously modified chitosan (Jabli 2020) and then examined for the presence of methylene blue and acid blue. After applying multiple beads, the adsorption capacity increased 1.4 times for acid blue 25 and three times for methylene blue, in comparison with the capacity of the original chitosan beads.

Adding tiny volumes of chitosan and Yttrium trivalent to the acid-based fly ash created another chitosan hybrid composite with a saturation adsorption amount of 627 mg g^{-1} (Li et al. 2020a). The researchers put much effort into improving chitosan's selectivity towards metal ions. For instance, developing highly selective sorbents is possible by grafting 2-mercapto benzimidazole onto chitosan microparticles. Another tactical component for the feasible recovery process of small chitosan particles is the integration of magnetite particles (Elwakeel et al. 2021). The sorbent demonstrated high eligibility for valued metals over base metals. Chitosan and 2-mercapto benzimidazole can create a very effective sorbent for recovering valuable metals from acidic leachates. Batch experiments were performed to estimate the adsorption capacities of the heavy metal pollutants (manganese, iron, cobalt, nickel, copper, and zinc) on chitosan relative to their comparable anions, sulfate, chloride, and nitrate (Weißpflog et al. 2020). The various heavy metal ions removal efficacy was analyzed using column tests. Upon comparison, the chloride anions and nitrate salts, respectively, the heavy metal cations of the sulfate salts and the sulfate ions adsorb to a substantially greater amount (Weißpflog et al. 2020).

To effectively eradicate chromium from wastewater, Luo et al. (2021) produced fluorescent chitosan built on hydrogel that contained titanate and cellulose nanofibers improved with carbon dots. The sorbent's increased capacity for adsorbing chromium of 228.2 mg g^{-1} may be primarily attributable to its porous design and the addition of titanate and cellulose nanofibers treated with carbon dots. By inserting co-polymerization on the surface of the chitosan/iron oxide composite, a sequence of magnetically modified chitosan adsorbents in conjunction with core-brush topology was produced. These sorbents were consequently applied to remove two water contaminants (e.g., diclofenac sodium and tetracycline hydrochloride) from the contaminated medium (Zhang et al. 2016).

Calcium carbonate is regarded as one of the most adaptable substances ever created by humans. It is pervasive and makes up more than 4% of the earth's crust. The common forms of calcium carbonate include chalk, marble, and limestone. The primary source of bio-calcium is the skeletons of some marine creatures, such as shellfish, crustacean shells, coral, seaweed, bivalves, and snails (Elwakeel et al. 2020). Aragonite, calcite, and vaterite are the three primary types of carbonate (Hoque et al. 2013). Even though the chemical makeup of all these forms is similar, they differ in terms of whiteness, homogeneity, thickness, and purity. Calcium carbonate has a distinctive white hue and is widely used in cement. In coatings features, including plastics, dyes, and paper productions, it has a wide range of purposes as a padding and/or coating material (Thilagan et al. 2015). Additionally, due to its antacid qualities, calcium carbonate is utilized in industrial locations to neutralize acidic mediums in soil and water (Correa et al. 2013).

A different fast-developing class of materials called MXenes is based on carbides or nitrides of transition metals (e.g., Titanium, Niobium, and Vanadium) and is applied for various purposes. MXenes have a large specific surface area, are chemically stable, and have various effective adsorption sites originating from external functional groups such as hydroxyl (Jeon et al. 2020). Due to its negative surface charge and robust-sheet-like structure, which contains plenty of active surface areas, titanium carbide ($\text{Ti}_3\text{C}_2\text{T}_x$), for example, removed 180 and 225 mg g^{-1} of barium and strontium ions in fracturing effluent. Metal–organic frameworks are crystalline hybrid inorganic–organic compounds. They have incredibly high specific surface areas reaching up to $6500 \text{ m}^2 \text{ g}^{-1}$ (Wang et al. 2015). They are excellent contenders for the adsorption of contaminants because they have a convenient pore volume and a spatial topology with an arranged porous composition originating from positive metal ions, metal groups, and organic connections (Huang et al. 2021a). Metal–organic frameworks are unstable in moist environments, but this can be remedied by changing the

surface with appropriate functionalization, such as water-balanced. Metal–organic framework with a great specific surface area ($1288 \text{ m}^2 \text{ g}^{-1}$) called MIL-53 (MIL stands for Matériaux de l'Institut Lavoisier) was applied to remove amoxicillin, which from the primary concentration of 150 mg L^{-1} , at a quantity of 0.1 g L^{-1} (Imanipoor et al. 2020). Another study found that a mercaptosuccinic-functionalized zirconium-based metal–organic framework with an adsorption amount of 1080 mg g^{-1} for Mercury ions and 510 mg g^{-1} for lead ions at pH 4.0 might potentially adsorb the harmful metals from wastewater (Wang et al. 2020a). Along with the substances mentioned overhead, carbonaceous materials such as carbon aerogels (Kalotra and Mehta 2022), carbon hydrogels (Yang et al. 2020b), and carbon xerogels (Girgis et al. 2012) also reported for the elimination of pollutants. These materials would share characteristics including an enormous specific surface area, great porosity, and organized structures even if they were created using various synthesis processes.

Graphene oxide and reduced graphene oxide, which are the graphene compound derivatives, own special sheet-like constructions, stand out among the numerous carbon nanostructures for their elevated specific surface area, high thermal stability, mechanical stability, and unique functional groups (Thakur et al. 2019). Although such materials exhibit strong adsorption capability, a significant problem that prevents various active sites from being available for contaminant remediation is their propensity to agglomerate. Aggregation is handled by including functional groups, such as oxygenated functional groups, or insertion constituents amongst graphene sheets (Baig et al. 2019). As an illustration, the reusability findings of fixed-bed removal revealed that a silica gel/graphene oxide-based adsorbent with an adsorption dosage of 147 mg g^{-1} for indium ions demonstrated successful regeneration (Li et al. 2021). The electrical characteristics, oxygen content, and interactions with contaminants of both graphene oxide and reduced graphene oxide-based adsorbents remain significantly influenced by structural intactness, which is sensitive to uncertain environments such as temperature, radiation, and specific pH media. The adsorption capacity of lead (Pb^{2+}) improved with irradiation doses. Nevertheless, an opposite tendency happened for chromium hexavalent, according to a rapid, substantial-ion-band and electron-beam radiation that altered the oxygen content of graphene oxide (Bai et al. 2016; Yang et al. 2021).

Another derivative of carbon nanomaterials is carbon nanotubes, comprising functionalized carbon nanotubes. Carbon nanotubes have fascinating structures, for instance, elevated thermal constancy, great chemical steadiness, nano-composition, uniform pore volume, exclusive specific surface area, ease of functional group formation, and tube-shaped construction, all of which produce great records of adsorption pore sites for removing different contaminants

such as heavy metals and synthetic dyes (Mashkooor and Nasar 2020; Sarkar et al. 2018).

A distinct category of carbon nanomaterials comprising functionalized carbon nanotubes is the diatomite-carbon nanotubes made through acid modification and chemical vapor deposition. It had a specific surface area of $50 \text{ m}^2 \text{ g}^{-1}$ and demonstrated two different adsorption capabilities. The high thermal and chemical steadiness, nano-composition, uniform pore size, great specific surface area, easiness of functionalization, and tube-shaped construction of carbon nanotubes are altogether intriguing properties that result in a significant number of adsorption sites for contaminants like metal ions and dyes.

Regeneration of spent adsorbents

Adsorbents that exhibit superior aquatic permanence can be easily separated from wastewater effluents after removing contaminants. The potential of exhausted adsorbents to be recovered, decontaminated, and regenerated will decide how useful they can be again (Yang et al. 2020a). A quality sorbent can be recycled and recovered for manufacturing, greatly reducing the cost of making adsorbents (Gupta et al. 2020). The restoration of used adsorbents can be done repeatedly; nevertheless, the restored adsorbent's adsorption capacity is lesser than that of recent adsorbents (Reddy et al. 2017). The effectiveness of the contaminant's desorption can be increased using the appropriate regeneration procedure. The viability of the industrial-scale application relies on numerous aspects, involving the sort of adsorbent, the pollutant, the adsorbent's stability, the toxicity of used adsorbents, and the expense and energy supplies of the recyclability method. Several methods involving magnetic separation (Tamjidi et al. 2019), filtration (Da'na and Awad 2017), thermal regeneration (Hwang et al. 2020), solvent reusability (Jiang et al. 2018), microwave treatment (Zhang et al. 2014b), supercritical fluid restoration (Shahadat and Isamil 2018), advanced oxidation method (Acevedo-García et al. 2020), and microbial-assisted pathway (Abromaitis et al. 2016) are used to recover the saturated adsorbents. Evaluating various recovery and regeneration procedures is crucial to recognize the ultimate recycling and dumping of exhausted adsorbents. Regeneration efficiencies of different sorbents in removing heavy metals, dyes or other contaminants and their adsorption efficiency are summarized in Tables 6, 7 and 8.

Regeneration methods

Thermal regeneration

Thermal desorption is a new technique for recovering metal from the used adsorbent. Thermal regeneration involves

Table 6 Regeneration efficiencies of adsorbents after adsorbing heavy metals from wastewater

Pollutant	Exhausted adsorbent	Regeneration method	Regeneration conditions	Removal%	References
Copper	Activated carbon	Filtration and acid treatment	pH = 5.5, temperature = 60 °C, time = 1 h, batch type, and 6M HCl/0.1M NaOH	87% (number of cycles = 10)	Da'na and Awad (2017)
Copper	Peat-based adsorbent	Hydrothermal carbonization	Temperature = 230 °C, time = 3 h, batch type, and aqua regia	25%	Kasiulienė et al. (2019b)
Copper	Biochar	Chemical regeneration	Batch type, and 0.1M NaOH	87% (number of cycles = 6)	Salvador et al. (2015)
Copper	Rice husk	Thermal treatment	pH = 6, temperature = 25 °C, time = 2 h, batch type, and methanol, HCl & NaOH	98% (number of cycles = 5)	Akhtar et al. (2006)
Copper	Pineapple leaf biochar	Chemical regeneration	pH = 4.5, temperature = 25 °C, time = 20 h, batch type, and 1M HCl	96% (number of cycles = 6)	Iamsaard et al. (2022)
Copper	Crosslinked carboxymethyl chitosan beads	Chemical regeneration	pH = 5, temperature = 25 °C, time = 24 h, batch type, and 0.1M HCl	99% (number of cycles = 1)	Yan et al. (2011)
Copper	Biochar/pectin/alginate hydrogel beads	Chemical regeneration	pH = 6, temperature = 30 °C, time = 24 h, batch type, and 0.2M HCl	81% (number of cycles = 5)	Zhang et al. (2020)
Copper	Chitosan coated sand	Chemical regeneration	pH = 1, temperature = 25 °C, time = 4 h, batch type, and 1.0 N HCl	99% (number of cycles = 1)	Wan et al. (2010)
Copper	Binary modified biochar	Chemical regeneration	Time = 12 h, batch type, and ethylenediamine-tetraacetic acid disodium salt (EDTA-2Na) solutions (0.1 mol L ⁻¹)	98.76% (number of cycles = 5)	Liu et al. (2021a)
Copper	Polyaniline/chitosan beads	Chemical regeneration	pH = 4, temperature = 25 °C, time = 3 h, batch type, and 0.01–0.5M HCl/HNO ₃ eluent	97% (number of cycles = 3)	Igberase et al. (2014)
Copper	<i>Eichhornia crassipes</i> biochar	Chemical regeneration	Temperature = 30 °C, batch type, and 0.5 mol L ⁻¹ HCl	41% (number of cycles = 10)	Lin et al. (2020a)
Copper	Calcite-modified biochar	Chemical regeneration	batch type, and 1M NaOH	97.87% (number of cycles = 4)	Wang et al. (2021)
Copper	Triphosphate crosslinked chitosan	Chemical regeneration	pH = 1, temperature = 25 °C, time = 3 h, batch type, and 1.0M HNO ₃ and ethylenediaminetetraacetic acid	88.7% (number of cycles = 1)	Laus and De Favere (2011)
Copper	Magnetic biochar	Chemical regeneration	Fixed-bed column, 0.1M NaOH	85% (number of cycles = 2)	Pan et al. (2020)
Copper	Hydroxyapatite-biochar	Chemical regeneration	Batch type, 0.2M HCl	98% (number of cycles = 5)	Wang et al. (2018b)

Table 6 (continued)

Pollutant	Exhausted adsorbent	Regeneration method	Regeneration conditions	Removal%	References
Zinc	Pineapple leaf biochar	Chemical regeneration	pH=4.5, temperature = 25 °C, time = 20 h, batch type, and 1M HCl	89% (number of cycles = 6)	Iamsaard et al. (2022)
Zinc	Chitosan/ferric-hydroxyapatite	Chemical regeneration	pH=6, temperature = 25 °C, time = 20 h, batch type, and 0.2–0.8M HCl	98% (number of cycles = 3)	Maleki et al. (2015)
Zinc	Oxidized <i>Eichhornia crassipes</i> biochar	Chemical regeneration	Temperature = 30 °C, batch type, and 0.5 mol L ⁻¹ HCl	47.5% (number of cycles = 10)	Lin et al. (2020a)
Zinc	Hydroxyapatite-biochar	Chemical regeneration	Batch type, and 0.2M HCl	95% (number of cycles = 5)	Wang et al. (2018b)
Cadmium	Chitosan with epichlorohydrin and triphosphate	Chemical regeneration	Temperature = 25 °C, time = 48 h, batch type, and 0.1M HCl and HNO ₃	89.9%	Laus et al. (2010)
Cadmium	<i>Eichhornia crassipes</i> biochar	Chemical regeneration	Temperature = 25 °C, batch type, and 0.5 mol L ⁻¹ HCl	44.5% (number of cycles = 10)	Lin et al. (2020a)
Cadmium	Alginate beads with attapulgite	Chemical regeneration	Temperature = 55 °C, time = 1 h, batch type, and 0.2M HCl	Number of cycles = 5	Wang et al. (2018c)
Cadmium	Modified biochar-based porous hydrogel	Chemical regeneration	Batch type, 0.3M HNO ₃ + 0.03M NaOH	9.3% (number of cycles = 5)	Wu et al. (2020)
Cadmium	Virgin biochar hydrogel	Chemical regeneration	Batch type, 0.3M HNO ₃ + 0.03M NaOH	0.13% (number of cycles = 5)	Wu et al. (2020)
Cadmium	Carboxymethyl βcyclodextrin polymer	Chemical regeneration	0.01M HNO ₃ /0.1M	Number of cycles = 4	Badruddoza et al. (2013)
Cadmium	Modified biochar	Chemical regeneration	1M NaOH	15.3% (number of cycles = 5)	Wu et al. (2021)
Cadmium	Chitosan/iron-hydroxyapatite	Chemical regeneration	pH = 6, time = 20 h, batch type, and 0.6M HCl	99% (number of cycles = 3)	Maleki et al. (2015)
Cadmium	Magnesium oxide-modified Crofton weed biochar	Chemical regeneration	pH = 5, batch type, and 1M NaOH	40% (number of cycles = 3)	Cheng et al. (2022)
Cadmium	Ethylene glycol tetraacetic acid (EGTA)-chitosan	Chemical regeneration	2M HNO ₃	99% (number of cycles = 10)	Zhao et al. (2013)
Cadmium	Potassium hydroxide-activated biochar	Chemical regeneration	pH = 6, temperature = 25 °C, time = 1 h, batch type, and 0.1M HCl	13% (number of cycles = 6)	Herath et al. (2021)
Cadmium	Peanut shell biochar	Chemical regeneration	pH = 5, temperature = 25 °C, and 0.2M HCl + 4% calcium chloride	85% (number of cycles = 5)	Wan et al. (2018)
Nickel	Chitosan- <i>Laminaria japonica</i>	Chemical regeneration	Batch type, HCl	71.73% (number of cycles = 1)	Fan et al. (2011)
Nickel	Pineapple leaf biochar	Chemical regeneration	pH = 4.5, temperature = 25 °C, time = 20 h, batch type, and 1M HCl	33% (number of cycles = 6)	Iamsaard et al. (2022)

Several methods can be used for regeneration, including chemical, thermal, hydrothermal, and microwave treatments. However, chemical regeneration is the most widely used method for desorption due to its popularity and cost-effectiveness. HCl, NaOH, and HNO₃ are hydrochloric acid, sodium hydroxide, and nitric acid, respectively

Table 7 Regeneration efficiencies of adsorbents after adsorbing dyes from wastewater

Pollutant	Exhausted adsorbent	Regeneration method	Regeneration conditions	Removal%	References
Basic blue 12	Wood residue biochar	Chemical regeneration	Batch type, and 0.3M HCl	25.3% (number of cycles = 3)	do Nascimento et al. (2021)
Methylene blue	Raw jujube shells	Chemical regeneration	Temperature = 24 °C, time = 50 min, batch type, and 0.5M HNO ₃	73.12% (number of cycles = 4)	Bereksi et al. (2018)
Methylene blue	Sulfuric acid-modified jujube shells	Chemical regeneration	Temperature = 24 °C, time = 50 min, batch type, and 0.5M HNO ₃	84% (number of cycles = 4)	El Messaoudi et al. (2021)
Methylene blue	Glomerata-based biochar	Chemical regeneration	Batch type, and 0.1M HCl	90% (number of cycles = 5)	Parsa et al. (2019)
Methylene blue	Cellulose/graphene oxide	Chemical regeneration	Temperature = 30 °C, time = 2 h, batch type, and dilute NaOH solution	93% (number of cycles = 3)	Parsa et al. (2019)
Methylene blue	Durian shell and jackfruit peel activated carbon	Microwave treatment	Temperature = 120 °C, time = 3 h, column reactor type	81.63% (number of cycles = 5)	Foo and Hameed (2012)
Reactive yellow 81	Porifera biochar	Chemical regeneration	Batch type, NaOH	99.3% (number of cycles = 3)	Foo and Hameed (2012)
Malachite green	Sulfur-treated tapioca peel	Chemical regeneration	Batch type, 0.1 NaOH	57% (number of cycles = 5)	Vigneshwaran et al. (2021b)
Congo red	Switchgrass-biochar	Chemical regeneration	Batch type, 3% HCl	46% (number of cycles = 5)	Iqbal et al. (2021)
Cibacron blue	Activated empty fruit fibers biochar	Chemical regeneration	Batch type, 0.3M HCl	91% (number of cycles = 7)	Jabar and Odusote (2020)

Chemical regeneration is also widely used for adsorbent regeneration. However, it is worth noting that most experiments have been conducted on a batch scale, which means that column bed systems need to be utilized to confirm the experimental results. HCl, NaOH, and HNO₃ are hydrochloric acid, sodium hydroxide, and nitric acid, respectively

raising a sorbent's temperature to a specified point to break the chemical and physical bonds that hold sorbate and sorbent together (Shahadat and Isamil 2018). Activated carbon is regenerated using this process on an industrial and commercial scale.

The carbon format and its volatile components will be eliminated from biochar when heated in the atmosphere at temperatures lower than 500 °C (Zhang et al. 2019a). Discarded-painting paper biochar with a superior preservative matter reduced lead metal ions from liquid media with the highest adsorption volume of 1555 mg g⁻¹ (Xu et al. 2017). Moreover, the wasted biochar was pyrolyzed at around 350 °C, which assisted in the gain of lead metal ions and subsequent conversion to lead oxide nanoparticles on the nano-biochar's surface with higher purity (greater than 96%). Turning exhausted adsorbents into beneficial products over thermal regeneration has received relatively little attention up to this point and is still in its beginning. However, the process's discharge of volatile compounds into the atmosphere could be a potential cause of secondary pollution. Potential impacts towards the ecosystem and

human health can be observed in the emission of Polycyclic aromatic hydrocarbons and dioxin as process byproducts. As a result, the benefit of biochar in carbon immobilization is eradicated (Toński et al. 2021). Multi-walled carbon nanotubes were effectively recycled, and it was used to remove cyclophosphamide, ifosfamide, and 5-fluorouracil along with a superior adsorption potential. For the greatest recovery of carbon nanotubes, the temperature and duration of the thermal recyclability requirements are varied, and the ideal circumstances are discovered to be 300 °C for 2 h. Findings further demonstrate that the adsorption capacity is unaffected even after 5 sets of adsorption and desorption.

In a further analysis, heat-treated gilsonite was utilized as an efficient adsorbent for removing toluene from wastewater (Saffarian Delkhosh et al. 2021). After four thermal recyclability sets, 250 °C and 20 min are used for regeneration, with adsorption effectiveness of 62.12%. Thermal regeneration demonstrated a higher toluene removal efficiency than acetone and ethanol washing. However, due to its quickness, selectivity, and regulated heating, microwave treatment technology is currently used to replace thermal regeneration

Table 8 Adsorption efficiencies of adsorbents towards different contaminants from wastewater

Pollutant	Adsorbent	Operational parameters	Adsorption mechanism	Adsorption capacity-removal%	References
Copper	Ethylenediamine-functionalized zirconium metal–organic framework	Sorbent mass = 50 mg; $C_0 = 100 \text{ mg L}^{-1}$; pH = 1.5–7, contact time = 20–360 min	Electron exchange, sharing, and covalent interactions	243.90 mg g^{-1}	Ahmadijokani et al. (2021)
Lead	Ethylenediamine-functionalized zirconium metal–organic framework	Sorbent mass = 3 g L^{-1} ; $C_0 = 140 \text{ mg L}^{-1}$; pH = 6, contact time = 360 min	Electron exchange, sharing, and covalent interactions	243.90 mg g^{-1}	Ahmadijokani et al. (2021)
Cadmium	Ethylenediamine-functionalized zirconium metal–organic framework	Sorbent mass = 100 mg; $C_0 = 20\text{--}300 \text{ mg L}^{-1}$; pH = 7, contact time = 24 h	Electron exchange, sharing, and covalent interactions	217.9 mg g^{-1}	Ahmadijokani et al. (2021)
Copper	Metal–organic framework modified bacterial cellulose/chitosan composite aerogel	Sorbent mass = 1 g; $C_0 = 1 \text{ g L}^{-1}$; pH = 6, contact time = 24 h	Coordination, ion exchange, and electrostatic interaction	200.6 mg g^{-1} , 100%	Li et al. (2020b)
Copper	Magnetic metal–organic framework–core–shell composite	Sorbent mass = 10 mg; $C_0 = 20 \text{ mg L}^{-1}$; pH = <2.5, contact time = 1 h	Ion-exchange and coordination reactions	301.33 mg g^{-1}	Jiang et al. (2021b)
Chromium	Hydroxypropyl chitosan/polyacrylamide/polyvinyl alcohol composite	Sorbent mass = 1 g; $C_0 = 100 \text{ mg L}^{-1}$; pH = 2, contact time = 48 h	Chemical adsorption	95.31 mg g^{-1}	Cao et al. (2021)
Copper	Chitosan/orange peel hydrogel composite	Sorbent mass = 4 g; $C_0 = 100 \text{ mg L}^{-1}$; pH = 5, contact time = 360 min	Not mentioned	181.884 mg g^{-1} , – 82.47%	Pavithra et al. (2021)
Copper	Functionalized cotton charcoal/chitosan biomass-based hydrogel	Sorbent mass = 0.01 g; $C_0 = 25 \text{ mg L}^{-1}$; pH = 6, contact time = 48 h	Surface complexation and electrostatic attraction	678.04 mg g^{-1}	(Fan et al. 2022)
Copper	Chitosan–montmorillonite composite aerogel	$C_0 = 22.5 \text{ mg L}^{-1}$; pH = 6, contact time = 50 min	Cation exchange	98.21%, 86.95 mg g^{-1}	Ye et al. (2021)
Copper	Nanocomposite beads (chitosan with paper sludge)	Sorbent mass = 0.1 g; $C_0 = 100 \text{ mg L}^{-1}$; pH = 4–8, contact time = 5 h	Physical diffusion and chemical sorption	114.6 mg g^{-1}	Xu et al. (2022)
Lead	Magnetic metal–organic framework (Fe ₃ O ₄ @ZIF-8) core–shell composite	Sorbent mass = 10 mg; $C_0 = 20 \text{ mg L}^{-1}$; pH = 2.5–3, contact time = 1 h	Ion exchange and coordination reactions	719.42 mg g^{-1}	Jiang et al. (2021b)
Lead	Zirconium metal–organic framework	Sorbent mass = 1.8 g; $C_0 = 1000 \text{ mg L}^{-1}$; contact time = 30 min	Ion-exchange	629 mg g^{-1}	Tamihara et al. (2021)
Lead	Zirconium metal–organic framework	Sorbent mass = 1 g L^{-1} ; $C_0 = 10$, 15 and 20 ppm; pH = 6.5, contact time = 120 min	Electrostatic, π – π , and surface interactions	937 mg g^{-1} , – 99.5%	Ahmad et al. (2021a)
Lead	Chitosan-assisted metal–organic framework	$C_0 = 0.1 \text{ mol L}^{-1}$; pH = 6, contact time = 2 h	Ion exchange, electrostatic adsorption, and coordination reactions	555.56 mg g^{-1}	Hu et al. (2022)
Lead	Modified magnetic-metal organic framework	Sorbent mass = 10 mg; $C_0 = 100 \text{ mg L}^{-1}$; pH = 6, contact time = 20 min	Intraparticle diffusion	397 mg g^{-1} , – 95 to 99%	Ragheb et al. (2022)

Table 8 (continued)

Pollutant	Adsorbent	Operational parameters	Adsorption mechanism	Adsorption capacity-removal%	References
Lead	Alginate-modified graphitic carbon nitride	Sorbent mass = 0.02 g; $C_0 = 500 \text{ mg L}^{-1}$; pH = 6, contact time = 110 min	Chemisorption	383.4 mg g^{-1}	Shen et al. (2020)
Lead	Calcium carbonate	$C_0 = 0.1 \text{ }\mu\text{M}$; pH = 5.4, contact time = 24 h	Heterogeneous nucleation and surface co-precipitation	100%	Fiorito et al. (2022)
Lead	Amino-modified chitosan/gold tailings composite	Sorbent mass = 20 mg; $C_0 = 200 \text{ mg L}^{-1}$; pH = 5, contact time = 24 h	Complexation, electrostatic interactions, and ion exchange	192.78 mg g^{-1}	Zhang et al. (2022d)
Cadmium	Modified magnetic-metal organic framework	Sorbent mass = 10 mg; $C_0 = 0.5 \text{ mol L}^{-1}$; pH = 6, contact time = 30 min	Intra-particle diffusion and liquid film diffusion	393 mg g^{-1} , – 95 to 99%	Ragheb et al. (2022)
Cadmium	Network nanostructured calcium alginate	Sorbent mass = 20 mg; $C_0 = 10 \text{ mg L}^{-1}$; pH = 5, contact time = 40 min	Diffusion-controlled process	86.69%	Tao et al. (2021)
Cadmium	Iron and manganese oxides modified biochar	Sorbent mass = 4 g L^{-1} ; $C_0 = 2 \text{ g L}^{-1}$; pH = 5.0 \pm 0.1, contact time = 30–60 min	Ion exchange, redox, electrostatic attraction, and cation- π interaction	120.77 mg g^{-1}	Tan et al. (2022)
Cadmium	Lanthanum-iron incorporated chitosan beads	Sorbent mass = 0.5 g L^{-1} ; $C_0 = 0.2 \text{ mg L}^{-1}$; pH = 6.5, contact time = 24 h	Chemical interaction	35.5 mg g^{-1} , – 80%	Lan et al. (2022)
Cadmium	Tin oxide-formaldehyde-chitosan	Sorbent mass = 0.05 mg; $C_0 = 1500 \text{ }\mu\text{mol g}^{-1}$; pH = 6, contact time = 10 s	Heterogeneous surface complexation	1050 $\mu\text{mol g}^{-1}$, – 99.2%	Mahmoud et al. (2022b)
Uranium	Oxidized rice straw biochar	Sorbent mass = 0.01 g; $C_0 = 50 \text{ mg L}^{-1}$; pH = 5.5, contact time = 4 h	Surface complexation	242.65 mg g^{-1}	Ahmed et al. (2021c)
Uranium	Magnetite-graphene oxide-chitosan	Sorbent mass = 15 mg; $C_0 = 50 \text{ ppm}$; pH = 6, contact time = 30 min	Surface complexation	504 mg g^{-1} , – 84.39%	Sharma et al. (2022)
Thorium	Chitosan-based aerogel	Sorbent mass = 0.1 g L^{-1} ; $C_0 = 4 \text{ mg L}^{-1}$; pH = 4, contact time = 20 min	Electrostatic interactions, surface complexation, and cation- π effect	526.2 mg g^{-1} , – 99.4%	Chen et al. (2022a)
Congo red	Microporous photoresponsive azobenzene dicarboxylate metal-organic framework	$C_0 = 100\text{--}400 \text{ mg L}^{-1}$; pH = 4, contact time = 24 h	Chemisorption	456.6 mg g^{-1}	Mogale et al. (2022)
Congo red	Magnetic chitosan	Sorbent mass = 0.045 g; $C_0 = 100 \text{ mL}$, 200 mg L^{-1} ; pH = 4, contact time = 2 h	Electrostatic interaction, hydrogen bond	727.8 mg g^{-1} , – 98.4%	Wang et al. (2022)
Tetracycline	Light-responsive iron benzene dicarboxylate	Sorbent mass = 20 mg; $C_0 = 50 \text{ mg L}^{-1}$; contact time = 6 h	Electrostatic interactions	97.05%	Zhang et al. (2022c)

Table 8 (continued)

Pollutant	Adsorbent	Operational parameters	Adsorption mechanism	Adsorption capacity-removal%	References
Tetracycline	Alkali-acid modified magnetic rice straw biochar	Sorbent mass = 30 mg; $C_0 = 50 \text{ mg L}^{-1}$; pH = 3–10, contact time = 120 min	Hydrogen bonding and pore-filling effect	98.33 mg g^{-1}	Dai et al. (2020)
Tetracycline	Modified Chitosan with zirconium and perlite	$C_0 = 20 \text{ mg L}^{-1}$; pH = 4, contact time = 24 h	Electron exchange	104.17 mg g^{-1}	Turan et al. (2022)
Methylene blue dye	Graphene oxide-chitosan composite	Sorbent mass = 1250 mg L^{-1} , $C_0 = 0.35 \text{ M}$; pH = 10, contact time = 50 min	Cross-linking	99.36%	Bryan et al. (2022)
Methylene blue dye	Chitosan–montmorillonite/poly-aniline	Sorbent mass = 0.05 g; $C_0 = 100 \text{ mg L}^{-1}$; contact time = 2 h	Electrostatic attraction	111 mg g^{-1} , – 98%	Mimisy et al. (2021)
Methylene blue dye	Lychee seed-based biochar	Sorbent mass = 50 mg; $C_0 = 50 \text{ mg L}^{-1}$; pH = 6, contact time = 45 min	Electrostatic force of interaction, hydrogen bonding interaction, and pi–pi interaction	124.5 mg g^{-1}	Sahu et al. (2020)

The adsorption mechanism involves several processes, including electron exchange, covalent interactions, ion exchange, π – π interactions, and surface interactions. This illustrates the non-selective behavior of various adsorbents and their ability to utilize different mechanisms in the adsorption process. The mechanism employed depends on various parameters, such as the reaction conditions, the type of pollutant (organic or inorganic), the characteristics of the adsorbent, and the interaction between the adsorbent and adsorbate. C_0 is the initial concentration

(Falciglia et al. 2018). This method entails the transformation of microwave radiation into heat at the molecular phase using adsorbent material (Falciglia et al. 2017). The sorbent is uniformly heated by microwave treatment from the exterior to the interior.

In contrast to traditional thermal heating, microwave heating preserved the sorbent's porous feature and the adsorbate's properties (Dai et al. 2019). Microwave irradiation technology effectively utilizes controlled heating to regenerate used sorbents. This technique takes advantage of the interaction between the delocalized electrons of activated carbon, the adsorbent material, and the microwave electrons. These interactions can facilitate the regeneration of activated carbon exhausted by perfluoroalkyl and polyfluoroalkyl substances. The dielectric properties of activated carbon, combined with the high volatility of the organic contaminants, contribute to the success of this regeneration process. In addition to being expensive to set up the plant, using microwave irradiation on an industrial scale to thermally desorb adsorbents is also an energy-intensive procedure. However, further research is necessary to determine whether microwave treatment may regenerate used sorbents (Gagliano et al. 2020).

Recently, pollutants loaded onto the exhausted adsorbents have been dissolved using a thermal process, producing a new material with a different porous composition and surface-chemical properties. Following this heat treatment of the used adsorbent, the resultant adsorbent was used to reabsorb similar contaminants with slightly reduced elimination capacities. For instance, Sonmez Baghizade et al. (2021) suggested a thermally adjusted method for efficiently reusing granular activated carbon loaded with perfluoroalkyl and polyfluoroalkyl materials. This method involves mineralizing the persistent Perfluoroalkyl and Polyfluoroalkyl Substances to recover the used granular activated carbon. Perfluoroalkyl and polyfluoroalkyl substances have been shown to desorb and volatilize at temperatures as low as 175 °C. However, they can also be mineralized at much higher temperatures, up to 700 °C (Xiao et al. 2020). High-temperature thermal desorption, in particular, leads to significant energy requirements that impede its sustainable use and applicable industrial manufacture. Thermally treated, wasted granular activated carbon may exhibit a growth in specific surface area and micropore size with temperature, although extremely high temperatures (over 1200 °C) may permanently damage the pore structure. Following removing the antidepressant medication contaminant amitriptyline, Chang et al. (2021) used a 600 °C modification for 2 h to renew a montmorillonite substance. The regenerated adsorbent's physicochemical characteristics changed, showing a removal of amitriptyline of 71.7 mg g^{-1} , or around 26% of the original montmorillonite. Therefore, using the thermal decomposition approach, it is crucial to use the

right temperature and treatment conditions (such as a gaseous atmosphere) to successfully regenerate an adsorbent. Future research is necessary for scientific advancement and process scaling because the thermal treatment settings can fluctuate based on the nature of adsorbents, pollutants, and the intent of the resulting product.

Chemical regeneration

Chemical regeneration is one of the most common methods for renewing adsorbent materials (Alsawy et al. 2022; Wu et al. 2020). It primarily depends on the concentration of the adsorbate and the forces interacting with the adsorbent. Chemical regeneration may better suit organic adsorbents with low boiling points and limited thermal stability (Dai et al. 2019). Solvents and chemical reagents are used in the chemical regeneration process. Acids and alkalis like phosphoric acid, nitric acid, sulfuric acid, ethylenediaminetetraacetic acid, calcium nitrate, sodium hydroxide, and sodium nitrate have been employed as regenerating solvents (Gupta et al. 2020; Hassan et al. 2020; Yang et al. 2020a). Baig et al. (2014) demonstrated that applying 0.5 M sodium hydroxide allowed arsenic ions to be regenerated from magnetic sorbent materials and subsequent magnetic sorbents to be recycled (Baig et al. 2014). A sizable desorption efficiency is monitored when acids are employed as regeneration solvents. In an acidic environment, adsorbent renewals and causes metals desorption from the surface of the adsorbent. Notably, the sorbent should have chemical stability as the adsorbent structure may be distorted by the chemical's action (Dai et al. 2019).

Supercritical fluid desorption

A substance is transformed into a supercritical fluid when heated over its critical temperature and squeezed past its critical pressure (Shahadat and Isamil 2018). Supercritical fluid desorption to regenerate used adsorbents is widespread and is considered a replacement for chemical-solvent and incineration methods (Efaq et al. 2015). The supercritical fluid desorption behaves as a typical solvent in the soil matrix and speeds up the process of pollutant desorption. The pollutant is further condensed by lowering the pressure until it can eventually be collected into a small container. Due to its incombustibility, non-hazardousness, and affordability, carbon dioxide is the most preferred for supercritical fluid desorption and is commonly utilized (Noman et al. 2020).

Additionally, supercritical fluid desorption exhibits a rapid mass transfer rate and reduced surface tension. Despite its advantages, carbon dioxide has a lower capacity for regeneration with phenol-loaded adsorbents (Humayun et al. 1998). To tackle this problem, authors substituted carbon dioxide with supercritical water, which completely

regenerated phenol from the phenol-loaded sorbent material and achieved effectiveness levels of about 100% (Salvador et al. 2013). The use of supercritical water has benefits and drawbacks. For example, it has a short process time, significantly lowering costs. Still, it also requires elevated pressure, which raises the method's cost and limits its industrial application. Supercritical water regeneration can only be used on a small scale. Zhang et al. (2019b) used an alkali metal catalyst and supercritical water regeneration to regenerate activated carbon using hydrogen peroxide. With a recyclability efficacy of 107%, the supercritical water regenerated trials had improved specific surface area ($813 \text{ m}^2 \text{ g}^{-1}$), contrary to the original samples ($765 \text{ m}^2 \text{ g}^{-1}$). Additionally, it has been revealed that the restoration temperatures ($385 \text{ }^\circ\text{C}$, $405 \text{ }^\circ\text{C}$, and $425 \text{ }^\circ\text{C}$), the hydrogen peroxide concentration, and the base metal behaving as a catalyst all impact the phenol contamination's capability to fasten to surfaces. In a unique study, Granular activated carbon is restored utilizing supercritical carbon dioxide (Carmona et al. 2014). Here, the pressure (e.g., 6, 15, 20, 31 MPa) and temperature (e.g., $45 \text{ }^\circ\text{C}$, $60 \text{ }^\circ\text{C}$) influenced the desorption yield of the contaminants. Intended for phenol, 2-chlorophenol, 4-chlorophenol, and 2,4-dichlorophenol, respectively, desorption yields of up to 97.9%, 68.3%, 71.5%, and 64.5% were achieved at 31 MPa and $45 \text{ }^\circ\text{C}$. To remove salicylic acid from bentonite that has been biologically functionalized, salgin used ethanol (Salgin et al. 2004). When no ethanol was used, the desorption efficiency was 76%, and when 10% (v/v) ethanol was applied, it was 98%. These results demonstrate the possible contribution of supercritical fluid desorption and the purpose of a co-solvent in the regeneration of toxins and recyclability of exhausted adsorbents. Nevertheless, for this procedure to be used on an industrial scale, creative methods for lowering the cost must be discovered.

Chemical versus thermal regeneration

The adsorption capabilities of such exhausted carbonaceous material are best enhanced by combining thermal and chemical regeneration. Compared to the temperature settings, acidic medium, and both treatment-washing steps, the latter brought more encouraging results in the regeneration process than the other recyclability treatments. The method was repeated five times to assess the consistency and removal efficacy of the carbonaceous material. The effectiveness and efficiency of the recycled adsorbent for removing various contaminants were demonstrated by the fact that this substance has nearly equal adsorption stability measurements and kinetic rate (Nahm et al. 2012). By using chemical, thermal, and electrochemical methods, the recyclability tests of phenol adsorbed on carbon-rich material (activated carbon) have been studied and evaluated. The sodium hydroxide-based alkaline medium improved phenol

desorption efficiency compared to pure water. A clearance efficacy of greater than 60% cannot be attained with this procedure. In this work, the phenol compounds were eliminated after 3 h of electrochemical exposure; however, thermal recyclability requires at least 450–600 °C to produce equivalent results. This study found that, when run under ideal operational parameters, electrochemical regeneration could remove particles with an efficiency of about 80% and produce surfaces with more functionality and surface area than thermal regeneration testing (77%). As a result, it might be suggested that chemical regeneration (in the electric field) is a better method than thermal regeneration (Berenguer et al. 2010). When *Enteromorpha Porifera*-derived biochar polluted with polycyclic aromatic hydrocarbon compound (Pyrene) was regenerated at 80, 150, and 200 °C, the renewal effectiveness was 35%, 45%, and 48%, respectively, indicating a correlation between the heat and the removal capability.

In experiments using iron-based biochar to remove microcystin-LR from polluted aqueous media, quartet sets of persulfate recyclability experiments achieved a removal efficacy of 92.81% and a regeneration efficiency of 82.89% in lake water. Furthermore, increasing the temperature from 20 to 50 °C significantly enhanced microcystin-LR oxidation and the impact of persulfate during the persulfate recyclability tests on iron-based biochar (Zeng and Kan 2022). A peroxy monosulfate-enhanced novel electrochemical method was used to regenerate rice-based biochar. Regeneration was successfully achieved under suboptimal conditions using a 75:1 ratio of peroxy monosulfate (PMS) to fluoxetine, 150 mA of appropriate current, and 0.15 mM of citric acid. Multiple adsorption–desorption cycles were completed successfully with minimal heat while maintaining the biochar's consistency. This technique demonstrates the applicability of chemical regeneration, which can be used under optimal conditions without external heat (Escudero-Curiel et al. 2021).

The regeneration process using the (water cleansing + nitrogen purging + alkali soaking) method was successful. The iron-copper-potassium hydroxide/biochar reusability test was conducted under medium conditions of 500 °C and 13% potassium hydroxide soaking matter. After three cycles of this test, the findings showed that the sulfur desorption had reached 42.64 mg sulfur g⁻¹, close to the adsorbent's initial removal capability of 48.58 mg sulfur g⁻¹. The nitrogen-wide approach reduced the ferric sulfate (Fe₂(SO₄)₃) into ferric oxide (Fe₂O₃), recovering a sizable amount of pre-diameter and effective components. However, the oxidation of the used-up biochar at a high temperature decreased regeneration effectiveness. The alkaline soaking procedure supplied the hydroxyl group. It reclaimed its alkaline strength, which helped with the desorption of sulfur. However, the high alkalinity levels in the medium resulted in the clogging of the pores of the employed biochar. It thus

decreased the capacity for desorption. The block influence of the potassium hydroxide in the medium was blamed for the reduced removal capacity (Song et al. 2017).

Exhausted adsorbent management and disposal

Secondary contamination is the primary restriction on chemical regeneration. It should be thought about managing used adsorbents sustainably to protect the environment. Disposal methods were suggested for reuse, incineration, and landfilling (Baskar et al. 2022; Lata et al. 2015). The old adsorbents can be recycled for soil fertilizers, energy transfer, storage devices, capacitors, and catalyst/catalyst support. Findings showed that nutrient-enriched biochar is an organic fertilizer that might replace synthetic fertilizers (Liu et al. 2019). Shortly, metal-impregnated green materials could replace carbon nanotubes and be utilized as supercapacitors or to remove tar (Baskar et al. 2022). When exhausted adsorbent material is applied as a supplier of thermal power rather than coal, incinerating waste results in less corrosiveness and harmful gas emissions. This process is known as waste-to-energy (Martín-Lara et al. 2016). Landfilling is a method for disposing of exhausted adsorbents, where the concentration of pollutants in the used adsorbent is identified before dumping to determine the acceptability of this method. For materials contaminated with heavy metals, pretreatment is required before landfilling. Other strategies, such as microwave irradiation, phyto-capping, and phytoremediation, could also be applied (Alsawy et al. 2022; Fuke et al. 2021).

Perspective

In order to release wastewater into the environment, it must first undergo a cleaning process to remove various organic and inorganic impurities. Adsorption using organic and inorganic adsorbent materials such as charcoal, activated carbon, clay minerals, and zeolite is a standard method for removing unwanted substances from wastewater. Exhausted adsorbents can often be recycled for the circular economy through various techniques, including filtration, chemical and thermal regeneration, and advanced oxidation methods. The recovery and regeneration approaches are significantly impacted by the type of pollutant and the adsorbent used. Regenerated samples perform exceptionally well in terms of wastewater adsorption. There is a growing interest in developing advanced, high-capacity adsorbents for extracting and recovering pollutants from wastewater. Researchers are also focusing on the cost and safety of the adsorption process. The recovery of sorbed pollutants after disposing of end-of-life adsorbents has been a significant challenge until recently. The adsorbents can now be recycled as catalysts,

capacitors, or soil amendments, or they can be safely disposed of through incineration or landfilling.

Reusing used adsorbents not only reduces application costs but also has environmental benefits. Chitosan-based materials have many applications, including tissue engineering, medication delivery, bioimaging, and wound healing (Ahmad et al. 2017, 2019, 2021b). Repurposing used chitosan-based materials for such applications would be interesting. Life cycle analysis is a valuable tool for assessing a system's environmental and financial viability, including wastewater treatment. This method considers both positive and negative effects, considering waste management, cost, energy use, and safety. For example, a life cycle analysis was conducted on activated carbon from discarded cherry and sour cherry kernels (Vukelic et al. 2018). This complex process involves various components: transportation, management, chemical handling, water and acid usage, energy consumption, rinsing, waste paper utilization, and wastewater treatment. The results indicate that utilizing waste cherry and sour cherry kernels for this process is economically and environmentally feasible, with minimal environmental impact when implemented at a production scale. Researchers must focus on life cycle analysis, especially for new adsorbents, to better understand their environmental impact. In order to successfully implement the regeneration technology for practical applications, several challenges need to be addressed in future research works:

- Many studies have focused on using adsorbents to remove a single contaminant from synthetic wastewater, which is impractical for real-world applications. Therefore, future studies should consider using genuine sewage wastewater with a mixture of contaminants to assess the effectiveness of the regeneration method.
- Developing cost-effective technologies for recycling pollutants from used adsorbents should be a key research focus.
- Characterizing the adsorbent material (e.g., surface structure, porosity, and functionality) after each regeneration cycle is essential to fully understanding the regeneration process. Therefore, artificial intelligence technologies can be developed to predict optimal recovery conditions and facilitate the long-term use of the adsorbent in wastewater treatment applications.
- The surface of many adsorbents can be modified to enhance their adsorption capacity while reducing regeneration problems. Therefore, researchers should suggest further modification methods that could aid in the complete chemical regeneration of the adsorbent material.
- The potential benefits of using biomass feedstocks in situ for functionalization and material improvement should be explored to reduce costs and improve sustainability.

- Previous experiments have demonstrated the effectiveness of using certain adsorbents to extract and recover precious metals from wastewater, but the scale of these experiments was limited. Therefore, further research is needed to scale up the use of adsorbents in wastewater treatment and to strengthen the technical feasibility of the adsorption/desorption process.
- The oxidative breakdown of organic contaminants is necessary for chemical regeneration, but it is still unclear whether harmful by-products may be produced. Thus, further research is required to ensure the safety and environmental impact of the regeneration process.

Conclusion

The success of biosorbents depends on their physical and surface chemistry characteristics, and understanding the removal mechanisms of each class of adsorbent is crucial to ensure high adsorption performance. The use of raw industrial waste and its functionalization offers a promising strategy for sanitation and water reuse, aligning with sustainable development objectives. This review has discussed various preparation and modification techniques to produce efficient biosorbents using various materials, including wood, bacteria, algae, herbaceous materials, agricultural waste, and animal waste. The preparation method to control the magnetic sorbents' shape, morphology, magnetic property, and particle size was also discussed.

Adsorption processes using different adsorbents were evaluated for removing various contaminants from wastewater and water, providing insights into isotherm and kinetic models for optimizing adsorption behavior and designing effective pollutant-adsorbent systems. The review also covers techniques for recovering, decontaminating, and regenerating exhausted adsorbents, emphasizing the importance of maximizing their reuse. Finally, future recommendations on biosorbents and magnetic sorbents are highlighted. Overall, this review emphasizes the crucial role of biosorbents and adsorption processes in promoting sustainable development and the circular economy.

Acknowledgements Dr. Ahmed I. Osman and Prof. David W. Rooney wish to acknowledge the support of The Bryden Centre project (Project ID VA5048), which was awarded by The European Union's INTERREG VA Programme, managed by the Special EU Programmes Body (SEUPB), with match funding provided by the Department for the Economy in Northern Ireland and the Department of Business, Enterprise and Innovation in the Republic of Ireland. The researcher (Mohamed Hosny) is funded by a full scholarship (MM32/21) from the Egyptian Ministry of Higher Education & Scientific Research represented by the Egyptian Bureau for Cultural & Educational Affairs in London.

Funding The authors have not disclosed any funding.

Declarations

Conflict of interest The authors declare no conflict of interest.

Open Access This article is licensed under a Creative Commons Attribution 4.0 International License, which permits use, sharing, adaptation, distribution and reproduction in any medium or format, as long as you give appropriate credit to the original author(s) and the source, provide a link to the Creative Commons licence, and indicate if changes were made. The images or other third party material in this article are included in the article's Creative Commons licence, unless indicated otherwise in a credit line to the material. If material is not included in the article's Creative Commons licence and your intended use is not permitted by statutory regulation or exceeds the permitted use, you will need to obtain permission directly from the copyright holder. To view a copy of this licence, visit <http://creativecommons.org/licenses/by/4.0/>.

References

- Abbasi M et al (2021) Enhanced adsorption of heavy metals in groundwater using sand columns enriched with graphene oxide: lab-scale experiments and process modeling. *J Water Process Eng* 40:101961. <https://doi.org/10.1016/j.jwpe.2021.101961>
- Abdel Maksoud MIA et al (2020) Insight on water remediation application using magnetic nanomaterials and biosorbents. *Coord Chem Rev* 403:213096. <https://doi.org/10.1016/j.ccr.2019.213096>
- Abdel Maksoud MIA et al (2021) MoS₂-based nanocomposites: synthesis, structure, and applications in water remediation and energy storage: a review. *Environ Chem Lett* 19(5):3645–3681. <https://doi.org/10.1007/s10311-021-01268-x>
- Abdel Maksoud MIA et al (2022) Engineered magnetic oxides nanoparticles as efficient sorbents for wastewater remediation: a review. *Environ Chem Lett* 20(1):519–562. <https://doi.org/10.1007/s10311-021-01351-3>
- Abdelfatah AM et al (2021) Efficient adsorptive removal of tetracycline from aqueous solution using phytosynthesized nano-zero valent iron. *J Saudi Chem Soc*. <https://doi.org/10.1016/j.jscs.2021.101365>
- Abdić Š et al (2018) Adsorptive removal of eight heavy metals from aqueous solution by unmodified and modified agricultural waste: tangerine peel. *Int J Environ Sci Technol* 15(12):2511–2518. <https://doi.org/10.1007/s13762-018-1645-7>
- Abdullah H et al (2021) Bisphenol A removal by adsorption using waste biomass: isotherm and kinetic studies. *Biointerface Res Appl Chem* 11(1):8467–8481. <https://doi.org/10.33263/BRIAC111.84678481>
- Abromaitis V et al (2016) Biodegradation of persistent organics can overcome adsorption–desorption hysteresis in biological activated carbon systems. *Chemosphere* 149:183–189
- Abu-Saqr KK, Lubbad SH (2019) Assessment of various treatment methods and reagents for cleanup and conditioning of sphagnum peat moss as sorbents in removal of malachite green as a cationic organic dye probe from water. *SN Appl Sci* 1(1):1–10. <https://doi.org/10.1007/s42452-018-0021-z>
- Acemioğlu B (2022) Removal of a reactive dye using NaOH-activated biochar prepared from peanut shell by pyrolysis process. *Int J Coal Prep Util* 42(3):671–693. <https://doi.org/10.1080/19392699.2019.1644326>
- Acevedo-García V et al (2020) Synthesis and use of efficient adsorbents under the principles of circular economy: waste valorisation and electroadvanced oxidation process regeneration. *Sep Purif Technol* 242:116796. <https://doi.org/10.1016/j.seppur.2020.116796>
- Adeyemi AJW (2020) Chemically modified biosorbents and their role in the removal of emerging pharmaceutical waste in the water system. *Water* 12(6):1551. <https://doi.org/10.3390/w12061551>
- Afshariani F, Roosta A (2019) Experimental study and mathematical modeling of biosorption of methylene blue from aqueous solution in a packed bed of microalgae *Scenedesmus*. *J Clean Prod* 225:133–142. <https://doi.org/10.1016/j.jclepro.2019.03.275>
- Ahmad M et al (2017) Chitosan centered bionanocomposites for medical specialty and curative applications: a review. *Int J Pharm* 529(1–2):200–217. <https://doi.org/10.1016/j.ijpharm.2017.06.079>
- Ahmad M et al (2019) Chitosan-based nanocomposites for cardiac, liver, and wound healing applications. In: Inamuddin AM, Mohammad-Asiri A (eds) *Applications of nanocomposite materials in orthopedics*. Elsevier, Amsterdam, pp 253–262. <https://doi.org/10.1016/B978-0-12-813740-6.00013-2>
- Ahmad K et al (2021a) Effect of metal atom in zeolitic imidazolate frameworks (ZIF-8 & 67) for removal of Pb²⁺ & Hg²⁺ from water. *Food Chem Toxicol* 149:112008. <https://doi.org/10.1016/j.fct.2021.112008>
- Ahmad S et al (2021b) Chitosan-based bionanocomposites in drug delivery. In: Sharma S, Malik A, Gupta P (eds) *Bionanocomposites in tissue engineering and regenerative medicine*. Elsevier, Amsterdam, pp 187–203. <https://doi.org/10.1016/B978-0-12-821280-6.00024-6>
- Ahmad K et al (2022) Synthesis and evaluation of Ca-doped ferrihydrite as a novel adsorbent for the efficient removal of fluoride. *Environ Sci Pollut Res* 29(4):6375–6388. <https://doi.org/10.1007/s11356-021-16105-5>
- Ahmadijokani F et al (2021) Ethylenediamine-functionalized Zr-based MOF for efficient removal of heavy metal ions from water. *Chemosphere* 264(Pt 2):128466. <https://doi.org/10.1016/j.chemosphere.2020.128466>
- Ahmed MJ (2016) Application of agricultural based activated carbons by microwave and conventional activations for basic dye adsorption. *J Environ Chem Eng* 4(1):89–99. <https://doi.org/10.1016/j.jece.2015.10.027>
- Ahmed W et al (2021a) Fabrication, characterization and U (VI) sorption properties of a novel biochar derived from *Tribulus terrestris* via two different approaches. *Sci Total Environ* 780:146617. <https://doi.org/10.1016/j.scitotenv.2021.146617>
- Ahmed W et al (2021b) Oxidized biochar obtained from rice straw as adsorbent to remove uranium (VI) from aqueous solutions. *J Environ Chem Eng* 9(2):105104. <https://doi.org/10.1016/j.jece.2021.105104>
- Ahmed W et al (2021c) Oxidized biochar obtained from rice straw as adsorbent to remove uranium (VI) from aqueous solutions. *J Environ Chem Eng* 9(2):105104. <https://doi.org/10.1016/j.jece.2021.105104>
- Ahn S-K et al (2022) Adsorption mechanisms on perfluorooctanoic acid by FeCl₃ modified granular activated carbon in aqueous solutions. *Chemosphere*. <https://doi.org/10.1016/j.chemosphere.2022.134965>
- Ai Y et al (2022) Waste non-burn-free brick derived sulfhydryl functionalized magnetic zeolites and their efficient removal of uranium (VI) ions. *Appl Surf Sci* 571:151241. <https://doi.org/10.1016/j.apsusc.2021.151241>
- Akar ST et al (2012) Biosorption potential of the waste biomaterial obtained from *Cucumis melo* for the removal of Pb²⁺ ions from aqueous media: equilibrium, kinetic, thermodynamic and mechanism analysis. *Chem Eng J* 185:82–90. <https://doi.org/10.1016/j.cej.2012.01.032>
- Akbour RA et al (2020) Adsorption of anionic dyes from aqueous solution using polyelectrolyte PDAD-PDADMAC-modified-montmorillonite

- clay. *Desalin Water Treat* 208:407–422. <https://doi.org/10.5004/dwt.2020.26446>
- Akemoto Y et al (2021) Interpretation of the interaction between cesium ion and some clay minerals based on their structural features. *Environ Sci Pollut Res* 28(11):14121–14130. <https://doi.org/10.1007/s11356-020-11476-7>
- Akhtar M et al (2006) Sorption potential of rice husk for the removal of 2, 4-dichlorophenol from aqueous solutions: kinetic and thermodynamic investigations. *J Hazard Mater* 128(1):44–52. <https://doi.org/10.1016/j.jhazmat.2005.07.025>
- Akram M et al (2017) Biocomposite efficiency for Cr (VI) adsorption: kinetic, equilibrium and thermodynamics studies. *J Environ Chem Eng* 5(1):400–411. <https://doi.org/10.1016/j.jece.2016.12.002>
- Alamudy HA, Cho K (2018) Selective adsorption of cesium from an aqueous solution by a montmorillonite-prussian blue hybrid. *Chem Eng J* 349:595–602. <https://doi.org/10.1080/19392699.2020.1792456>
- Albayati TM et al (2019) Adsorption of binary and multi heavy metals ions from aqueous solution by amine functionalized SBA-15 mesoporous adsorbent in a batch system. *Desalin Water Treat* 151:315–321. <https://doi.org/10.5004/dwt.2019.23937>
- Al-dahri T et al (2022) Preparation and characterization of Linde-type A zeolite (LTA) from coal fly ash by microwave-assisted synthesis method: its application as adsorbent for removal of anionic dyes. *Int J Coal Prep Util* 42(7):2064–2077. <https://doi.org/10.1080/19392699.2020.1792456>
- Al-Ghouti MA, Da'ana DA (2020) Guidelines for the use and interpretation of adsorption isotherm models: a review. *J Hazard Mater* 393:122383. <https://doi.org/10.1016/j.jhazmat.2020.122383>
- Ali S (2018) Fabrication of a nanocomposite from an agricultural waste and its application as a biosorbent for organic pollutants. *Int J Environ Sci Technol* 15(6):1169–1178. <https://doi.org/10.1007/s13762-017-1477-x>
- Aljohani FS et al (2021) Water treatment from MB using Zn–Ag MWCNT synthesized by double arc discharge. *Materials* 14(23):7205. <https://doi.org/10.3390/ma14237205>
- Alsawy T et al (2022) A comprehensive review on the chemical regeneration of biochar adsorbent for sustainable wastewater treatment. *npj Clean Water* 5(1):1–21
- Al-Shehri BM et al (2021) A significant improvement in adsorption behavior of mesoporous TUD-1 silica through neodymium incorporation. *J Rare Earths* 39(4):469–476. <https://doi.org/10.1016/j.jre.2020.07.004>
- Alver E, Metin AÜ (2012) Anionic dye removal from aqueous solutions using modified zeolite: adsorption kinetics and isotherm studies. *Chem Eng J* 200:59–67
- Amabilis-Sosa LE et al (2022) Biochar-assisted bioengineered strategies for metal removal: mechanisms, key considerations, and perspectives for the treatment of solid and liquid matrices. *Sustainability* 14(24):17049. <https://doi.org/10.3390/su142417049>
- Amin M, Chetpattananondh P (2019) Biochar from extracted marine *Chlorella* sp. residue for high efficiency adsorption with ultrasonication to remove Cr (VI), Zn (II) and Ni (II). *Bioresour Technol* 289:121578
- Amin FR et al (2016) Biochar applications and modern techniques for characterization. *Clean Technol Environ Policy* 18(5):1457–1473. <https://doi.org/10.1007/s10098-016-1218-8>
- Amrhar O et al (2021) Removal of methylene blue dye by adsorption onto Natural Muscovite Clay: experimental, theoretical and computational investigation. *Int J Environ Anal Chem.* <https://doi.org/10.1080/03067319.2021.1897119>
- Anastopoulos I, Kyzas GZ (2016) Are the thermodynamic parameters correctly estimated in liquid-phase adsorption phenomena? *J Mol Liq* 218:174–185
- Aniagor CO et al (2021) Evaluation of the aqueous Fe (II) ion sorption capacity of functionalized microcrystalline cellulose. *J Environ Chem Eng* 9(4):105703. <https://doi.org/10.1016/j.jece.2021.105703>
- Aniagor CO et al (2022) Preparation of amidoxime modified biomass and subsequent investigation of their lead ion adsorption properties. *Clean Chem Eng.* <https://doi.org/10.1016/j.clce.2022.100013>
- Ansari MJ et al (2022) Synthesis and stability of magnetic nanoparticles. *BioNanoScience* 12(2):627–638
- Arasi MA et al (2021) Production of mesoporous and thermally stable silica powder from low grade kaolin based on eco-friendly template free route via acidification of appropriate zeolite compound for removal of cationic dye from wastewater. *Sustain Chem Pharm* 19:100366. <https://doi.org/10.1016/j.scp.2020.100366>
- Armah EK et al (2022) Biochar: production, application and the future. In: Bartoli M, Giorcelli M, Tagliaferro A (eds) *Biochar-productive technologies, properties and application*. IntechOpen, London. <https://doi.org/10.5772/intechopen.105070>
- Arora N, Sharma N (2014) Arc discharge synthesis of carbon nanotubes: comprehensive review. *Diam Relat Mater* 50:135–150
- Arslanoglu H (2021) Production of low-cost adsorbent with small particle size from calcium carbonate rich residue carbonation cake and their high performance phosphate adsorption applications. *J Mater Res Technol* 11:428–447
- Ashraf MA et al (2019) Treatment of Taman Beringin landfill leachate using the column technique. *Desalin Water Treat* 149:370–387. <https://doi.org/10.5004/dwt.2019.23839>
- Attallah OA et al (2016) Synthesis of non-aggregated nicotinic acid coated magnetite nanorods via hydrothermal technique. *J Magn Magn Mater* 399:58–63
- Atun G, Bascetin E (2003) Adsorption of barium on kaolinite, illite and montmorillonite at various ionic strengths. *Radiochim Acta* 91(4):223–228. <https://doi.org/10.1524/ract.91.4.223.19964>
- Aziz K et al (2022) Enhanced biosorption of bisphenol A from wastewater using hydroxyapatite elaborated from fish scales and camel bone meal: a RSM@BBD optimization approach. *Ceram Int* 48(11):15811–15823. <https://doi.org/10.1016/j.ceramint.2022.02.119>
- Badruddoza AZM et al (2013) Fe₃O₄/cyclodextrin polymer nanocomposites for selective heavy metals removal from industrial wastewater. *Carbohydr Polym* 91(1):322–332
- Bai J et al (2016) Oxygen-content-controllable graphene oxide from electron-beam-irradiated graphite: synthesis, characterization, and removal of aqueous lead [Pb (II)]. *ACS Appl Mater Interfaces* 8(38):25289–25296
- Bai M et al (2023) Enhancing cadmium removal efficiency through spinel ferrites modified biochar derived from agricultural waste straw. *J Environ Chem Eng* 11(1):109027. <https://doi.org/10.1016/j.jece.2022.109027>
- Baig SA et al (2014) Effect of synthesis methods on magnetic Kans grass biochar for enhanced As (III, V) adsorption from aqueous solutions. *Biomass Bioenergy* 71:299–310
- Baig N et al (2019) Graphene-based adsorbents for the removal of toxic organic pollutants: a review. *J Environ Manag* 244:370–382
- Bartczak P et al (2018) Removal of nickel (II) and lead (II) ions from aqueous solution using peat as a low-cost adsorbent: a kinetic and equilibrium study. *Arab J Chem* 11(8):1209–1222. <https://doi.org/10.1016/j.arabjc.2015.07.018>
- Baskar AV et al (2022) Recovery, regeneration and sustainable management of spent adsorbents from wastewater treatment streams: a review. *Sci Total Environ* 822:153555
- Bayramoglu G et al (2022) Preparation of effective green sorbents using *O. Princeps* alga biomass with different composition

- of amine groups: comparison to adsorption performances for removal of a model acid dye. *J Mol Liq* 347:118375. <https://doi.org/10.1016/j.molliq.2021.118375>
- Belousov P et al (2021) Sorption of ¹³⁷Cs and ⁹⁰Sr on organic sorbents. *Appl Sci* 11(23):11531. <https://doi.org/10.3390/app112311531>
- Belviso C et al (2021) Efficiency in Ofloxacin antibiotic water remediation by magnetic zeolites formed combining pure sources and wastes. *Processes* 9(12):2137. <https://doi.org/10.3390/pr9122137>
- Bensedira A et al (2022) Study of methylene blue dye elimination from water using polyaniline (PANI) and PANI/SiO₂ composite. *Polym Polym Compos* 30:09673911221141747. <https://doi.org/10.1177/09673911221141747>
- Benvenuti J et al (2020) Hybrid sol–gel silica adsorbent material based on grape stalk applied to cationic dye removal. *Environ Prog Sustain Energy* 39(4):e13398. <https://doi.org/10.1002/ep.13398>
- Bereksi ZS et al (2018) Effects of some operating parameters on sorption and desorption kinetics related to spotted golden thistle stalks and methylene blue; isotherm study at optimal pH and sorbent regeneration. *Prog React Kinet Mech* 43(2):173–188
- Berenguer R et al (2010) Comparison among chemical, thermal, and electrochemical regeneration of phenol-saturated activated carbon. *Energy Fuels* 24(6):3366–3372
- Bergaya F, Lagaly G (2013) General introduction: clays, clay minerals, and clay science. In: *Developments in clay science*, vol 5. Elsevier, Amsterdam, pp 1–19. [https://doi.org/10.1016/S1572-4352\(05\)01001-9](https://doi.org/10.1016/S1572-4352(05)01001-9)
- Bhatnagar A et al (2015) Agricultural waste peels as versatile biomass for water purification—a review. *Chem Eng J* 270:244–271
- Bhatti HN et al (2007) Removal of Zn (II) ions from aqueous solution using *Moringa oleifera* Lam. (horseradish tree) biomass. *Process Biochem* 42(4):547–553
- Biglari H (2017) Removal of Acid Orange 7 dye from aqueous solutions by adsorption onto Kenya tea pulps. *Electron Physician* 9(5):4312–4321. <https://doi.org/10.19082/4312>
- Bordelet G et al (2018) Chemical reactivity of natural peat towards U and Ra. *Chemosphere* 202:651–660. <https://doi.org/10.1016/j.chemosphere.2018.03.140>
- Bordoloi N et al (2017) Biosorption of Co (II) from aqueous solution using algal biochar: kinetics and isotherm studies. *Bioresour Technol* 244:1465–1469
- Boulaiche W et al (2019) Removal of heavy metals by chitin: equilibrium, kinetic and thermodynamic studies. *Appl Water Sci* 9(2):1–10
- Boulika H et al (2022) Definitive screening design applied to cationic & anionic adsorption dyes on Almond shells activated carbon: isotherm, kinetic and thermodynamic studies. *Mater Today Proc* 72:3336–3346
- Brunauer S et al (1938) Adsorption of gases in multimolecular layers. *J Am Chem Soc* 60(2):309–319
- Bryan MYK et al (2022) Graphene oxide-chitosan composite material as adsorbent in removing methylene blue dye from synthetic wastewater. *Mater Today Proc* 64:1587–1596
- Bu J et al (2019) Adsorption mechanisms of cesium at calcium–silicate–hydrate surfaces using molecular dynamics simulations. *J Nucl Mater* 515:35–51. <https://doi.org/10.1016/j.jnucmat.2018.12.007>
- Bursztyn Fuentes AL et al (2022) Paracetamol and ibuprofen removal from aqueous phase using a ceramic-derived activated carbon. *Arab J Sci Eng* 48:525–537
- Bushra R et al (2021) Current approaches and methodologies to explore the perceptive adsorption mechanism of dyes on low-cost agricultural waste: a review. *Microporous Mesoporous Mater* 319:111040
- Cao G et al (2020) Asymmetric gemini surfactants modified vermiculite-and silica nanosheets-based adsorbents for removing methyl orange and crystal violet. *Colloids Surf A Physicochem Eng Asp* 596:124735. <https://doi.org/10.1016/j.colsurfa.2020.124735>
- Cao J et al (2021) Hydroxypropyl chitosan-based dual self-healing hydrogel for adsorption of chromium ions. *Int J Biol Macromol* 174:89–100
- Carmona M et al (2014) Adsorption of phenol and chlorophenols onto granular activated carbon and their desorption by supercritical CO₂. *J Chem Technol Biotechnol* 89(11):1660–1667
- Cavalcante EH et al (2022) 3-Aminopropyl-triethoxysilane-functionalized tannin-rich grape biomass for the adsorption of methyl orange dye: synthesis, characterization, and the adsorption mechanism. *ACS Omega* 7(22):18997–19009. <https://doi.org/10.1021/acsomega.2c02101>
- Çelebi H (2020) Recovery of detox tea wastes: usage as a lignocellulosic adsorbent in Cr⁶⁺ adsorption. *J Environ Chem Eng* 8(5):104310. <https://doi.org/10.1016/j.jece.2020.104310>
- Chan SS et al (2022) Recent advances biodegradation and biosorption of organic compounds from wastewater: microalgae-bacteria consortium—a review. *Bioresour Technol* 344:126159
- Chang P-H et al (2021) Unravelling the mechanism of amitriptyline removal from water by natural montmorillonite through batch adsorption, molecular simulation and adsorbent characterization studies. *J Colloid Interface Sci* 598:379–387
- Chatterjee S et al (2005) Adsorption of a model anionic dye, eosin Y, from aqueous solution by chitosan hydrobeads. *J Colloid Interface Sci* 288(1):30–35. <https://doi.org/10.1016/j.jcis.2005.02.055>
- Chauhan M et al (2020a) Enhancement in selective adsorption and removal efficiency of natural clay by intercalation of Zr-pillars into its layered nanostructure. *J Clean Prod* 258:120686. <https://doi.org/10.1016/j.jclepro.2020.120686>
- Chauhan M et al (2020b) Ti-pillared montmorillonite clay for adsorptive removal of amoxicillin, imipramine, diclofenac-sodium, and paracetamol from water. *J Hazard Mater* 399:122832. <https://doi.org/10.1016/j.jhazmat.2020.122832>
- Chen K-L et al (2017) Adsorption of sulfamethoxazole and sulfapyridine antibiotics in high organic content soils. *Environ Pollut* 231:1163–1171. <https://doi.org/10.1016/j.envpol.2017.08.011>
- Chen B et al (2019a) A magnetically recyclable chitosan composite adsorbent functionalized with EDTA for simultaneous capture of anionic dye and heavy metals in complex wastewater. *Chem Eng J* 356:69–80
- Chen H et al (2019b) Upcycling food waste digestate for energy and heavy metal remediation applications. *Resour Conserv Recycl* X 3:100015. <https://doi.org/10.1016/j.rcrx.2019.100015>
- Chen S et al (2019c) Study on the adsorption of dyestuffs with different properties by sludge-rice husk biochar: adsorption capacity, isotherm, kinetic, thermodynamics and mechanism. *J Mol Liq* 285:62–74. <https://doi.org/10.1016/j.molliq.2019.04.035>
- Chen T et al (2019d) Integrated comparisons of thorium (IV) adsorption onto alkali-treated duckweed biomass and duckweed-derived hydrothermal and pyrolytic biochar. *Environ Sci Pollut Res* 26(3):2523–2530. <https://doi.org/10.1007/s11356-018-3789-x>
- Chen B et al (2022a) High efficient adsorption for thorium in aqueous solution using a novel tentacle-type chitosan-based aerogel: adsorption behavior and mechanism. *Int J Biol Macromol* 222:1747–1757
- Chen X et al (2022b) Isotherm models for adsorption of heavy metals from water—a review. *Chemosphere* 307:135545
- Cheng S et al (2022) High-efficiency removal of lead/cadmium from wastewater by MgO modified biochar derived from crofton weed. *Bioresour Technol* 343:126081
- Chien S, Clayton W (1980) Application of Elovich equation to the kinetics of phosphate release and sorption in soils. *Soil Sci Soc Am J* 44(2):265–268

- Chien CC et al (2011) Efficiency of moso bamboo charcoal and activated carbon for adsorbing radioactive iodine. *CLEAN Soil Air Water* 39(2):103–108. <https://doi.org/10.1002/clen.201000012>
- Chin AB, Yaacob II (2007) Synthesis and characterization of magnetic iron oxide nanoparticles via w/o microemulsion and Massart's procedure. *J Mater Process Technol* 191(1–3):235–237
- Cho E et al (2020) Cesium ion-exchange resin using sodium dodecylbenzenesulfonate for binding to Prussian blue. *Chemosphere* 244:125589. <https://doi.org/10.1016/j.chemosphere.2019.125589>
- Choudhary V, Philip L (2022) Sustainability assessment of acid-modified biochar as adsorbent for the removal of pharmaceuticals and personal care products from secondary treated wastewater. *J Environ Chem Eng* 10(3):107592. <https://doi.org/10.1016/j.jece.2022.107592>
- Chranioti C et al (2016) Comparison of spray, freeze and oven drying as a means of reducing bitter aftertaste of steviol glycosides (derived from *Stevia rebaudiana* Bertoni plant)—evaluation of the final products. *Food Chem* 190:1151–1158
- Chu TTH, Nguyen MV (2023) Improved Cr (VI) adsorption performance in wastewater and groundwater by synthesized magnetic adsorbent derived from Fe₃O₄ loaded corn straw biochar. *Environ Res* 216:114764. <https://doi.org/10.1016/j.envres.2022.114764>
- Chwastowski J, Staroń P (2022) Influence of *Saccharomyces cerevisiae* yeast cells immobilized on *Cocos nucifera* fibers for the adsorption of Pb(II) ions. *Colloids Surf A Physicochem Eng Asp* 632:127735. <https://doi.org/10.1016/j.colsurfa.2021.127735>
- Çiftçi H (2022) Removal of methylene blue from water by ultrasound-assisted adsorption using low-cost bentonites. *Chem Phys Lett.* <https://doi.org/10.1016/j.cplett.2022.139758>
- Conde-Cid M et al (2019) Competitive adsorption/desorption of tetracycline, oxytetracycline and chlortetracycline on pine bark, oak ash and mussel shell. *J Environ Manag* 250:109509. <https://doi.org/10.1016/j.jenvman.2019.109509>
- Contreras-Cortés AG et al (2019) Toxicological assessment of cross-linked beads of chitosan-alginate and *Aspergillus australensis* biomass, with efficiency as biosorbent for copper removal. *Polymers* 11(2):222
- Cordeiro NC, Kini MS (2018) A review on adsorption of cationic dyes using activated carbon. In: MATEC web of conferences
- Correa F et al (2013) Study of Co (II) and Cr (VI) adsorption from aqueous solution by CaCO₃/sub 3. *J Chem Soc Pak* 35(4):1088–1095
- Crini G et al (2019a) Conventional and non-conventional adsorbents for wastewater treatment. *Environ Chem Lett* 17(1):195–213. <https://doi.org/10.1007/s10311-018-0786-8>
- Crini G et al (2019b) Dye removal by biosorption using cross-linked chitosan-based hydrogels. *Environ Chem Lett* 17(4):1645–1666. <https://doi.org/10.1007/s10311-019-00903-y>
- da Fontoura JT et al (2017) Defatted microalgal biomass as biosorbent for the removal of Acid Blue 161 dye from tannery effluent. *J Environ Chem Eng* 5(5):5076–5084
- da Rosa ALD et al (2018) Biosorption of rhodamine B dye from dyeing stones effluents using the green microalgae *Chlorella pyrenoidosa*. *J Clean Prod* 198:1302–1310
- Da'na E, Awad A (2017) Regeneration of spent activated carbon obtained from home filtration system and applying it for heavy metals adsorption. *J Environ Chem Eng* 5(4):3091–3099
- Dada AO et al (2021) Two–three parameters isotherm modeling, kinetics with statistical validity, desorption and thermodynamic studies of adsorption of Cu (II) ions onto zerovalent iron nanoparticles. *Sci Rep* 11(1):1–15
- Dai Y et al (2019) The adsorption, regeneration and engineering applications of biochar for removal organic pollutants: a review. *Chemosphere* 223:12–27
- Dai J et al (2020) Effects of modification and magnetization of rice straw derived biochar on adsorption of tetracycline from water. *Bioresour Technol* 311:123455
- Daneshvar E et al (2017) A comparative study of methylene blue biosorption using different modified brown, red and green macroalgae—effect of pretreatment. *Chem Eng J* 307:435–446
- Das L et al (2021) Experimental and numerical modeling on dye adsorption using pyrolyzed mesoporous biochar in Batch and fixed-bed column reactor: isotherm, thermodynamics, mass transfer, Kinetic analysis. *Surf Interfaces* 23:100985. <https://doi.org/10.1016/j.surfin.2021.100985>
- Dasgupta S et al (2021) Copper and chromium removal from synthetic textile wastewater using clay minerals and zeolite through the effect of pH. *J Iran Chem Soc* 18(12):3377–3386. <https://doi.org/10.1007/s13738-021-02273-1>
- de Farias MB et al (2022) Natural and synthetic clay-based materials applied for the removal of emerging pollutants from aqueous medium. In: Giannakoudakis DA, Meili L, Anastopoulos I (eds) *Advanced materials for sustainable environmental remediation*. Elsevier, Amsterdam, pp 359–392. <https://doi.org/10.1016/b978-0-323-90485-8.00012-6>
- de Queiroga LNF et al (2019) Functionalized bentonites for dye adsorption: depollution and production of new pigments. *J Environ Chem Eng* 7(5):103333. <https://doi.org/10.1016/j.jece.2019.103333>
- De Rossi A et al (2018) Chromium (VI) biosorption by *Saccharomyces cerevisiae* subjected to chemical and thermal treatments. *Environ Sci Pollut Res* 25(19):19179–19186
- De Rossi A et al (2020) Synthesis, characterization, and application of *Saccharomyces cerevisiae*/alginate composites beads for adsorption of heavy metals. *J Environ Chem Eng* 8(4):104009. <https://doi.org/10.1016/j.jece.2020.104009>
- del Mar Orta OM et al (2019) Adsorption of propranolol onto montmorillonite: kinetic, isotherm and pH studies. *Appl Clay Sci* 173:107–114. <https://doi.org/10.1016/j.clay.2019.03.015>
- Demey H et al (2019) Boron removal from aqueous solutions by using a novel alginate-based sorbent: comparison with Al₂O₃ particles. *Polymers* 11(9):1509
- Dirbaz M, Roosta A (2018) Adsorption, kinetic and thermodynamic studies for the biosorption of cadmium onto microalgae *Parachlorella* sp. *J Environ Chem Eng* 6(2):2302–2309
- do Nascimento JM et al (2019) Biosorption Cu (II) by the yeast *Saccharomyces cerevisiae*. *Biotechnol Rep* 21:e00315. <https://doi.org/10.1016/j.btre.2019.e00315>
- do Nascimento BF et al (2021) Adsorption of reactive black 5 and basic blue 12 using biochar from gasification residues: batch tests and fixed-bed breakthrough predictions for wastewater treatment. *Bioresour Technol Rep* 15:100767
- Dobe N et al (2022) Removal of amaranth dye by modified Ngassa clay: linear and non-linear equilibrium, kinetics and statistical study. *Chem Phys Lett.* <https://doi.org/10.1016/j.cplett.2022.139707>
- dos Reis GS et al (2021) Preparation and application of efficient biobased carbon adsorbents prepared from spruce bark residues for efficient removal of reactive dyes and colors from synthetic effluents. *Coatings* 11(7):772. <https://doi.org/10.3390/coatings11070772>
- Duan S et al (2015) Effective removal of Pb (II) using magnetic Co₀. 6Fe₂. 4O₄ micro-particles as the adsorbent: synthesis and study on the kinetic and thermodynamic behaviors for its adsorption. *Colloids Surf A* 469:211–223
- Duan C et al (2020) Removal of heavy metals from aqueous solution using carbon-based adsorbents: a review. *J Water Process Eng* 37:101339

- Dubin M (1947) The equation of the characteristic curve of activated charcoal. Dokl Akad Nauk SSSR 55:327–329
- Dzieniańska A et al (2019) Effect of auxiliary substances on the adsorption of anionic dyes on low-moor peat. Desalin Water Treat 177:209–226. <https://doi.org/10.5004/dwt.2020.24933>
- Eberhardt TL, Min S-H (2008) Biosorbents prepared from wood particles treated with anionic polymer and iron salt: effect of particle size on phosphate adsorption. Bioresour Technol 99(3):626–630. <https://doi.org/10.1016/j.biortech.2006.12.037>
- Efaq A et al (2015) Supercritical carbon dioxide as non-thermal alternative technology for safe handling of clinical wastes. Environ Process 2(4):797–822
- El-Borady OM et al (2021) Antioxidant, anticancer and enhanced photocatalytic potentials of gold nanoparticles biosynthesized by common reed leaf extract. Appl Nanosci. <https://doi.org/10.1007/s13204-021-01776-w>
- El-Magied A et al (2021) Development of functionalized activated carbon for uranium removal from groundwater. Int J Environ Res 15(3):543–558. <https://doi.org/10.1007/s41742-021-00333-1>
- El-Monaem EMA et al (2021) Cobalt nanoparticles supported on reduced amine-functionalized graphene oxide for catalytic reduction of nitroanilines and organic dyes. NANO 16(04):2150039
- El-Monaem A et al (2022) Zero-valent iron supported-lemon derived biochar for ultra-fast adsorption of methylene blue. Biomass Convers Biorefinery. <https://doi.org/10.1007/s13399-022-02362-y>
- El-Nahas S et al (2020) Facile and affordable synthetic route of nano powder zeolite and its application in fast softening of water hardness. J Water Process Eng 33:101104. <https://doi.org/10.1016/j.jwpe.2019.101104>
- El-Shazly E et al (2021a) Kinetic and isotherm studies for the sorption of ¹³⁴Cs and ⁶⁰Co radionuclides onto supported titanium oxide. J Radioanal Nucl Chem 330(1):127–139. <https://doi.org/10.1007/s10967-021-07956-w>
- El-Shazly E et al (2021b) Sorption of ¹³⁴Cs radionuclide onto insoluble ferrocyanide loaded silica-gel. J Radioanal Nucl Chem 329(1):437–449. <https://doi.org/10.1007/s10967-021-07789-7>
- El Kassimi A et al (2021) Removal of two cationic dyes from aqueous solutions by adsorption onto local clay: experimental and theoretical study using DFT method. Int J Environ Anal Chem. <https://doi.org/10.1080/03067319.2021.1873306>
- El Messaoudi N et al (2017) Valorization and characterization of wood of the jujube shell: application to the removal of cationic dye from aqueous solution. J Eng Sci Technol 12(2):421–436
- El Messaoudi N et al (2021) Desorption study and reusability of raw and H₂SO₄ modified jujube shells (*Zizyphus lotus*) for the methylene blue adsorption. Int J Environ Anal Chem. <https://doi.org/10.1080/03067319.2021.1912338>
- El Naga AOA et al (2019) Fast removal of diclofenac sodium from aqueous solution using sugar cane bagasse-derived activated carbon. J Mol Liq 285:9–19. <https://doi.org/10.1016/j.molliq.2019.04.062>
- Elgarahy AM et al (2019) Microwave-accelerated sorption of cationic dyes onto green marine algal biomass. Environ Sci Pollut Res 26(22):22704–22722
- Elgarahy A et al (2020) Multifunctional eco-friendly sorbent based on marine brown algae and bivalve shells for subsequent uptake of Congo red dye and copper (II) ions. J Environ Chem Eng 8(4):103915
- Elgarahy A et al (2021) A critical review of biosorption of dyes, heavy metals and metalloids from wastewater as an efficient and green process. Clean Eng Technol 4:100209
- Elgarahy AM et al (2022) Magnetically separable solid phase extractor for static anionic dyes adsorption from aqueous solutions. Surf Interfaces 30:101962
- Elgazzar A et al (2020) Preparation of various sorbents from agro waste to remove some radionuclides and organic species from aqueous solutions. J Radioanal Nucl Chem 326(3):1733–1748. <https://doi.org/10.1007/s10967-020-07476-z>
- Eltaweil A et al (2020) Mesoporous magnetic biochar composite for enhanced adsorption of malachite green dye: characterization, adsorption kinetics, thermodynamics and isotherms. Adv Powder Technol 31(3):1253–1263
- Eltaweil AS et al (2022a) Recent developments in alginate-based adsorbents for removing phosphate ions from wastewater: a review. RSC Adv 12(13):8228–8248. <https://doi.org/10.1039/d1ra09193j>
- Eltaweil AS et al (2022b) Synthesis of a new magnetic sulfacetamide-ethylacetoacetate hydrazone-chitosan Schiff-base for Cr (VI) removal. Int J Biol Macromol. 222:1465–1475
- Elwakeel KZ et al (2018) Efficient retention of chromate from industrial wastewater onto a green magnetic polymer based on shrimp peels. J Polym Environ 26(5):1–12
- Elwakeel K et al (2020) Microwave assist sorption of crystal violet and Congo red dyes onto amphoteric sorbent based on upcycled Sepia shells. J Environ Health Sci Eng 18(1):35–50
- Elwakeel KZ et al (2021) 2-Mercaptobenzimidazole derivative of chitosan for silver sorption—contribution of magnetite incorporation and sonication effects on enhanced metal recovery. Chem Eng J 403:126265
- Escudero LB et al (2019) Recent advances on elemental biosorption. Environ Chem Lett 17(1):409–427
- Escudero-Curiel S et al (2021) Eco-approach for pharmaceutical removal: thermochemical waste valorisation, biochar adsorption and electro-assisted regeneration. Electrochim Acta 389:138694
- Essebaai H et al (2022) Green and eco-friendly montmorillonite clay for the removal of Cr (III) metal ion from aqueous environment. Int J Environ Sci Technol 19(4):2443–2454. <https://doi.org/10.1007/s13762-021-03303-4>
- Falciglia PP et al (2017) Remediation of Hg-contaminated marine sediments by simultaneous application of enhancing agents and microwave heating (MWH). Chem Eng J 321:1–10
- Falciglia PP et al (2018) A review on the microwave heating as a sustainable technique for environmental remediation/detoxification applications. Renew Sustain Energy Rev 95:147–170
- Fan W et al (2011) Biosorption of nickel ion by chitosan-immobilized brown algae *Laminaria japonica*. Chem Biochem Eng Q 25(2):247–254
- Fan S et al (2021) Fabrication of a CO₂-responsive chitosan aerogel as an effective adsorbent for the adsorption and desorption of heavy metal ions. J Hazard Mater 416:126225
- Fan X et al (2022) Functionalized cotton charcoal/chitosan biomass-based hydrogel for capturing Pb²⁺, Cu²⁺ and MB. J Hazard Mater 423:127191. <https://doi.org/10.1016/j.jhazmat.2021.127191>
- Fan Q et al (2019) Radionuclides sorption on typical clay minerals: modeling and spectroscopies. In: Interface science and technology, vol 29. Elsevier, Amsterdam, pp 1–38. <https://doi.org/10.1016/B978-0-08-102727-1.00001-7>
- Faraji M et al (2010) Magnetic nanoparticles: synthesis, stabilization, functionalization, characterization, and applications. J Iran Chem Soc 7(1):1–37
- Farghali M et al (2023) Seaweed for climate mitigation, wastewater treatment, bioenergy, bioplastic, biochar, food, pharmaceuticals, and cosmetics: a review. Environ Chem Lett 21(1):97–152. <https://doi.org/10.1007/s10311-022-01520-y>
- Febrianto J et al (2009) Equilibrium and kinetic studies in adsorption of heavy metals using biosorbent: a summary of recent studies. J Hazard Mater 162(2–3):616–645
- Ferkous H et al (2022) The removal of a textile dye from an aqueous solution using a biocomposite adsorbent. Polymers 14(12):2396. <https://doi.org/10.3390/polym14122396>

- Fernando IS et al (2019) Advances in functionalizing fucoidans and alginates (bio) polymers by structural modifications: a review. *Chem Eng J* 355:33–48
- Fiorito E et al (2022) Calcium carbonate as sorbent for lead removal from wastewaters. *Chemosphere* 296:133897
- Foo K, Hameed B (2012) A cost effective method for regeneration of durian shell and jackfruit peel activated carbons by microwave irradiation. *Chem Eng J* 193:404–409
- Franco DSP et al (2021) Conversion of the forest species *Inga marginata* and *Tipuana tipu* wastes into biosorbents: dye biosorption study from isotherm to mass transfer. *Environ Technol Innov* 22:101521. <https://doi.org/10.1016/j.eti.2021.101521>
- Freundlich H (1907) Über die adsorption in lösungen. *Z Phys Chem* 57(1):385–470
- Frišták V et al (2017) Sorption separation of Eu and As from single-component systems by Fe-modified biochar: kinetic and equilibrium study. *J Iran Chem Soc* 14(3):521–530. <https://doi.org/10.1007/s13738-016-1000-1>
- Fuke P et al (2021) Role of microbial diversity to influence the growth and environmental remediation capacity of bamboo: a review. *Ind Crops Prod* 167:113567
- Gagliano E et al (2020) Removal of poly-and perfluoroalkyl substances (PFAS) from water by adsorption: role of PFAS chain length, effect of organic matter and challenges in adsorbent regeneration. *Water Res* 171:115381
- Gao Y et al (2021) Functional biochar fabricated from waste red mud and corn straw in China for acidic dye wastewater treatment. *J Clean Prod* 320:128887. <https://doi.org/10.1016/j.jclepro.2021.128887>
- García D et al (2019) Sorption of Eu (III) on quartz at high salt concentrations. *Colloids Surf A Physicochem Eng Asp* 578:123610. <https://doi.org/10.1016/j.colsurfa.2019.123610>
- García-Rosero H et al (2022) Adsorption and thermal degradation of Atenolol using carbon materials: towards an advanced and sustainable drinking water treatment. *J Water Process Eng* 49:102987. <https://doi.org/10.1016/j.jwpe.2022.102987>
- Gaskin J et al (2008) Effect of low-temperature pyrolysis conditions on biochar for agricultural use. *Trans ASABE* 51(6):2061–2069
- Gemeay AH et al (2020) Chemical insight into the adsorption of reactive wool dyes onto amine-functionalized magnetite/silica core-shell from industrial wastewaters. *Environ Sci Pollut Res* 27(26):32341–32358. <https://doi.org/10.1007/s11356-019-06530-y>
- Gemicí BT et al (2021) Removal of methylene blue onto forest wastes: adsorption isotherms, kinetics and thermodynamic analysis. *Environ Technol Innov* 22:101501. <https://doi.org/10.1016/j.eti.2021.101501>
- Giannakoudakis DA et al (2016) Multi-parametric adsorption effects of the reactive dye removal with commercial activated carbons. *J Mol Liq* 213:381–389. <https://doi.org/10.1016/j.molliq.2015.07.010>
- Girgis BS et al (2012) Textural and adsorption characteristics of carbon xerogel adsorbents for removal of Cu (II) ions from aqueous solution. *J Non Cryst Solids* 358(4):741–747
- Goher ME et al (2015) Removal of aluminum, iron and manganese ions from industrial wastes using granular activated carbon and Amberlite IR-120H. *Egypt J Aquat Res* 41(2):155–164. <https://doi.org/10.1016/j.ejar.2015.04.002>
- Gollakota AR et al (2020) Synthesis of novel ZSM-22 zeolite from Taiwanese coal fly ash for the selective separation of Rhodamine 6G. *J Mater Res Technol* 9(6):15381–15393. <https://doi.org/10.1016/j.jmrt.2020.10.070>
- Gollakota AR et al (2023) Ionic liquid [bmim][TFSI] templated Na-X zeolite for the adsorption of (Cd²⁺, Zn²⁺), and dyes (AR, R6). *Environ Res* 216:114525. <https://doi.org/10.1016/j.envres.2022.114525>
- Gomaa H et al (2022) A hybrid mesoporous CuO@ barley straw-derived SiO₂ nanocomposite for adsorption and photocatalytic degradation of methylene blue from real wastewater. *Colloids Surf A Physicochem Eng Asp* 644:128811. <https://doi.org/10.1016/j.colsurfa.2022.128811>
- Goswami R et al (2016) Characterization of cadmium removal from aqueous solution by biochar produced from *Ipomoea fistulosa* at different pyrolytic temperatures. *Ecol Eng* 97:444–451. <https://doi.org/10.1016/j.ecoleng.2016.10.007>
- Goyal N et al (2018) Removal of emerging contaminants daidzein and coumestrol from water by nanozeolite beta modified with tetrasubstituted ammonium cation. *J Hazard Mater* 344:417–430. <https://doi.org/10.1016/j.jhazmat.2017.10.051>
- Guilhen SN et al (2019) Pyrolytic temperature evaluation of macauba biochar for uranium adsorption from aqueous solutions. *Biomass Bioenergy* 122:381–390. <https://doi.org/10.1016/j.biombioe.2019.01.008>
- Gul S et al (2019) A comprehensive review of magnetic nanomaterials modern day theranostics. *Front Mater* 6:179
- Gul S et al (2022) Efficient removal of methyl red dye by using bark of hopbush. *Water* 14(18):2831. <https://doi.org/10.3390/w14182831>
- Guo J et al (2017a) Dynamic and thermodynamic mechanisms of TFA adsorption by particulate matter. *Environ Pollut* 225:175–183
- Guo X et al (2017b) Sorption mechanisms of sulfamethazine to soil humin and its subfractions after sequential treatments. *Environ Pollut* 221:266–275. <https://doi.org/10.1016/j.envpol.2016.11.073>
- Guo S et al (2020) Dipyrindyl-based organo-silica nanosheets for three emerging micropollutants efficient removal: adsorption performance and mechanisms. *J Clean Prod* 260:121149. <https://doi.org/10.1016/j.jclepro.2020.121149>
- Guo J et al (2023) Macro-constructing zeolitic imidazole frameworks functionalized sponge for enhanced removal of heavy metals: the significance of morphology and structure modulation. *J Colloid Interface Sci* 630:666–675. <https://doi.org/10.1016/j.jcis.2022.10.019>
- Gupta NK et al (2019) Biosorption-a green method for the preconcentration of rare earth elements (REEs) from waste solutions: a review. *J Mol Liq* 274:148–164
- Gupta S et al (2020) Latest trends in heavy metal removal from wastewater by biochar based sorbents. *J Water Process Eng* 38:101561
- Gupta R et al (2022) Potential and future prospects of biochar-based materials and their applications in removal of organic contaminants from industrial wastewater. *J Mater Cycles Waste Manag.* <https://doi.org/10.1007/s10163-022-01391-z>
- Gurav R et al (2021) Application of macroalgal biomass derived biochar and bioelectrochemical system with *Shewanella* for the adsorptive removal and biodegradation of toxic azo dye. *Chemosphere* 264:128539. <https://doi.org/10.1016/j.chemosphere.2020.128539>
- Guy M et al (2022) process parameters optimization, characterization, and application of KOH-activated Norway spruce bark graphitic biochars for efficient azo dye adsorption. *Molecules* 27(2):456. <https://doi.org/10.3390/molecules27020456>
- Hamad HN, Idrus S (2022) Recent developments in the application of bio-waste-derived adsorbents for the removal of methylene blue from wastewater: a review. *Polymers* 14(4):783. <https://doi.org/10.3390/polym14040783>
- Hamed MM et al (2016) Preparation of activated carbon from doum stone and its application on adsorption of 60Co and 152+ 154Eu: equilibrium, kinetic and thermodynamic studies. *J Environ Radiat* 164:113–124. <https://doi.org/10.1016/j.jenvrad.2016.07.005>
- Haounati R et al (2021) Elaboration and properties of a new SDS/CTAB@ Montmorillonite organoclay composite as a superb adsorbent for the removal of malachite green from aqueous

- solutions. *Sep Purif Technol* 255:117335. <https://doi.org/10.1016/j.seppur.2020.117335>
- Haque ANMA et al (2020) Physicochemical properties of film fabricated from cotton gin trash. *Mater Chem Phys* 239:122009
- Haque ANMA et al (2021) A review on cotton gin trash: sustainable commodity for material fabrication. *J Clean Prod* 281:125300
- Hashem A et al (2021a) Application of novel butane-1, 4-dioic acid-functionalized cellulosic biosorbent for aqueous cobalt ion sequestration. *Cellulose* 28(6):3599–3615. <https://doi.org/10.1007/s10570-021-03726-9>
- Hashem A et al (2021b) Utilization of low-cost sugarcane waste for the adsorption of aqueous Pb (II): kinetics and isotherm studies. *Curr Res Green Sustain Chem* 4:100056. <https://doi.org/10.1016/j.crgsc.2021.100056>
- Hashem A et al (2022a) Instrumental characteristics and acid blue 193 dye sorption properties of novel lupine seed powder. *Clean Chem Eng*. <https://doi.org/10.1016/j.clce.2022.100011>
- Hashem A et al (2022b) *Lepidium sativum* seed powder: a novel biosorbent for acid orange 142 dye uptake. *Environ Process* 9(4):1–20. <https://doi.org/10.1007/s40710-022-00607-6>
- Hashem A et al (2022c) Apricot seed shell: an agro-waste biosorbent for acid blue 193 dye adsorption. *Biomass Convers Biorefinery*. <https://doi.org/10.1007/s13399-022-03272-9>
- Hassan M et al (2020) Critical review of magnetic biosorbents: their preparation, application, and regeneration for wastewater treatment. *Sci Total Environ* 702:134893
- Heidarinejad Z et al (2020) Methods for preparation and activation of activated carbon: a review. *Environ Chem Lett* 18(2):393–415. <https://doi.org/10.1007/s10311-019-00955-0>
- Herath A et al (2021) KOH-activated high surface area Douglas Fir biochar for adsorbing aqueous Cr (VI), Pb (II) and Cd (II). *Chemosphere* 269:128409
- Herrera-Barros A et al (2020) Cd (II) and Ni (II) uptake by novel biosorbent prepared from oil palm residual biomass and Al₂O₃ nanoparticles. *Sustain Chem Pharm* 15:100216. <https://doi.org/10.1016/j.scp.2020.100216>
- Hespanhol I, Prost A (1994) WHO guidelines and national standards for reuse and water quality. *Water Res* 28(1):119–124
- Ho Y-S (2006) Review of second-order models for adsorption systems. *J Hazard Mater* 136(3):681–689
- Ho S (2020) Removal of dyes from wastewater by adsorption onto activated carbon: mini review. *J Geosci Environ Prot* 8(5):120–131. <https://doi.org/10.4236/gep.2020.85008>
- Ho Y-S, McKay G (1999) Pseudo-second order model for sorption processes. *Process Biochem* 34(5):451–465
- Holt GA et al (2012) Fungal mycelium and cotton plant materials in the manufacture of biodegradable molded packaging material: evaluation study of select blends of cotton byproducts. *J Biobased Mater Bioenergy* 6(4):431–439
- Hoque ME et al (2013) Processing and characterization of cockle shell calcium carbonate (CaCO₃) bioceramic for potential application in bone tissue engineering. *J Mater Sci Eng* 2(4):132
- Hosny M et al (2021) Comparative study between *Phragmites australis* root and rhizome extracts for mediating gold nanoparticles synthesis and their medical and environmental applications. *Adv Powder Technol* 32(7):2268–2279. <https://doi.org/10.1016/j.apt.2021.05.004>
- Hosny M et al (2022) Phytofabrication of bimetallic silver-copper/biochar nanocomposite for environmental and medical applications. *J Environ Manag* 316:115238. <https://doi.org/10.1016/j.jenvman.2022.115238>
- Hu S et al (2022) Chitosan-assisted MOFs dispersion via covalent bonding interaction toward highly efficient removal of heavy metal ions from wastewater. *Carbohydr Polym* 277:118809
- Huang L et al (2021a) Adsorptive removal of pharmaceuticals from water using metal-organic frameworks: a review. *J Environ Manag* 277:111389
- Huang Q et al (2021b) Amorphous molybdenum sulfide mediated EDTA with multiple active sites to boost heavy metal ions removal. *Chin Chem Lett* 32(9):2797–2802
- Huang T et al (2022) A comprehensive investigation of zeolite-rich tuff functionalized with 3-mercaptopropionic acid intercalated green rust for the efficient removal of HgII and CrVI in a binary system. *J Environ Manag* 324:116344. <https://doi.org/10.1016/j.jenvman.2022.116344>
- Hugouenq P et al (2012) Iron oxide monocrystalline nanoflowers for highly efficient magnetic hyperthermia. *J Phys Chem C* 116(29):15702–15712
- Humayun R et al (1998) Supercritical fluid extraction and temperature-programmed desorption of phenol and its oxidative coupling products from activated carbon. *Ind Eng Chem Res* 37(8):3089–3097
- Huo H et al (2022) Phosphorylated wood designed as a biosorbent for effectively removing Ni²⁺ from wastewater. *Ind Crops Prod* 188:115727. <https://doi.org/10.1016/j.indcrop.2022.115727>
- Husnain SM et al (2017) Recyclable superparamagnetic adsorbent based on mesoporous carbon for sequestration of radioactive Cesium. *Chem Eng J* 308:798–808
- Hwang SY et al (2020) Pre-treatment methods for regeneration of spent activated carbon. *Molecules* 25(19):4561
- Iamsaard K et al (2022) Adsorption of metal on pineapple leaf biochar: key affecting factors, mechanism identification, and regeneration evaluation. *Bioresour Technol* 344:126131
- Igberase E et al (2014) The adsorption of copper (II) ions by polyaniline graft chitosan beads from aqueous solution: equilibrium, kinetic and desorption studies. *J Environ Chem Eng* 2(1):362–369
- Ighalo JO, Eletta OA (2020) Response surface modelling of the biosorption of Zn (II) and Pb (II) onto *Micropogonias undulatus* scales: Box–Behnken experimental approach. *Appl Water Sci* 10(8):1–12
- Ighalo JO et al (2022a) Recent advances in hydrochar application for the adsorptive removal of wastewater pollutants. *Chem Eng Res Des*. <https://doi.org/10.1016/j.cherd.2022.06.028>
- Ighalo JO et al (2022b) Utilization of avocado (*Persea americana*) adsorbents for the elimination of pollutants from water: a review. *Biomass Deriv Mater Environ Appl*. <https://doi.org/10.1016/B978-0-323-91914-2.00016-7>
- Ighalo JO et al (2022c) Adsorption of persistent organic pollutants (POPs) from the aqueous environment by nano-adsorbents: a review. *Environ Res* 212:113123. <https://doi.org/10.1016/j.envres.2022.113123>
- Igwegbe CA et al (2021) Environmental protection by the adsorptive elimination of acetaminophen from water: a comprehensive review. *J Ind Eng Chem* 104:117–135. <https://doi.org/10.1016/j.jiec.2021.08.015>
- Imanipoor J et al (2020) Adsorption and desorption of amoxicillin antibiotic from water matrices using an effective and recyclable MIL-53 (Al) metal-organic framework adsorbent. *J Chem Eng Data* 66(1):389–403
- Imran A et al (2012) Removal of direct red 81 dye from aqueous solution by native and citric acid modified bamboo sawdust: kinetic study and equilibrium isotherm analyses. *Gazi Univ J Sci* 25(1):59–87
- Iqbal MM et al (2021) Effective sequestration of Congo red dye with ZnO/cotton stalks biochar nanocomposite: modeling, reusability and stability. *J Saudi Chem Soc* 25(2):101176
- Iwanow M et al (2017) Preparation of supported palladium catalysts using deep eutectic solvents. *Chem A Eur J* 23(51):12467–12470. <https://doi.org/10.1002/chem.201702790>

- Iwanow M et al (2020) Activated carbon as catalyst support: precursors, preparation, modification and characterization. *Beilstein J Org Chem* 16(1):1188–1202. <https://doi.org/10.3762/bjoc.16.104>
- Jabar JM, Odusote YA (2020) Removal of cibacron blue 3G-A (CB) dye from aqueous solution using chemo-physically activated biochar from oil palm empty fruit bunch fiber. *Arab J Chem* 13(5):5417–5429
- Jaber M et al (2013) Synthesis of clay minerals. In: *Developments in clay science*, vol 5. Elsevier, Amsterdam, pp. 223–241. <https://doi.org/10.1016/B978-0-08-098258-8.00009-2>
- Jabli M (2020) Synthesis, characterization, and assessment of cationic and anionic dye adsorption performance of functionalized silica immobilized chitosan bio-polymer. *Int J Biol Macromol* 153:305–316
- Jabłońska B (2021) Optimization of Ni (II), Pb (II), and Zn (II) ion adsorption conditions on pliocene clays from post-mining waste. *Minerals* 11(6):568. <https://doi.org/10.3390/min11060568>
- Jadhav AC, Jadhav NC (2021) Treatment of textile wastewater using adsorption and adsorbents. In: *Sustainable technologies for textile wastewater treatments*. Elsevier, Amsterdam, pp. 235–273. <https://doi.org/10.1016/B978-0-323-85829-8.00008-0>
- Jalali R et al (2002) Removal and recovery of lead using nonliving biomass of marine algae. *J Hazard Mater* 92(3):253–262. [https://doi.org/10.1016/S0304-3894\(02\)00021-3](https://doi.org/10.1016/S0304-3894(02)00021-3)
- Jayakumar R et al (2014) Sorption of hexavalent chromium from aqueous solution using marine green algae *Halimeda gracilis*: optimization, equilibrium, kinetic, thermodynamic and desorption studies. *J Environ Chem Eng* 2(3):1261–1274
- Jayakumar V et al (2021) Sustainable removal of cadmium from contaminated water using green alga—optimization, characterization and modeling studies. *Environ Res* 199:111364
- Jeon M et al (2020) A review on MXene-based nanomaterials as adsorbents in aqueous solution. *Chemosphere* 261:127781
- Ji Y et al (2019) Single and simultaneous adsorption of methyl orange and p-chlorophenol on organo-vermiculites modified by an asymmetric gemini surfactant. *Colloids Surf A Physicochem Eng Asp* 580:123740. <https://doi.org/10.1016/j.colsurfa.2019.123740>
- Jiang D et al (2018) Removal and recovery of phosphate from water by Mg-laden biochar: batch and column studies. *Colloids Surf A* 558:429–437
- Jiang K et al (2021a) Adsorption of Pb (II) and Zn (II) ions on humus-like substances modified montmorillonite. *Colloids Surf, A* 631:127706
- Jiang X et al (2021b) Magnetic metal-organic framework (Fe₃O₄@ZIF-8) core-shell composite for the efficient removal of Pb (II) and Cu (II) from water. *J Environ Chem Eng* 9(5):105959
- Jodeh S et al (2022) Experimental and theoretical study for removal of trimethoprim from wastewater using organically modified silica with pyrazole-3-carbaldehyde bridged to copper ions. *BMC Chem* 16(1):1–17. <https://doi.org/10.1186/s13065-022-00814-0>
- Jose J et al (2020) Evaluation of selected solvent systems for the single-cycle separation of Am (III) from Eu (III) using aqueous soluble sulphonated bis-triazinylpyridine. *J Mol Liq* 306:112893. <https://doi.org/10.1016/j.molliq.2020.112893>
- Jose S et al (2022) Biochar from oil cakes: an efficient and economical adsorbent for the removal of acid dyes from wool dye house effluent. *Clean Technol Environ Policy*. <https://doi.org/10.1007/s10098-021-02253-2>
- Joseph CG et al (2019) Application of modified red mud in environmentally-benign applications: a review. *Environ Eng Res* 25(6):795–806. <https://www.eeer.org/articles/archive.phphttps://doi.org/10.4491/eeer.2019.374>
- Jóźwiak T, Filipkowska U (2020) Sorption kinetics and isotherm studies of a Reactive Black 5 dye on chitosan hydrogel beads modified with various ionic and covalent cross-linking agents. *J Environ Chem Eng* 8(2):103564
- Kakavandi B et al (2018) Efficient adsorption of cobalt on chemical modified activated carbon: characterization, optimization and modeling studies. *Desalin Water Treat* 111:310–321. <https://doi.org/10.5004/dwt.2018.22238>
- Kalkan E, Nadaroglu H (2021) Adsorptive removal of Acid Fuchsin dye using by-product silica fume and laccase-modified silica fume. *Iran J Chem Chem Eng: IJCCE* 40(2):551–564
- Kalotra S, Mehta R (2022) Carbon aerogel and polyaniline/carbon aerogel adsorbents for Acid Green 25 dye: synthesis, characterization and an adsorption study. *Chem Eng Commun* 209(6):757–773
- Kannan P et al (2021) Neutralization of Bayer bauxite residue (red mud) by various brines: a review of chemistry and engineering processes. *Hydrometallurgy* 206:105758
- Karaman C et al (2022) Congo red dye removal from aqueous environment by cationic surfactant modified-biomass derived carbon: equilibrium, kinetic, and thermodynamic modeling, and forecasting via artificial neural network approach. *Chemosphere* 290:133346. <https://doi.org/10.1016/j.chemosphere.2021.133346>
- Karunakara N et al (2015) Evaluation of radon adsorption characteristics of a coconut shell-based activated charcoal system for radon and thoron removal applications. *J Environ Radioact* 142:87–95. <https://doi.org/10.1016/j.jenvrad.2014.12.017>
- Kasiulienė A et al (2019a) Treatment of metal (loid) contaminated solutions using iron-peat as sorbent: is landfilling a suitable management option for the spent sorbent? *Environ Sci Pollut Res* 26(21):21425–21436. <https://doi.org/10.1007/s11356-019-05379-5>
- Kasiulienė A et al (2019b) Hydrothermal carbonisation of peat-based spent sorbents loaded with metal (loid) s. *Environ Sci Pollut Res* 26:23730–23738
- Kaur H et al (2018) Effect of hydrophobicity of pharmaceuticals and personal care products for adsorption on activated carbon: adsorption isotherms, kinetics and mechanism. *Environ Sci Pollut Res* 25(21):20473–20485. <https://doi.org/10.1007/s11356-017-0054-7>
- Keerthan S et al (2020) Engineered tea-waste biochar for the removal of caffeine, a model compound in pharmaceuticals and personal care products (PPCPs), from aqueous media. *Environ Technol Innov* 19:100847. <https://doi.org/10.1016/j.eti.2020.100847>
- Khandaker S et al (2018) Adsorptive removal of cesium from aqueous solution using oxidized bamboo charcoal. *Water Resour Ind* 19:35–46. <https://doi.org/10.1016/j.wri.2018.01.001>
- Khandaker S et al (2021) Efficient cesium encapsulation from contaminated water by cellulosic biomass based activated wood charcoal. *Chemosphere* 262:127801. <https://doi.org/10.1016/j.chemosphere.2020.127801>
- Kim D-G et al (2022) Enhanced adsorption of tetracycline by thermal modification of coconut shell-based activated carbon. *Int J Environ Res Public Health* 19(21):13741. <https://doi.org/10.3390/ijerph192113741>
- Kolay PK, Taib SNL (2018) *Physical and geotechnical properties of tropical peat and its stabilization*. IntechOpen, London, pp 93–106. <https://doi.org/10.5772/intechopen.74173>
- Komissarov M, Ogura S (2019) International soil and water conservation research. *Int Soil Water Conserv Res: ISWCR* 8:56–65
- Koyuncu DDE, Okur M (2021) Investigation of dye removal ability and reusability of green and sustainable silica and carbon-silica hybrid aerogels prepared from paddy waste ash. *Colloids Surf A Physicochem Eng Asp* 628:127370. <https://doi.org/10.1016/j.colsurfa.2021.127370>
- Kumar S et al (2022) Characterization of power ultrasound modified kappaphycus alvarezii biosorbent and its modeling by artificial neural networks. *Water Air Soil Pollut* 233(7):1–20

- Kumari R, Dey S (2019) A breakthrough column study for removal of malachite green using coco-peat. *Int J Phytorem* 21(12):1263–1271. <https://doi.org/10.1080/15226514.2019.1633252>
- Kwikima MM et al (2021) Potentials of agricultural wastes as the ultimate alternative adsorbent for cadmium removal from wastewater. A review. *Sci Afr* 13:e00934. <https://doi.org/10.1016/j.sciaf.2021.e00934>
- Kwon S et al (2020) Selective and rapid capture of Sr²⁺ with LTA zeolites: effect of crystal sizes and mesoporosity. *Appl Surf Sci* 506:145029. <https://doi.org/10.1016/j.apsusc.2019.145029>
- Lagergren S (1898) Zur theorie der sogenannten adsorption gelöster stoffe. *Kungliga Svenska Vetenskapsakademiens Handlingar* 24:1–39
- Lahiri SK, Liu L (2021) Fabrication of a nanoporous silica hydrogel by cross-linking of SiO₂–H₃BO₃–hexadecyltrimethoxysilane for excellent adsorption of azo dyes from wastewater. *Langmuir* 37(29):8753–8764. <https://doi.org/10.1021/acs.langmuir.1c01046>
- Lan Z et al (2022) Lanthanum-iron incorporated chitosan beads for adsorption of phosphate and cadmium from aqueous solutions. *Chem Eng J* 448:137519
- Langmuir I (1916) The constitution and fundamental properties of solids and liquids. Part I. Solids. *J Am Chem Soc* 38(11):2221–2295
- Langmuir I (1918) The adsorption of gases on plane surfaces of glass, mica and platinum. *J Am Chem Soc* 40(9):1361–1403
- Largitte L et al (2016) Comparison of the adsorption of lead by activated carbons from three lignocellulosic precursors. *Microporous Mesoporous Mater* 219:265–275. <https://doi.org/10.1016/j.micromeso.2015.07.005>
- Lata S et al (2015) Regeneration of adsorbents and recovery of heavy metals: a review. *Int J Environ Sci Technol* 12(4):1461–1478
- Laus R, De Favere VT (2011) Competitive adsorption of Cu (II) and Cd (II) ions by chitosan crosslinked with epichlorohydrin-triphosphate. *Bioresour Technol* 102(19):8769–8776
- Laus R et al (2010) Adsorption and desorption of Cu (II), Cd (II) and Pb (II) ions using chitosan crosslinked with epichlorohydrin-triphosphate as the adsorbent. *J Hazard Mater* 183(1–3):233–241
- Lawchoochaisakul S et al (2021) Cationic starch intercalated montmorillonite nanocomposites as natural based adsorbent for dye removal. *Carbohydr Polym* 253:117230. <https://doi.org/10.1016/j.carbpol.2020.117230>
- Lee LY et al (2016) Effective removal of Acid Blue 113 dye using overripe *Cucumis sativus* peel as an eco-friendly biosorbent from agricultural residue. *J Clean Prod* 113:194–203. <https://doi.org/10.1016/j.jclepro.2015.11.016>
- Li K et al (2010) Characterization and lead adsorption properties of activated carbons prepared from cotton stalk by one-step H₃PO₄ activation. *J Hazard Mater* 181(1–3):440–447. <https://doi.org/10.1016/j.jhazmat.2010.05.030>
- Li D et al (2014) Aqueous 99Tc, 129I and 137Cs removal from contaminated groundwater and sediments using highly effective low-cost sorbents. *J Environ Radioact* 136:56–63. <https://doi.org/10.1016/j.jenvrad.2014.05.010>
- Li H et al (2019a) Analytical model and experimental investigation of the adsorption thermodynamics of coalbed methane. *Adsorption* 25(2):201–216
- Li M et al (2019b) Synthesis of magnetic biochar composites for enhanced uranium (VI) adsorption. *Sci Total Environ* 651:1020–1028. <https://doi.org/10.1016/j.scitotenv.2018.09.259>
- Li Y et al (2019c) Utilizing low-cost natural waste for the removal of pharmaceuticals from water: mechanisms, isotherms and kinetics at low concentrations. *J Clean Prod* 227:88–97. <https://doi.org/10.1016/j.jclepro.2019.04.081>
- Li B et al (2020a) Superior adsorption of direct dye from aqueous solution by Y (III)-chitosan-doped fly ash composite as low-cost adsorbent. *J Polym Environ* 28(6):1811–1821
- Li D et al (2020b) Multifunctional adsorbent based on metal-organic framework modified bacterial cellulose/chitosan composite aerogel for high efficient removal of heavy metal ion and organic pollutant. *Chem Eng J* 383:123127
- Li Y et al (2020c) Rapid removal of Sr²⁺, Cs⁺ and UO₂²⁺ from solution with surfactant and amino acid modified zeolite Y. *Microporous Mesoporous Mater* 302:110244. <https://doi.org/10.1016/j.micromeso.2020.110244>
- Li Y et al (2020d) Gradient adsorption of methylene blue and crystal violet onto compound microporous silica from aqueous medium. *ACS Omega* 5(43):28382–28392. <https://doi.org/10.1021/acscomega.0c04437>
- Li M et al (2021) Experimental and DFT studies on highly selective separation of indium ions using silica gel/graphene oxide based ion-imprinted composites as a sorbent. *Chem Eng Res Des* 168:135–145
- Li H et al (2022a) Comparison of adsorption capacity and removal efficiency of strontium by six typical adsorption materials. *Sustainability* 14(13):7723. <https://doi.org/10.3390/su14137723>
- Li W et al (2022b) Characterizing aqueous Cd²⁺ removal by plant biochars from Qinghai-Tibet Plateau. *Water* 14(24):4085. <https://doi.org/10.1016/j.scitotenv.2018.09.259>
- Lin S et al (2020a) Recycling application of waste long-root *Eichhornia crassipes* in the heavy metal removal using oxidized biochar derived as adsorbents. *Bioresour Technol* 314:123749
- Lin S et al (2020b) Machine-learning-assisted screening of pure-silica zeolites for effective removal of linear siloxanes and derivatives. *J Mater Chem A* 8(6):3228–3237. <https://doi.org/10.1039/C9TA11909D>
- Ling Y et al (2019) QSARs to predict adsorption affinity of organic micropollutants for activated carbon and β-cyclodextrin polymer adsorbents. *Water Res* 154:217–226. <https://doi.org/10.1016/j.watres.2019.02.012>
- Liu X et al (2019) Black liquor-derived calcium-activated biochar for recovery of phosphate from aqueous solutions. *Bioresour Technol* 294:122198
- Liu C et al (2020a) Removal of Cadmium (II) using water hyacinth (*Eichhornia crassipes*) biochar alginate beads in aqueous solutions. *Environ Pollut* 264:114785
- Liu S et al (2020b) Preparation, surface functionalization and application of Fe₃O₄ magnetic nanoparticles. *Adv Colloid Interface Sci* 281:102165
- Liu J et al (2021a) Preparation of Si–Mn/biochar composite and discussions about characterizations, advances in application and adsorption mechanisms. *Chemosphere* 281:130946
- Liu R et al (2021b) Reductive and adsorptive elimination of U (VI) ions in aqueous solution by SFeS@ Biochar composites. *Environ Sci Pollut Res* 28(39):55176–55185. <https://doi.org/10.1007/s11356-021-14835-0>
- Liu T et al (2022a) Technologies for removing pharmaceuticals and personal care products (PPCPs) from aqueous solutions: recent advances, performances, challenges and recommendations for improvements. *J Mol Liq* 1:121144. <https://doi.org/10.1016/j.molliq.2022.121144>
- Liu T et al (2022b) Recent developments in the utilization of modified graphene oxide to adsorb dyes from water: a review. *J Ind Eng Chem*. <https://doi.org/10.1016/j.jiec.2022.10.008>
- Liu T et al (2022c) Adsorption of cadmium and lead from aqueous solution using modified biochar: a review. *J Environ Chem Eng* 10(1):106502. <https://doi.org/10.1016/j.jece.2021.106502>
- Liu Y et al (2023) Enhanced cadmium removal by biochar and iron oxides composite: material interactions and pore structure. *J*

- Environ Manag 330:117136. <https://doi.org/10.1016/j.jenvman.2022.117136>
- Lodygin E (2019) Sorption of Cu²⁺ and Zn²⁺ ions by humic acids of tundra peat gley soils (histic reductaquic cryosols). Eurasian Soil Sci 52(7):769–777. <https://doi.org/10.1134/S1064229319070093>
- Lodygin ED et al (2020) Complexation of lead and cadmium ions with humic acids from arctic peat soils. Environ Res 191:110058. <https://doi.org/10.1016/j.envres.2020.110058>
- Lombardo S, Thielemans WJC (2019) Thermodynamics of adsorption on nanocellulose surfaces. Cellulose 26(1):249–279
- López-Quintela MA et al (2004) Microemulsion dynamics and reactions in microemulsions. Curr Opin Colloid Interface Sci 9(3–4):264–278
- Luo Q et al (2021) Fluorescent chitosan-based hydrogel incorporating titanate and cellulose nanofibers modified with carbon dots for adsorption and detection of Cr (VI). Chem Eng J 407:127050
- Lv Y et al (2009) Synthesis, characterization and growing mechanism of monodisperse Fe₃O₄ microspheres. J Cryst Growth 311(13):3445–3450
- Mahmoud AED et al (2022a) Biogenic synthesis of reduced graphene oxide from *Ziziphus spina-christi* (Christ's thorn jujube) extracts for catalytic, antimicrobial, and antioxidant potentialities. Environ Sci Pollut Res 29:89772–89787
- Mahmoud ME et al (2022b) The design of SnO₂-crosslinked-chitosan nanocomposite for microwave-assisted adsorption of aqueous cadmium and mercury ions. Sustain Chem Pharm 28:100731
- Maia LC et al (2021) A review on the use of lignocellulosic materials for arsenic adsorption. J Environ Manag 288:112397. <https://doi.org/10.1016/j.jenvman.2021.112397>
- Maity JP et al (2018) Removal of fluoride from water through bacterial-surfactin mediated novel hydroxyapatite nanoparticle and its efficiency assessment: adsorption isotherm, adsorption kinetic and adsorption thermodynamics. Environ Nanotechnol Monit Manag 9:18–28
- Majd MM et al (2021) Adsorption isotherm models: a comprehensive and systematic review (2010–2020). Sci Total Environ 812:151334
- Maksoud MA et al (2020) Insight on water remediation application using magnetic nanomaterials and biosorbents. Coord Chem Rev 403:213096
- Malana MA et al (2011) Adsorption studies of arsenic on nano aluminium doped manganese copper ferrite polymer (MA, VA, AA) composite: kinetics and mechanism. Chem Eng J 172(2–3):721–727
- Maleki A et al (2015) Ethyl acrylate grafted chitosan for heavy metal removal from wastewater: equilibrium, kinetic and thermodynamic studies. J Taiwan Inst Chem Eng 51:127–134
- Marcińczyk M et al (2022) From waste to fertilizer: nutrient recovery from wastewater by pristine and engineered biochars. Chemosphere. <https://doi.org/10.1016/j.chemosphere.2022.135310>
- Marques BS et al (2019) Adsorption of a textile dye onto piacava fibers: kinetic, equilibrium, thermodynamics, and application in simulated effluents. Environ Sci Pollut Res 26(28):28584–28592
- Martín J et al (2019) Evaluation of a modified mica and montmorillonite for the adsorption of ibuprofen from aqueous media. Appl Clay Sci 171:29–37. <https://doi.org/10.1016/j.clay.2019.02.002>
- Martín-Lara M et al (2016) Kinetic study of the pyrolysis of pine cone shell through non-isothermal thermogravimetry: effect of heavy metals incorporated by biosorption. Renew Energy 96:613–624
- Mashkour F, Nasar A (2020) Carbon nanotube-based adsorbents for the removal of dyes from waters: a review. Environ Chem Lett 18(3):605–629
- Mayakaduwa S et al (2017) Insights into aqueous carbofuran removal by modified and non-modified rice husk biochars. Environ Sci Pollut Res 24(29):22755–22763. <https://doi.org/10.1007/s11356-016-7430-6>
- Mdlalose L et al (2021) Performance evaluation of polypyrrole–montmorillonite clay composite as a re-usable adsorbent for Cr (VI) remediation. Polym Bull 78(8):4685–4697. <https://doi.org/10.1007/s00289-020-03338-6>
- Minisy IM et al (2021) Adsorption of methylene blue onto chitosan–montmorillonite/polyaniline nanocomposite. Appl Clay Sci 203:105993
- Mittal N et al (2022) Adsorption studies on hydrophobic disperse dye using cellulose derived mesoporous activated carbon. Mater Today Proc 62:7595–7599
- Mogale R et al (2022) Dye adsorption of aluminium-and zirconium-based metal organic frameworks with azobenzene dicarboxylate linkers. J Environ Manag 304:114166
- Mohamed LA et al (2021) Isotherms and kinetic modelling of mycoremediation of hexavalent chromium contaminated wastewater. Clean Eng Technol 4:100192. <https://doi.org/10.1016/j.clet.2021.100192>
- Mohammad SG et al (2022) Removal of copper (II) ions by eco-friendly raw eggshells and nano-sized eggshells: a comparative study. Chem Eng Commun 209(1):83–95
- Mohammed BB et al (2020) Fe-ZSM-5 zeolite for efficient removal of basic Fuchsin dye from aqueous solutions: synthesis, characterization and adsorption process optimization using BBD-RSM modeling. J Environ Chem Eng 8(5):104419. <https://doi.org/10.1016/j.clet.2021.100192>
- Mohanasrinivasan V et al (2014) Studies on heavy metal removal efficiency and antibacterial activity of chitosan prepared from shrimp shell waste. 3 Biotech 4(2):167–175
- Mokhtar N et al (2017) Biosorption of azo-dye using marine macro-alga of *Eucheuma Spinosum*. J Environ Chem Eng 5(6):5721–5731
- Moloukhia H et al (2016) Removal of Eu³⁺, Ce³⁺, Sr²⁺, and Cs⁺ ions from radioactive waste solutions by modified activated carbon prepared from coconut shells. Chem Ecol 32(4):324–345. <https://doi.org/10.1080/02757540.2016.1139089>
- Moreno-Marengo AR et al (2020) Adsorption of n-butylparaben from aqueous solution on surface of modified granular activated carbons prepared from African palm shell. Thermodynamic study of interactions. J Environ Chem Eng 8(4):103969. <https://doi.org/10.1016/j.jece.2020.103969>
- Motaghi H et al (2021) Simultaneous adsorption of cobalt ions, azo dye, and imidacloprid pesticide on the magnetic chitosan/activated carbon@ UiO-66 bio-nanocomposite: optimization, mechanisms, regeneration, and application. Sep Purif Technol 284:120258
- Mundim HSDSL et al (2022) Optimization of Pb²⁺, Cd²⁺, Ni²⁺ and Ba²⁺ adsorption onto light expanded clay aggregate (LECA). Ciência e Natura 44:e3. <https://doi.org/10.5902/2179460X68809>
- Muralikrishnan R, Jodhi C (2020) Biodecolorization of reactive dyes using biochar derived from coconut shell: batch, isotherm, kinetic and desorption studies. ChemistrySelect 5(26):7734–7742. <https://doi.org/10.1002/slct.202001454>
- Naderi P et al (2018) Efficient removal of crystal violet from aqueous solutions with *Centaurea stem* as a novel biodegradable bio-adsorbent using response surface methodology and simulated annealing: kinetic, isotherm and thermodynamic studies. Ecotoxicol Environ Saf 163:372–381
- Nagy E (2018) Basic equations of mass transport through a membrane layer. Elsevier, Amsterdam. <https://doi.org/10.1016/B978-0-12-416025-5.00001-6>
- Nahm SW et al (2012) Thermal and chemical regeneration of spent activated carbon and its adsorption property for toluene. Chem Eng J 210:500–509

- Najafloo S et al (2021) Removal of Pb (II) from contaminated waters using cellulose sulfate/chitosan aerogel: equilibrium, kinetics, and thermodynamic studies. *J Environ Manag* 286:112167
- Naraghi B et al (2017) Removal of Acid Orange 7 dye from aqueous solutions by adsorption onto Kenya tea pulps; granulated shape. *Electron Physician* 9(5):4312. <https://doi.org/10.19082/4312>
- Natrayan L et al (2022) Synthesis and analysis of impregnation on activated carbon in multiwalled carbon nanotube for Cu adsorption from wastewater. *Bioinorg Chem Appl*. <https://doi.org/10.1155/2022/7470263>
- Naymushina O, Gaskova O (2019) Adsorption of Cu (II) from aqueous solution using raw peat: preliminary results. In: E3S web of conferences
- Nayyar D et al (2022) Remediation of emerging contaminants by naturally derived adsorbents. *New Trends Emerg Environ Contam*. https://doi.org/10.1007/978-981-16-8367-1_11
- Nezhad MM et al (2021) Efficient removal and recovery of uranium from industrial radioactive wastewaters using functionalized activated carbon powder derived from zirconium carbide process waste. *Environ Sci Pollut Res* 28(40):57073–57089. <https://doi.org/10.1007/s11356-021-14638-3>
- Nguyen T-B et al (2021) Mesoporous and adsorption behavior of algal biochar prepared via sequential hydrothermal carbonization and ZnCl₂ activation. *Bioresour Technol*. <https://doi.org/10.1016/j.biortech.2021.126351>
- Nindjio GFK et al (2022) Lignocellulosic-based materials from bean and pistachio pod wastes for dye-contaminated water treatment: optimization and modeling of indigo carmine sorption. *Polymers* 14(18):3776. <https://doi.org/10.3390/polym14183776>
- Noman E et al (2020) Qualitative characterization of healthcare wastes. In: Al-Gheethi AA, Mohamed RM, Noman EA, Kassim AH (eds) *Prospects of fresh market wastes management in developing countries*. Springer, Berlin, pp 167–178
- Nyankson E et al (2020) Synthesis and kinetic adsorption characteristics of Zeolite/CeO₂ nanocomposite. *Sci Afr* 7:e00257. <https://doi.org/10.1016/j.sciaf.2019.e00257>
- Obradović M et al (2022) Ibuprofen and diclofenac sodium adsorption onto functionalized minerals: equilibrium, kinetic and thermodynamic studies. *Microporous Mesoporous Mater* 335:111795. <https://doi.org/10.1016/j.micromeso.2022.111795>
- Okewale A et al (2013) Adsorption isotherms and kinetics models of starchy adsorbents on uptake of water from ethanol–water systems. *Int J Appl Sci Technol* 3(1):35–42
- Osman AI et al (2020a) The production and application of carbon nanomaterials from high alkali silicate herbaceous biomass. *Sci Rep* 10(1):2563. <https://doi.org/10.1038/s41598-020-59481-7>
- Osman AI et al (2020b) Upcycling brewer's spent grain waste into activated carbon and carbon nanotubes for energy and other applications via two-stage activation. *J Chem Technol Biotechnol* 95(1):183–195. <https://doi.org/10.1002/jctb.6220>
- Osman AI et al (2022a) Facile synthesis and life cycle assessment of highly active magnetic sorbent composite derived from mixed plastic and biomass waste for water remediation. *ACS Sustain Chem Eng* 10(37):12433–12447. <https://doi.org/10.1021/acssuschemeng.2c04095>
- Osman AI et al (2022b) Biochar for agronomy, animal farming, anaerobic digestion, composting, water treatment, soil remediation, construction, energy storage, and carbon sequestration: a review. *Environ Chem Lett* 20(4):2385–2485. <https://doi.org/10.1007/s10311-022-01424-x>
- Osman AI et al (2023) Biofuel production, hydrogen production and water remediation by photocatalysis, biocatalysis and electrocatalysis. *Environ Chem Lett*. <https://doi.org/10.1007/s10311-023-01581-7>
- Ouachtak H et al (2020) Experimental and molecular dynamics simulation study on the adsorption of Rhodamine B dye on magnetic montmorillonite composite γ -Fe₂O₃@ Mt. *J Mol Liq* 309:113142. <https://doi.org/10.1016/j.molliq.2020.113142>
- Pal D, Maiti SK (2020) An approach to counter sediment toxicity by immobilization of heavy metals using waste fish scale derived biosorbent. *Ecotoxicol Environ Saf* 187:109833. <https://doi.org/10.1016/j.ecoenv.2019.109833>
- Pamphile N et al (2019) Synthesis of a novel core-shell-structure activated carbon material and its application in sulfamethoxazole adsorption. *J Hazard Mater* 368:602–612. <https://doi.org/10.1016/j.jhazmat.2019.01.093>
- Pan J et al (2020) Waste-to-resources: green preparation of magnetic biogas residues-based biochar for effective heavy metal removals. *Sci Total Environ* 737:140283
- Parsa M et al (2019) Biochars derived from marine macroalgae as a mesoporous by-product of hydrothermal liquefaction process: characterization and application in wastewater treatment. *J Water Process Eng* 32:100942
- Patsula V et al (2016) Superparamagnetic Fe₃O₄ nanoparticles: synthesis by thermal decomposition of iron (III) glucuronate and application in magnetic resonance imaging. *ACS Appl Mater Interfaces* 8(11):7238–7247
- Pavithra S et al (2021) Batch adsorption studies on surface tailored chitosan/orange peel hydrogel composite for the removal of Cr (VI) and Cu (II) ions from synthetic wastewater. *Chemosphere* 271:129415
- Pavón González E, Alba MD (2022) Insight into the role of temperature, time and pH in the effective zirconium retention using clay minerals. *J Environ Manag* 308:114635. <https://doi.org/10.1016/j.jenvman.2022.114635>
- Pelinson Marques J et al (2020) Increase in Pb and Cd adsorption by the application of peat in a tropical soil. *Water Air Soil Pollut* 231(3):1–21. <https://doi.org/10.1007/s11270-020-04507-z>
- Peng X et al (2023) Recycling municipal, agricultural and industrial waste into energy, fertilizers, food and construction materials, and economic feasibility: a review. *Environ Chem Lett* 21(2):765–801. <https://doi.org/10.1007/s10311-022-01551-5>
- Perelomov L et al (2021) Trace elements adsorption by natural and chemically modified humic acids. *Environ Geochem Health* 43(1):127–138. <https://doi.org/10.1007/s10653-020-00686-0>
- Peres EC et al (2018) Treatment of leachates containing cobalt by adsorption on *Spirulina* sp. and activated charcoal. *J Environ Chem Eng* 6(1):677–685. <https://doi.org/10.1016/j.jece.2017.12.060>
- Pham TD et al (2020a) Adsorption characteristics of beta-lactam cefixime onto nanosilica fabricated from rice HUSK with surface modification by polyelectrolyte. *J Mol Liq* 298:111981. <https://doi.org/10.1016/j.molliq.2019.111981>
- Pham TD et al (2020b) Adsorptive removal of antibiotic ciprofloxacin from aqueous solution using protein-modified nanosilica. *Polymers* 12(1):57. <https://doi.org/10.3390/polym12010057>
- Pham TD et al (2021) Adsorptive removal of anionic azo dye new coccine using silica and silica-gel with surface modification by polycation. *Polymers* 13(10):1536. <https://doi.org/10.3390/polym13101536>
- Philipp T et al (2022) Effect of Ca (II) on U (VI) and Np (VI) retention on Ca-bentonite and clay minerals at hyperalkaline conditions—new insights from batch sorption experiments and luminescence spectroscopy. *Sci Total Environ* 842:156837. <https://doi.org/10.1016/j.scitotenv.2022.156837>
- Phouthavong V et al (2020) Magnetic BEA-type zeolites: preparation by dry-gel conversion method and assessment of dye removal performance. *J Mater Cycles Waste Manag* 22(2):375–382. <https://doi.org/10.1007/s10163-020-00994-8>
- Pirbazari AE et al (2014) Fe₃O₄–wheat straw: preparation, characterization and its application for methylene blue adsorption. *Water Resour Ind* 7:23–37. <https://doi.org/10.1016/j.wri.2014.09.001>

- Praveen S et al (2021) Techno-economic feasibility of biochar as biosorbent for basic dye sequestration. *J Indian Chem Soc* 98(8):100107. <https://doi.org/10.1016/j.jics.2021.100107>
- Priya A et al (2022) Biosorption of heavy metals by microorganisms: evaluation of different underlying mechanisms. *Chemosphere* 307:135957
- Qi Y (2021) The neutralization and recycling of red mud—a review. In: *Journal of physics: conference series*
- Qi G et al (2023) Microwave biochar produced with activated carbon catalyst: characterization and adsorption of heavy metals. *Environ Res* 216:114732. <https://doi.org/10.1016/j.envres.2022.114732>
- Radi S et al (2019) New hybrid adsorbent based on porphyrin functionalized silica for heavy metals removal: synthesis, characterization, isotherms, kinetics and thermodynamics studies. *J Hazard Mater* 370:80–90. <https://doi.org/10.1016/j.jhazmat.2017.10.058>
- Ragheb E et al (2022) Modified magnetic-metal organic framework as a green and efficient adsorbent for removal of heavy metals. *J Environ Chem Eng* 10(2):107297
- Rahmayanti M et al (2021) Isolation, characterization and application of humin from sumatran peat soils as adsorbent for naphthol blue black and indigosol blue dyes. *Molekul* 16(1):67–74. <https://doi.org/10.20884/1.jm.2021.16.1.700>
- Rai S et al (2013) Feasibility of red mud neutralization with seawater using Taguchi's methodology. *Int J Environ Sci Technol* 10(2):305–314
- Rangabhashiyam S et al (2016) Equilibrium and kinetics studies of hexavalent chromium biosorption on a novel green macroalgae *Enteromorpha* sp. *Res Chem Intermed* 42(2):1275–1294
- Rashad E et al (2022) Pinewood sawdust biochar as an effective biosorbent for PAHs removal from wastewater. *Biomass Convers Biorefinery*. <https://doi.org/10.1007/s13399-021-02181-7>
- Razak MR et al (2020) Phosphoric acid modified kenaf fiber (K-PA) as green adsorbent for the removal of copper (II) ions towards industrial waste water effluents. *React Funct Polym* 147:104466. <https://doi.org/10.1016/j.reactfunctpolym.2019.104466>
- Reddy DHK et al (2017) Valorisation of post-sorption materials: opportunities, strategies, and challenges. *Adv Coll Interface Sci* 242:35–58
- Richards S et al (2019) The potential use of natural vs commercial biosorbent material to remediate stream waters by removing heavy metal contaminants. *J Environ Manag* 231:275–281. <https://doi.org/10.1016/j.jenvman.2018.10.019>
- Rodrigues AE, Silva CM (2016) What's wrong with Lagergreen pseudo first order model for adsorption kinetics? *Chem Eng J* 306:1138–1142
- Rout PR et al (2016) Nutrient removal from binary aqueous phase by dolochar: highlighting optimization, single and binary adsorption isotherms and nutrient release. *Process Saf Environ Prot* 100:91–107. <https://doi.org/10.1016/j.psep.2016.01.001>
- Rwiza MJ et al (2018) Comparative sorption isotherms and removal studies for Pb(II) by physical and thermochemical modification of low-cost agro-wastes from Tanzania. *Chemosphere* 195:135–145. <https://doi.org/10.1016/j.chemosphere.2017.12.043>
- Saad SA et al (2010) Chemically modified sugarcane bagasse as a potentially low-cost biosorbent for dye removal. *Desalination* 264(1):123–128. <https://doi.org/10.1016/j.desal.2010.07.015>
- SafaÇelik M et al (2022) Biosorption of Rhodamine B dye from aqueous solution by *Rhus coriaria* L. plant: equilibrium, kinetic, thermodynamic and DFT calculations. *J Mol Struct* 1272:134158
- Saffarian Delkosh A et al (2021) Heat-treated gilsonite as an efficient natural material for removing toluene: a Box–Behnken experimental design approach. *Sci Iran* 28(3):1353–1365
- Sahu MK et al (2013) Removal of Pb (II) from aqueous solution by acid activated red mud. *J Environ Chem Eng* 1(4):1315–1324
- Sahu S et al (2020) Adsorption of methylene blue on chemically modified lychee seed biochar: dynamic, equilibrium, and thermodynamic study. *J Mol Liq* 315:113743
- Salam MA et al (2020) Effective decontamination of As (V), Hg (II), and U (VI) toxic ions from water using novel muscovite/zeolite aluminosilicate composite: adsorption behavior and mechanism. *Environ Sci Pollut Res* 27:13247–13260. <https://doi.org/10.1007/s11356-020-07945-8>
- Salgın U et al (2004) Desorption of salicylic acid from modified bentonite by using supercritical fluids in packed bed column. *Sep Sci Technol* 39(11):2677–2694
- Salishcheva O et al (2021) Analysis of kinetic and equilibrium adsorption of heavy metals by natural materials. In: *IOP conference series: earth and environmental science*
- Salleh MAM et al (2011) Cationic and anionic dye adsorption by agricultural solid wastes: a comprehensive review. *Desalination* 280(1–3):1–13
- Salvador F et al (2013) Regeneration of activated carbons contaminated by phenol using supercritical water. *J Supercrit Fluids* 74:1–7
- Salvador F et al (2015) Regeneration of carbonaceous adsorbents. Part II: chemical, microbiological and vacuum regeneration. *Microporous Mesoporous Mater* 202:277–296
- Sánchez-Duarte RG et al (2017) Síntesis de hidrogeles de quitosano a partir de cáscara de camarón para ensayos de adsorción de cobre. *Revista Internacional De Contaminación Ambiental* 33:93–98
- Saravana PS et al (2018) Green and efficient extraction of polysaccharides from brown seaweed by adding deep eutectic solvent in subcritical water hydrolysis. *J Clean Prod* 198:1474–1484
- Sari EO et al (2018) The 3 hours-hydrothermal synthesis of high surface area superparamagnetic Fe₃O₄ core-shell nanoparticles. *Jurnal Sains Materi Indonesia* 19(1):9–13
- Sarkar B et al (2018) Designer carbon nanotubes for contaminant removal in water and wastewater: a critical review. *Sci Total Environ* 612:561–581
- Sarma GK et al (2019) Removal of hazardous basic dyes from aqueous solution by adsorption onto kaolinite and acid-treated kaolinite: kinetics, isotherm and mechanistic study. *SN Appl Sci*. <https://doi.org/10.1007/s42452-019-0216-y>
- Sarti E et al (2020) High-silica zeolites as sorbent media for adsorption and pre-concentration of pharmaceuticals in aqueous solutions. *Molecules* 25(15):3331. <https://doi.org/10.3390/molecules25153331>
- Sayin F et al (2021) Chitosan immobilization and Fe₃O₄ functionalization of olive pomace: an eco-friendly and recyclable Pb²⁺ biosorbent. *Carbohydr Polym* 269:118266
- Sevim F et al (2021) Adsorption capacity, isotherm, kinetic, and thermodynamic studies on adsorption behavior of malachite green onto natural red clay. *Environ Prog Sustain Energy* 40(1):e13471. <https://doi.org/10.1002/ep.13471>
- Shahadat M, Isamil S (2018) Regeneration performance of clay-based adsorbents for the removal of industrial dyes: a review. *RSC Adv* 8(43):24571–24587
- Shahnaz T et al (2020) A comparative study of raw, acid-modified and EDTA-complexed *Acacia auriculiformis* biomass for the removal of hexavalent chromium. *Chem Ecol* 36(4):360–381
- Shalaby SM et al (2021) Green synthesis of recyclable iron oxide nanoparticles using *Spirulina platensis* microalgae for adsorptive removal of cationic and anionic dyes. *Environ Sci Pollut Res* 28(46):65549–65572
- Shao P et al (2020) Evaluating the adsorptivity of organo-functionalized silica nanoparticles towards heavy metals: quantitative comparison and mechanistic insight. *J Hazard Mater* 387:121676. <https://doi.org/10.1016/j.jhazmat.2019.121676>
- Sharma M et al (2022) Selective removal of uranium from an aqueous solution of mixed radionuclides of uranium, cesium, and

- strontium via a viable recyclable GO@ chitosan based magnetic nanocomposite. *Mater Today Commun* 32:104020
- Shen W et al (2020) Alginate modified graphitic carbon nitride composite hydrogels for efficient removal of Pb (II), Ni (II) and Cu (II) from water. *Int J Biol Macromol* 148:1298–1306
- Shi Q et al (2018) Mechanistic study of lead adsorption on activated carbon. *Langmuir* 34(45):13565–13573. <https://doi.org/10.1021/acs.langmuir.8b03096>
- Shukla S, Dhiman N (2017) Characterization and adsorption of disperse dyes from wastewater onto cenospheres activated carbon composites. *Environ Earth Sci* 76(20):1–12. <https://doi.org/10.1007/s12665-017-7030-x>
- Siddiqui SI et al (2019) *Nigella sativa* seed based nanocomposite-MnO₂/BC: an antibacterial material for photocatalytic degradation, and adsorptive removal of Methylene blue from water. *Environ Res* 171:328–340. <https://doi.org/10.1016/j.envres.2018.11.044>
- Silva TL et al (2016) Mesoporous activated carbon from industrial laundry sewage sludge: adsorption studies of reactive dye Remazol Brilliant Blue R. *Chem Eng J* 303:467–476. <https://doi.org/10.1016/j.molliq.2015.07.010>
- Silva RV et al (2021) Bioproducts from the pyrolysis of castor seed cake: basic dye adsorption capacity of biochar and antifungal activity of the aqueous phase. *J Environ Chem Eng* 9(1):104825. <https://doi.org/10.1016/j.jece.2020.104825>
- Slimani R et al (2014) Calcined eggshells as a new biosorbent to remove basic dye from aqueous solutions: thermodynamics, kinetics, isotherms and error analysis. *J Taiwan Inst Chem Eng* 45(4):1578–1587. <https://doi.org/10.1016/j.jtice.2013.10.009>
- Smiljanić S et al (2011) Study of factors affecting Ni²⁺ immobilization efficiency by temperature activated red mud. *Chem Eng J* 168(2):610–619
- Smiljanić D et al (2020) Removal of emerging contaminants from water by zeolite-rich composites: a first approach aiming at diclofenac and ketoprofen. *Microporous Mesoporous Mater* 298:110057. <https://doi.org/10.1016/j.micromeso.2020.110057>
- Smiljanić D et al (2021) Removal of non-steroidal anti-inflammatory drugs from water by zeolite-rich composites: the interference of inorganic anions on the ibuprofen and naproxen adsorption. *J Environ Manag* 286:112168. <https://doi.org/10.1016/j.jenvman.2021.112168>
- Soliman MA et al (2019) Organo-modification of montmorillonite for enhancing the adsorption efficiency of cobalt radionuclides from aqueous solutions. *Environ Sci Pollut Res* 26(10):10398–10413. <https://doi.org/10.1007/s11356-019-04478-7>
- Song X et al (2017) Regeneration performance and mechanism of modified walnut shell biochar catalyst for low temperature catalytic hydrolysis of organic sulfur. *Chem Eng J* 330:727–735
- Sonmez Baghirzade B et al (2021) Thermal regeneration of spent granular activated carbon presents an opportunity to break the forever PFAS cycle. *Environ Sci Technol* 55(9):5608–5619
- Southichak B et al (2006) *Phragmites australis*: a novel biosorbent for the removal of heavy metals from aqueous solution. *Water Res* 40(12):2295–2302. <https://doi.org/10.1016/j.watres.2006.04.027>
- Srivatsav P et al (2020) Biochar as an eco-friendly and economical adsorbent for the removal of colorants (dyes) from aqueous environment: a review. *Water* 12(12):3561. <https://doi.org/10.3390/w12123561>
- Stjepanović M et al (2021) From waste to biosorbent: removal of congo red from water by waste wood biomass. *Water* 13(3):279
- Sun K et al (2017) Extending surfactant-modified 2: 1 clay minerals for the uptake and removal of diclofenac from water. *J Hazard Mater* 323:567–574. <https://doi.org/10.1016/j.jhazmat.2016.05.038>
- Sun L et al (2022) Modified chicken manure biochar enhanced the adsorption for Cd²⁺ in aqueous and immobilization of Cd in contaminated agricultural soil. *Sci Total Environ* 851:158252. <https://doi.org/10.1016/j.scitotenv.2022.158252>
- Sun Q et al (2023a) Adsorption of Pb²⁺ and methylene blue by Al-incorporated magadiite. *Appl Clay Sci* 231:106745. <https://doi.org/10.1016/j.clay.2022.106745>
- Sun Y et al (2023b) Copper ion removal from aqueous media using banana peel biochar/Fe₃O₄/branched polyethyleneimine. *Colloids Surf A Physicochem Eng Asp* 658:130736. <https://doi.org/10.1016/j.colsurfa.2022.130736>
- Sutivisedsak N et al (2012) Evaluation of cotton byproducts as fillers for poly (lactic acid) and low density polyethylene. *Ind Crops Prod* 36(1):127–134
- Syeda HI, Yap P-S (2022) A review on three-dimensional cellulose-based aerogels for the removal of heavy metals from water. *Sci Total Environ* 807:150606. <https://doi.org/10.1016/j.scitotenv.2021.150606>
- Syeda HI et al (2022) Biosorption of heavy metals from aqueous solution by various chemically modified agricultural wastes: a review. *J Water Process Eng* 46:102446. <https://doi.org/10.1016/j.jwpe.2021.102446>
- Szewczuk-Karpisz K et al (2022) Immobilization mechanism of Cd²⁺/HCrO₄⁻/CrO₄²⁻ ions and carboxin on montmorillonite modified with *Rhizobium leguminosarum* bv trifolii exopolysaccharide. *J Hazard Mater* 428:128228. <https://doi.org/10.1016/j.jhazmat.2022.128228>
- Tamjidi S et al (2019) Application of magnetic adsorbents for removal of heavy metals from wastewater: a review study. *Mater Res Express* 6(10):102004
- Tan X et al (2016) Biochar-based nano-composites for the decontamination of wastewater: a review. *Bioresour Technol* 212:318–333. <https://doi.org/10.1016/j.biortech.2016.04.093>
- Tan W-T et al (2022) Enhancing Cd (II) adsorption on rice straw biochar by modification of iron and manganese oxides. *Environ Pollut* 300:118899
- Tanez M, Hurel C (2019) A review on the potential uses of red mud as amendment for pollution control in environmental media. *Environ Sci Pollut Res* 26(22):22106–22125
- Tanihara A et al (2021) Insight into the mechanism of heavy metal removal from water by monodisperse ZIF-8 fine particles. *Inorg Chem Commun* 131:108782
- Tao X et al (2021) Green synthesis of network nanostructured calcium alginate hydrogel and its removal performance of Cd²⁺ and Cu²⁺ ions. *Mater Chem Phys* 258:123931
- Tee GT et al (2022) Adsorption of pollutants in wastewater via biosorbents, nanoparticles and magnetic biosorbents: a review. *Environ Res* 212:113248
- Temkin M (1940) Kinetics of ammonia synthesis on promoted iron catalysts. *Acta Physiochim URSS* 12:327–356
- Tesfaye T et al (2017) Valorisation of chicken feathers: a review on recycling and recovery route—current status and future prospects. *Clean Technol Environ Policy* 19(10):2363–2378
- Thakur K et al (2019) Graphene and graphene oxide-based composites for removal of organic pollutants: a review. *J Chem Eng Data* 64(3):833–867
- Thilagan J et al (2015) Continuous fixed bed column adsorption of copper (II) ions from aqueous solution by calcium carbonate. *Int J Eng Res Technol* 4(12):413–416
- Thirumoorthy K, Krishna S (2020) Removal of cationic and anionic dyes from aqueous phase by Ball clay–Manganese dioxide nanocomposites. *J Environ Chem Eng* 8(1):103582. <https://doi.org/10.1016/j.jece.2019.103582>
- Thirunavukkarasu A et al (2021) Continuous fixed-bed biosorption process: a review. *Chem Eng J Adv* 8:100188
- Thompson KA et al (2016) Environmental comparison of biochar and activated carbon for tertiary wastewater treatment. *Environ*

- Sci Technol 50(20):11253–11262. <https://doi.org/10.1021/acs.est.6b03239>
- Tonk S et al (2022) Effectiveness and characterization of novel mineral clay in Cd²⁺ adsorption process: linear and non-linear isotherm regression analysis. *Water* 14(3):279. <https://doi.org/10.3390/w14030279>
- Toński M et al (2021) Regeneration and reuse of the carbon nanotubes for the adsorption of selected anticancer drugs from water matrices. *Colloids Surf A* 618:126355
- Tran TN et al (2018) Adsorption mechanisms of manganese (II) ions onto acid-treated activated carbon. *KSCE J Civ Eng* 22(10):3772–3782. <https://doi.org/10.1007/s12205-018-1334-6>
- Tripathi S et al (2018) Removal of U (VI) from aqueous solution by adsorption onto synthesized silica and zinc silicate nanotubes: equilibrium and kinetic aspects with application to real samples. *Environ Nanotechnol Monit Manag* 10:127–139. <https://doi.org/10.1016/j.enmm.2018.05.003>
- Tuomikoski S et al (2019) Zinc adsorption by activated carbon prepared from lignocellulosic waste biomass. *Appl Sci* 9(21):4583. <https://doi.org/10.3390/app9214583>
- Turan B et al (2022) Adsorption of tetracycline antibiotics using metal and clay embedded cross-linked chitosan. *Mater Chem Phys* 279:125781
- Uasuf A, Becker G (2011) Wood pellets production costs and energy consumption under different framework conditions in Northeast Argentina. *Biomass Bioenerg* 35(3):1357–1366
- Uddin MK (2017) A review on the adsorption of heavy metals by clay minerals, with special focus on the past decade. *Chem Eng J* 308:438–462. <https://doi.org/10.1016/j.cej.2016.09.029>
- Ugwu EI, Agunwamba JC (2020) A review on the applicability of activated carbon derived from plant biomass in adsorption of chromium, copper, and zinc from industrial wastewater. *Environ Monit Assess* 192(4):1–12. <https://doi.org/10.1007/s10661-020-8162-0>
- Vareda JP et al (2020) Silica aerogels/xerogels modified with nitrogen-containing groups for heavy metal adsorption. *Molecules* 25(12):2788. <https://doi.org/10.3390/molecules25122788>
- Vázquez-Durán A et al (2021) Potential of kale and lettuce residues as natural adsorbents of the carcinogen aflatoxin B1 in a dynamic gastrointestinal tract-simulated model. *Toxins* 13(11):771. <https://doi.org/10.3390/toxins13110771>
- Vidal-Vidal J et al (2006) Synthesis of monodisperse maghemite nanoparticles by the microemulsion method. *Colloids Surf A* 288(1–3):44–51
- Vigneshwaran S et al (2021a) Fabrication of sulfur-doped biochar derived from tapioca peel waste with superior adsorption performance for the removal of Malachite green and Rhodamine B dyes. *Surf Interfaces* 23:100920. <https://doi.org/10.1016/j.surfin.2020.100920>
- Vigneshwaran S et al (2021b) Facile synthesis of sulfur-doped chitosan/biochar derived from tapioca peel for the removal of organic dyes: isotherm, kinetics and mechanisms. *J Mol Liq* 326:115303
- Vilela PB et al (2019) Polyacrylic acid-based and chitosan-based hydrogels for adsorption of cadmium: equilibrium isotherm, kinetic and thermodynamic studies. *J Environ Chem Eng* 7(5):103327
- Volesky B (1994) Advances in biosorption of metals: selection of biomass types. *FEMS Microbiol Rev* 14(4):291–302
- Vukelic D et al (2018) Eco-design of a low-cost adsorbent produced from waste cherry kernels. *J Clean Prod* 174:1620–1628
- Wakkel M et al (2019) Basic red 2 and methyl violet adsorption by date pits: adsorbent characterization, optimization by RSM and CCD, equilibrium and kinetic studies. *Environ Sci Pollut Res* 26(19):18942–18960. <https://doi.org/10.1007/s11356-018-2192-y>
- Wan M-W et al (2010) Adsorption of copper (II) and lead (II) ions from aqueous solution on chitosan-coated sand. *Carbohydr Polym* 80(3):891–899
- Wan S et al (2018) Enhanced lead and cadmium removal using biochar-supported hydrated manganese oxide (HMO) nanoparticles: behavior and mechanism. *Sci Total Environ* 616:1298–1306
- Wan X et al (2022) Chitosan-based dual network composite hydrogel for efficient adsorption of methylene blue dye. *Int J Biol Macromol* 222:725–735
- Wang J, Guo X (2020) Adsorption isotherm models: classification, physical meaning, application and solving method. *Chemosphere* 258:127279
- Wang TC et al (2015) Ultrahigh surface area zirconium MOFs and insights into the applicability of the BET theory. *J Am Chem Soc* 137(10):3585–3591
- Wang G et al (2018a) Removal of Pb(II) from aqueous solutions by *Phytolacca americana* L. biomass as a low cost biosorbent. *Arab J Chem* 11(1):99–110. <https://doi.org/10.1016/j.arabjc.2015.06.011>
- Wang Y-Y et al (2018b) Competitive adsorption of Pb (II), Cu (II), and Zn (II) ions onto hydroxyapatite-biochar nanocomposite in aqueous solutions. *J Solid State Chem* 261:53–61
- Wang Y et al (2018c) Alginate-based attapulgite foams as efficient and recyclable adsorbents for the removal of heavy metals. *J Colloid Interface Sci* 514:190–198
- Wang Z et al (2018d) New insights from supercritical methane adsorption in coal: gas resource estimation, thermodynamics, and engineering application. *Energy Fuels* 32(4):5001–5009
- Wang C et al (2020a) Development of mercaptosuccinic anchored MOF through one-step preparation to enhance adsorption capacity and selectivity for Hg (II) and Pb (II). *J Mol Liq* 317:113896
- Wang J et al (2020b) Synthesis and characterization of sodium laurylsulfonate modified silicon dioxide for the efficient removal of europium. *J Mol Liq* 316:113846. <https://doi.org/10.1016/j.molliq.2020.113846>
- Wang Y et al (2020c) Removing Cd (II) from aqueous solution by inverse opal hybrid SiO₂. *NANO* 15(04):2050047. <https://doi.org/10.1142/S1793292020500472>
- Wang S et al (2021) Calcite modification of agricultural waste biochar highly improves the adsorption of Cu (II) from aqueous solutions. *J Environ Chem Eng* 9(5):106215
- Wang H et al (2022) Effective adsorption of Congo red dye by magnetic chitosan prepared by solvent-free ball milling. *Mater Chem Phys* 292:126857
- Weber WJ Jr, Morris JC (1963) Kinetics of adsorption on carbon from solution. *J Sanit Eng Div* 89(2):31–59
- Wee S-B et al (2017) Role of N-methyl-2-pyrrolidone for preparation of Fe₃O₄@ SiO₂ controlled the shell thickness. *J Nanopart Res* 19(4):1–8
- Weißpflog J et al (2020) Solubility and selectivity effects of the anion on the adsorption of different heavy metal ions onto chitosan. *Molecules* 25(11):2482
- Wu W et al (2008) Magnetic iron oxide nanoparticles: synthesis and surface functionalization strategies. *Nanoscale Res Lett* 3(11):397–415
- Wu Z et al (2020) A facile foaming-polymerization strategy to prepare 3D MnO₂ modified biochar-based porous hydrogels for efficient removal of Cd (II) and Pb (II). *Chemosphere* 239:124745
- Wu J et al (2021) A novel modified method for the efficient removal of Pb and Cd from wastewater by biochar: enhanced the ion exchange and precipitation capacity. *Sci Total Environ* 754:142150
- Xiang W et al (2022) Performance of lignin impregnated biochar on tetracycline hydrochloride adsorption: governing factors and mechanisms. *Environ Res* 215:114339

- Xiao F et al (2020) Thermal stability and decomposition of perfluoroalkyl substances on spent granular activated carbon. *Environ Sci Technol Lett* 7(5):343–350
- Xu C, Teja AS (2008) Continuous hydrothermal synthesis of iron oxide and PVA-protected iron oxide nanoparticles. *J Supercrit Fluids* 44(1):85–91
- Xu H et al (2012) Porous carbon spheres from energetic carbon precursors using ultrasonic spray pyrolysis. *Adv Mater* 24(45):6028–6033. <https://doi.org/10.1002/adma.201201915>
- Xu X et al (2017) Waste-art-paper biochar as an effective sorbent for recovery of aqueous Pb (II) into value-added PbO nanoparticles. *Chem Eng J* 308:863–871
- Xu K et al (2022) Efficient adsorption of heavy metals from wastewater on nanocomposite beads prepared by chitosan and paper sludge. *Sci Total Environ* 846:157399. <https://doi.org/10.1016/j.scitotenv.2022.157399>
- Yaashikaa P et al (2021) Advances in biosorbents for removal of environmental pollutants: a review on pretreatment, removal mechanism and future outlook. *J Hazard Mater* 420:126596
- Yan H et al (2011) Enhanced and selective adsorption of copper (II) ions on surface carboxymethylated chitosan hydrogel beads. *Chem Eng J* 174(2–3):586–594
- Yang KM et al (2014) Synthesis of water well-dispersed PEGylated iron oxide nanoparticles for MR/optical lymph node imaging. *J Mater Chem B* 2(21):3355–3364
- Yang J et al (2015) Adsorption of hexavalent chromium from aqueous solution by activated carbon prepared from longan seed: kinetics, equilibrium and thermodynamics. *J Ind Eng Chem* 21:414–422. <https://doi.org/10.1016/j.jiec.2014.02.054>
- Yang S-S et al (2019a) Generation of high-efficient biochar for dye adsorption using frass of yellow mealworms (larvae of *Tenebrio molitor* Linnaeus) fed with wheat straw for insect biomass production. *J Clean Prod* 227:33–47. <https://doi.org/10.1016/j.jclepro.2019.04.005>
- Yang Y et al (2019b) Preparation and characterization of cationic water-soluble pillar [5] arene-modified zeolite for adsorption of methyl orange. *ACS Omega* 4(18):17741–17751. <https://doi.org/10.1021/acsomega.9b02180>
- Yang H et al (2020a) Utilization of biochar for resource recovery from water: a review. *Chem Eng J* 397:125502
- Yang K et al (2020b) Facile synthesis of novel porous graphene-like carbon hydrogel for highly efficient recovery of precious metal and removal of organic dye. *Appl Surf Sci* 528:146928
- Yang X et al (2021) Increased structural defects of graphene oxide compromised reductive capacity of ZVI towards hexavalent chromium. *Chemosphere* 277:130308
- Yang X et al (2022) Characteristics and aqueous dye removal ability of novel biosorbents derived from acidic and alkaline one-step ball milling of hickory wood. *Chemosphere* 309:136610. <https://doi.org/10.1016/j.chemosphere.2022.136610>
- Yap P-S, Priyaa V (2019) Removal of crystal violet and acid green 25 from water using kaolin. In: IOP conference series: materials science and engineering
- Ye X et al (2021) Ultra-efficient adsorption of copper ions in chitosan–montmorillonite composite aerogel at wastewater treatment. *Cellulose* 28(11):7201–7212
- Yin Y et al (2019) Adsorption of arsenic by activated charcoal coated zirconium-manganese nanocomposite: performance and mechanism. *Colloids Surf A* 575:318–328. <https://doi.org/10.1016/j.colsurfa.2019.04.093>
- Younas F et al (2021) Current and emerging adsorbent technologies for wastewater treatment: trends, limitations, and environmental implications. *Water* 13(2):215. <https://doi.org/10.3390/w13020215>
- Youssef HF et al (2021) Preparation and characterization of different zeolites from andesite rock: product evaluation for efficient dye removal. *Microporous Mesoporous Mater* 328:111485. <https://doi.org/10.1016/j.micromeso.2021.111485>
- Yu J et al (2008) Enhanced and selective adsorption of Pb²⁺ and Cu²⁺ by EDTAD-modified biomass of baker's yeast. *Bioresour Technol* 99(7):2588–2593. <https://doi.org/10.1016/j.biortech.2007.04.038>
- Yu M et al (2019) Single and simultaneous adsorption of rhodamine B and congo red from aqueous solution by organo-vermiculites. *J Mol Liq* 292:111408. <https://doi.org/10.1016/j.molliq.2019.111408>
- Zabulonov Y et al (2021) Effect of the surface hydration of clay minerals on the adsorption of cesium and strontium from dilute solutions. *Adsorption* 27(1):41–48. <https://doi.org/10.1007/s10450-020-00263-y>
- Zein R et al (2020) Modification of rice husk silica with bovine serum albumin (BSA) for improvement in adsorption of metanil yellow dye. *J Iran Chem Soc* 17(10):2599–2612. <https://doi.org/10.1007/s13738-020-01955-6>
- Zeldowitsch J (1934) Über den mechanismus der katalytischen oxydation von CO an MnO₂. *Acta Physicochim URSS* 1:364–449
- Zeng S, Kan EJC (2022) Thermally enhanced adsorption and persulfate oxidation-driven regeneration on FeCl₃-activated biochar for removal of microcystin-LR in water. *Chemosphere* 286:131950
- Zeng H et al (2020) Optimization and regeneration of chitosan-alginate hybrid adsorbent embedding iron-manganese sludge for arsenic removal. *Colloids Surf A* 607:125500
- Zeng Z et al (2023) Preparation and characterization of sodium polyacrylate grafted montmorillonite nanocomposite for the adsorption of cadmium ions from aqueous solution. *Colloids Surf A Physicochem Eng Asp* 656:130389. <https://doi.org/10.1016/j.colsurfa.2022.130389>
- Zhang D et al (2010) Synthesis of clay minerals. *Appl Clay Sci* 50(1):1–11. <https://doi.org/10.1016/j.clay.2010.06.019>
- Zhang W et al (2012) Adsorption of anionic dyes from aqueous solutions using chemically modified straw. *Bioresour Technol* 117:40–47
- Zhang S et al (2014a) Protic ionic liquids and salts as versatile carbon precursors. *J Am Chem Soc* 136(5):1690–1693. <https://doi.org/10.1021/ja411981c>
- Zhang X et al (2014b) Adsorption of anionic dye on magnesium hydroxide-coated pyrolytic bio-char and reuse by microwave irradiation. *Int J Environ Sci Technol* 11(5):1439–1448
- Zhang S et al (2016) Adsorption of pharmaceuticals on chitosan-based magnetic composite particles with core-brush topology. *Chem Eng J* 304:325–334
- Zhang P et al (2019a) Catalytic degradation of estrogen by persulfate activated with iron-doped graphitic biochar: process variables effects and matrix effects. *Chem Eng J* 378:122141
- Zhang Y et al (2019b) Regeneration of phenol-saturated activated carbon by supercritical water: effect of H₂O₂ and alkali metal catalysts. *J Environ Eng* 145(12):04019083
- Zhang W et al (2020) Novel pectin based composite hydrogel derived from grapefruit peel for enhanced Cu (II) removal. *J Hazard Mater* 384:121445
- Zhang H et al (2021) The adsorption mechanism of montmorillonite for different tetracycline species at different pH conditions: the novel visual analysis of intermolecular interactions. *Water Air Soil Pollut* 232(2):1–15. <https://doi.org/10.1007/s11270-021-05012-7>
- Zhang M et al (2022a) Sorption of pharmaceuticals and personal care products (PPCPs) from water and wastewater by carbonaceous materials: a review. *Crit Rev Environ Sci Technol* 52(5):727–766. <https://doi.org/10.1080/10643389.2020.1835436>
- Zhang T et al (2022b) Ultrasound-assisted and hydroalcoholic-freezing combination modification for the preparation of biomass sorbent

- from waste peach wood branches to efficient removal of methylene blue. *Biomass Convers Biorefinery*. <https://doi.org/10.1007/s13399-022-03322-2>
- Zhang X et al (2022c) Fabrication of new MIL-53 (Fe)@ TiO₂ visible-light responsive adsorptive photocatalysts for efficient elimination of tetracycline. *Chem Eng J* 428:131077
- Zhang Y et al (2022d) Amino-modified chitosan/gold tailings composite for selective and highly efficient removal of lead and cadmium from wastewater. *Chemosphere* 308:136086
- Zhao F et al (2013) Adsorption of Cd (II) and Pb (II) by a novel EGTA-modified chitosan material: kinetics and isotherms. *J Colloid Interface Sci* 409:174–182
- Zhao YG et al (2021) Ultrasound-assisted synthesis of tetraethylenepentamine-modified graphene oxide/dispersible Fe₃O₄ composites with enhanced adsorption capacity for allergenic disperse dyes [Article]. *J Iran Chem Soc* 18(5):1113–1125. <https://doi.org/10.1007/s13738-020-02099-3>
- Zhou C et al (2016) Removal of Pb (II) and Zn (II) from aqueous solutions by raw crab shell: a comparative study. *Water Environ Res* 88(4):374–383
- Zhou Q et al (2023) Synthesis of high-quality NaP1 zeolite from municipal solid waste incineration fly ash by microwave-assisted hydrothermal method and its adsorption capacity. *Sci Total Environ* 855:158741. <https://doi.org/10.1016/j.scitotenv.2022.158741>
- Zhuravlev IZ et al (2022) Zirconium phosphates deposited on the granulated silica gel as adsorbents for the extraction of cesium, strontium radioisotope ions. *Sep Sci Technol* 57(5):671–682. <https://doi.org/10.1080/01496395.2021.1934024>
- Zubair M et al (2022) Nano-modified feather keratin derived green and sustainable biosorbents for the remediation of heavy metals from synthetic wastewater. *Chemosphere* 308:136339. <https://doi.org/10.1016/j.chemosphere.2022.136339>

Publisher's Note Springer Nature remains neutral with regard to jurisdictional claims in published maps and institutional affiliations.

Authors and Affiliations

Ahmed I. Osman¹  · Eman M. Abd El-Monaem² · Ahmed M. Elgarahy^{3,4} · Chukwunonso O. Aniagor⁵ · Mohamed Hosny⁶ · Mohamed Farghali^{7,8} · Emanne Rashad⁹ · Marcel I. Ejimofor⁵ · Eduardo A. López-Maldonado¹⁰ · Ikko Ihara⁷ · Pow-Seng Yap¹¹ · David W. Rooney¹ · Abdelazeem S. Eltaweil²

¹ School of Chemistry and Chemical Engineering, Queen's University Belfast, David Keir Building, Stranmillis Road, Belfast BT9 5AG, Northern Ireland, UK

² Chemistry Department, Faculty of Science, Alexandria University, Alexandria, Egypt

³ Egyptian Propylene and Polypropylene Company (EPPC), Port Said, Egypt

⁴ Environmental Chemistry Division, Environmental Science Department, Faculty of Science, Port Said University, Port Said, Egypt

⁵ Department of Chemical Engineering, Nnamdi Azikiwe University, P.M.B. 5025, Awka, Nigeria

⁶ Green Technology Group, Environmental Sciences Department, Faculty of Science, Alexandria University, Alexandria 21511, Egypt

⁷ Department of Agricultural Engineering and Socio-Economics, Kobe University, Kobe 657-8501, Japan

⁸ Department of Animal and Poultry Hygiene and Environmental Sanitation, Faculty of Veterinary Medicine, Assiut University, Assiut 71526, Egypt

⁹ Department of Environmental Sciences, Faculty of Science, Alexandria University, Alexandria, Egypt

¹⁰ Faculty of Chemical Sciences and Engineering, Autonomous University of Baja California, CP 22390 Tijuana, Baja California, Mexico

¹¹ Department of Civil Engineering, Xi'an Jiaotong-Liverpool University, Suzhou 215123, China